# A STUDY OF TWO HIGHLY CONSERVED BACULOVIRUS GENES

by

CHRISTOPHER J. LEHIY

B.A., Kansas State University, 2002

AN ABSTRACT OF A DISSERTATION

submitted in partial fulfillment of the requirements for the degree

DOCTOR OF PHILOSOPHY

Division of Biology
College of Arts and Science

KANSAS STATE UNIVERSITY
Manhattan, Kansas

2010

# Abstract

Baculoviruses are enveloped, rod shaped viruses with circular, double-stranded DNA genomes. These viruses infect arthropods, primarily in the order Lepidoptera, although members of this virus family also infect species of Diptera, Hymenoptera, and Crustacea. The majority of these viruses undergo a bi-phasic cycle with one phase defined by the production of a budded virus (BV) form, responsible for cell to cell transmission, and the other defined by the production of an occlusion-derived virus (ODV) form, responsible for host to host transmission. The proto-typical member of the Baculoviridae family is considered to be *Autographa californica* M Nucleopolyhedrovirus (Ac*M*NPV). Its 133,894 base pair genome is predicted to encode for 156 proteins, a large number of which are essential for virus replication..

In this current work, we have further characterized two viral proteins that are highly conserved among baculoviruses. The first of these is an ortholog of the fibroblast growth factor family of proteins with sequence homology to the *Drosophila* Branchless protein as well as the mammalian FGF- 9, -16 and -20 subfamily. Despite its high degree of conservation among Baculoviruses, the viral fibroblast growth factor (vFGF) is considered a non-essential protein, although its deletion from the genome does affect the lethality of the virus when ingested *per os*. In our study, we were able to localize vFGF to the membrane of BV. Its presence on the envelope affected the ability of the virus particle to bind to both heparin *in vitro* and to the cell surface *in vivo,* and may play a role in the attachment phase prior to virus entry.

We also characterized Ac*M*NPV's open reading frame 109 (Ac-orf109). Unlike vFGF, Ac-orf109 is essential for virus replication since its deletion results in a complete lack of BV production. Transmission electron microscopy of cells transfected with an Ac-orf109 deletion virus shows the full range of virus-associated structures including mature capsid formation but there appears to be a deficiency in capsid egress out of the nucleus. Furthermore, the ODV retained in the nucleus appear to lack microvesicular membranes, an essential component for host to host transmission of infection.

# A STUDY OF TWO HIGHLY CONSERVED BACULOVIRUS GENES

by

CHRISTOPHER J. LEHIY

B.A., Kansas State University, 2002

A DISSERTATION

submitted in partial fulfillment of the requirements for the degree

DOCTOR OF PHILOSOPHY

Division of Biology
College of Arts and Sciences

KANSAS STATE UNIVERSITY
Manhattan, Kansas

2010

Approved by:

Major Professor
A. Lorena Passarelli

# Copyright

# Abstract

Baculoviruses are enveloped, rod shaped viruses with circular, double-stranded DNA genomes. These viruses infect arthropods, primarily in the order Lepidoptera, although members of this virus family also infect species of Diptera, Hymenoptera, and Crustacea. The majority of these viruses undergo a bi-phasic cycle with one phase defined by the production of a budded virus (BV) form, responsible for cell to cell transmission, and the other defined by the production of an occlusion-derived virus (ODV) form, responsible for host to host transmission. The proto-typical member of the Baculoviridae family is considered to be *Autographa californica* M Nucleopolyhedrovirus (Ac*M*NPV). Its 133,894 base pair genome is predicted to encode for 156 proteins, a large number of which are essential for virus replication..

In this current work, we have further characterized two viral proteins that are highly conserved among baculoviruses. The first of these is an ortholog of the fibroblast growth factor family of proteins with sequence homology to the *Drosophila* Branchless protein as well as the mammalian FGF- 9, -16 and -20 subfamily. Despite its high degree of conservation among baculoviruses, the viral fibroblast growth factor (vFGF) is considered a non-essential protein, although its deletion from the genome does affect the lethality of the virus when ingested *per os*. In our study, we were able to localize vFGF to the membrane of BV. Its presence on the envelope affected the ability of the virus particle to bind to both heparin *in vitro* and to the cell surface *in vivo,* and may play a role in the attachment phase prior to virus entry.

We also characterized Ac*M*NPV's open reading frame 109 (Ac-orf109). Unlike vFGF, Ac-orf109 is essential for virus replication since its deletion results in a complete lack of BV production. Transmission electron microscopy of cells transfected with an Ac-orf109 deletion virus shows the full range of virus-associated structures including mature capsid formation but there appears to be a deficiency in capsid egress out of the nucleus. Furthermore, the ODV retained in the nucleus appear to lack microvesicular membranes, an essential component for host to host transmission of infection.

# Table of Contents

# List of Figures

# Acknowledgements

I would like to acknowledge a number of people who have been instrumental in this work. First, I would like to thank Dr. A. Lorena Passarelli who was instrumental in guiding the research and showing infinite patience as the work was progressing. I would also like to acknowledge members of my graduate committee who worked tirelessly refining ideas and providing critical feedback: Dr. Rollie Clem, Dr. Tonia Von Ohlen, and Dr. Micheal Kanost. And finally, for providing comraderie as well as many hours of illumninating discussion, I would like to thank current and past members of the Passarelli lab: Dr. Marcelo Berretta, Dr. Chanitchote Detvisitsakun, Dr. Wenbi Wu, Dr. John Means, Erica Cain, Mandar Deshpande, Olga Martinez, Emma Del Real, Justin Trowbridge and Erin Crouch.

# Dedication

To my family who without there support nothing would have been possible and to my lovely daughter, this is the big paper I was working on for so very long.

# CHAPTER 1 - Fibroblast Growth Factors, an Introduction

Fibroblast growth factors (FGFs) are a diverse family of typically secreted, paracrine signaling molecules first isolated from pituitary extracts and characterized as potent mitogens for mouse fibroblast cells (Armelin, 1973). Since their initial discovery, FGFs have been found in a wide variety of multi-cellular organisms ranging from nematodes, which encode just two FGFs, to vertebrates, which encode 18 distinct FGFs and 4 FGF homologous factors (Beeken and Mohammadi, 2009; Birnbaum et. al., 2005; Ornitz and Itoh, 2000). While structurally similar, these FGFs are functionally diverse, playing roles ranging from pattern determination during embryonic development to homeostatic maintenance and metabolism in adults (Itoh, 2007; Kharitonenkov, 2009; Olsen et al. 2003). Interestingly, an increasing numbers of studies have linked mutations in the vertebrate *fgf* genes to serious health concerns including several aggressive forms of mammary and prostrate cancers, Parkinson's Disease, and the metabolic disorder autosomal dominant hypophosphataemic rickets (Gattineni and Baum, 2009; Itoh, 2007; Krejci, et.al., 2009). Because of the serious nature of these illnesses, determining how FGFs function, and perhaps more importantly, how these functions can be modulated has been under intense scrutiny in the research community.

## What Makes a Fibroblast Growth Factor a Fibroblast Growth Factor?

There are approximately 300 distinct protein sequences identified by homology as fibroblast growth factors in the National Center of Biotechnology Information database (Altschul et. al, 1990). Most of these sequences were collected from a diverse array of multi-cellular organisms including species of chordates, arthropods, and nematodes with the majority of them having been characterized to various extents according to their expression pattern, structure, and cellular function. In addition to these somewhat well characterized FGFs, several hypothetical proteins with weak structural similarity to the vertebrate basic fibroblast growth factor have also been identified in various plants and fungi species, but these have yet to be functionally characterized and none of these species appear to encode a corresponding fibroblast growth factor receptor (FGFR). Outside of these multi-cellular organisms, proteins similar in sequence to fibroblast growth factors have not currently been identified, however orthologs to vertebrate FGFs have been discovered in virtually all the genome sequences of the Baculovirus family of

arthropod-infecting viruses, opening up interesting speculation as to their function and potential roles during virus infection.

### *Nomenclature and Classification of Fibroblast Growth Factors*

The first attempt to classify this particular class of proteins was based on the biochemical characteristics of two proteins isolated from bovine pituitary extracts which had previously been shown to induce cell proliferation in mouse embryonic 3T3 cells (Gospardowicz et. al., 1982; Gambrini and Armelin, 1981). The first of these proteins, which was resistant to both urea and β-mercaptoethanol treatment, was called the 'acidic' fibroblast growth factor because it had an isoelectric point of 4. The second purified FGF protein, with an isoelectric point above 8, was termed the 'basic' FGF. Aside from these differences in isoelectric point attributable to overall amino acid composition, the 'acidic' and 'basic' FGFs had remarkably similar functions in these early assays and were capable of stimulating cell proliferation at concentrations as low as 10 ng/mL (Gambrini and Armelin, 1981; Holley and Kiernan, 1974).

The discovery of multiple and distinct FGFs in vertebrates, with a wide range of isoelectric points, made the initial classification of fibroblast growth factors as basic or acidic to be largely moot. In its place, attempts to classify vertebrate FGFs by their specific cellular function were made, but this quickly proved impossible when it was realized the diverse number of roles that FGFs play during development and homeostatic maintenance (Goldfarb, 2005; Itoh, 2007). The discovery of fibroblast growth factor orthologs in arthropod, nematode, and baculovirus species further complicated FGF classification since these factors are somewhat divergent from their vertebrate counterparts in both sequence and function. *Drosophila's* Branchless protein, for example, with an overall size of 770 amino acids (84 kilodaltons) is approximately two times larger than the largest known vertebrate FGF and fulfills multiple functions throughout the fly's life cycle. A careful analysis of the Branchless amino acid sequence, however, shows it still retains a core element of ~120 amino acids which is markedly well conserved ( ~23%) with the vertebrate counterparts. Functional studies have further cemented its identification as a vertebrate fibroblast growth factor homolog since it has been shown Branchless works as a signal ligand binding to a tyrosine kinase receptor, Breathless, similar in structure to vertebrate FGF receptors (Glazer and Shilo, 1991; Sutherland et.al., 1996).

Because of the diversity seen here, the current acceptable classification of fibroblast growth factors is based on two separate criteria— sequence homology of the FGF core region

and the ability to stimulate a tyrosine kinase receptor (Goldfarb, 2005). Based on these conditions, there are 18 recognized vertebrate FGFs organized into six subfamilies by sequence: FGFs 1 (acidic) and 2 (basic) comprise one subfamily, FGF 3, 7, 10 and 22 another; FGFs 4, 5, and 6 a third subfamily; FGFS 8, 17, and 18 a fourth subfamily; 9, 16 and 20 a fifth subfamily; and FGFs 19 (FGF 15 is the mouse homolog), 21, and 23 a sixth subfamily (Coulier et. al., 1997; Ornitz and Itoh, 2004). FGFs 11 through 14 were initially classified as functional vertebrate growth factors, but subsequent studies have shown they were incapable of stimulating any of the known FGF receptors and have been reclassified as FGF homologous factors (Goldfarb, 2005; Olsen et. al., 2003). In addition to these 18 vertebrate FGFs, there are approximately 50 additional potential FGF orthologs identified in arthropod, nematode, and baculovirus species, but only a handful of these proteins have been functionally characterized and shown to work through stimulation of a tyrosine kinase receptor.

## The Structure-Function Relationship in FGF Signaling

The first crystal structures to be reported for vertebrate fibroblast growth factors were for the prototypical acidic and basic FGFs (Eriksson et. al., 1991; Zhang et. al, 1991; Zhu et. al., 1991). Each showed a characteristic tertiary folding of the core domain similar to the closed beta barrel formation described initially from the crystal structures of the two cytokines; interleukin 1α and interleukin 1β (Murzina et.al, 1992). This closed beta barrel, or β-trefoil structure, consists of twelve antiparallel β strands arranged into three distinct sheets of four strands each. Subsequent crystal structures of FGFs 4, 7, 8, 9, 14, and 19 showed similar core domain architectures; however there were several important differences Bellosta et. al., 2001; Harmer et al., 2004; Olsen et. al., 2003; Olsen et. al., 2006; Osslund et. al., 1998; Plotnikov et. al., 2001).

### *The FGF Heparin Binding Site*

One of the differences identified by comparing the various FGF crystal structures was how they interacted with extracellular heparan sulfate proteoglycans (HSPGs). These proteoglycans are remarkably abundant throughout nature and can be found on virtually every mammalian cell, but they are far from uniform. In fact, HSPGs can be organized into three broad classifications based on how their core proteins interact with the cell surface: glycosyl-phosphatidylinositol (GPI) anchored HSPGs (glypicans), transmembrane anchored HSPGs (syndecans), or secreted HSPGs (perlecan or agrin). Aside from their attachment differences, each of these proteins are heavily post-translationally modified beginning in the endoplasmic

reticulum where a short linker sequence is attached to specific SGD tripeptide binding sites (Costell et. al., 1997; Noonan et. al. 1991). Once the linker sequence is attached to the protein core, chain elongation begins in the Golgi with alternate glucuronic acid (GlcA) and N-acetylglucosamine (GlcNAc) being attached by their respective gluco-transferases. Chains constructed in this manner are of widely varying lengths which is illustrated by a visualization study of HSPGs from basement membranes which showed 38% variation in length with a mean average length of 143 +/- 53 nm (Laurie et. al., 1988). Once the sugar chains are covalently attached to the core protein, they can undergo modification as well via the action of a number of cell-specific enzymes. These modifications may include deacetylation and N-sulphation of GlcNAc, epimerisation of GlcA to iduronic acid (IdoA), and O-sulphation at the 2, 3 or 6 position of the disaccharides (Prydz and Dalen, 2000). The variable ratio of these modification enzymes, as well as the abundance of the sulfate donor group, 3'-phosphoadenosine-5'-phosphosulfate, lead to complex sulfation patterns which are tissue- and in some cases cell-specific (Carlson et. al., 2008).

The foundation for the interaction of FGFs with HSPGs was initially established before crystal structure analysis with work involving the culturing of human endothelial cells. It was demonstrated that the addition of heparin (highly sulfated repeating disaccharides similar to heparan sulfate, although the sulfation pattern is much greater yielding a very high net negative charge to mass ratio) to the culture medium, and not other negatively charged substrates such as chondroitin sulfate, dramatically increased cell proliferation even when very low concentrations of growth factors were present (Thornton et. al., 1983). Subsequent work showed that the addition of exogenous heparin not only affected the mitogenic activity of acidic FGF specifically, but that the nature of the heparin-FGF binding relationship could be exploited to prepare crude FGF-containing preparations from bovine extracts in a single two-step process (Shing et.al., 1984; Thomas et. al., 1985). Even with this early work indicating the importance of heparin in FGF signalling, it was clear that not all FGFs interacted with heparin in an identical manner. Both basic FGF and acidic FGF, for example, could be purified using a heparin-Sepharose column but basic FGF had a much higher affinity to heparin compared to acidic FGF (Shing et. al., 1985). In addition, basic FGFs mitogenic activity was largely unresponsive to the addition of exogenous heparin in endothelial cell cultures while acidic FGF required exogenous heparin to stimulate cell proliferation to basic FGF levels (Gimenez-Gallego et. al., 1986).

The differential binding and responsiveness to exogenous heparin of the two prototypical FGFs led researchers to question the role endogenous HSPG plays in FGF signaling. Early work showed secreted FGF bound to extracellular matrix (EM) HSPGs upon exocytosis, independent of the presence of FGF-specific receptors, thus forming a readily-releasable pool of signal factors (Vlodavsky et. al., 1987). Later work showed FGF-heparin complexes were protected from proteolytic degradation by plasmin, but this protection could be reversed if the cells were treated with heparinase prior to plasmin treatment (Saksela et. al., 1988). In addition, researchers were also able to independently demonstrate the role of heparin in FGF-specific signal transduction by using cells deficient in their ability to form endogenous HSPG or pre-treating cells to remove HSPGs. In either case, FGFs could not bind to or stimulate a FGF-specific receptor or trigger cell proliferation (Rapraeger et. al., 1991; Yayon et. al., 1991). This led to the hypothesis that HSPGs were acting as low affinity FGF receptors and were essential for FGF signaling (Moy et. al., 1997). As an extension of this hypothesis, researchers were also able to demonstrate that FGF signaling, at least in part, could be controlled by altering the sulfation pattern of HSPGs (Allen et. al., 2001; Pye et. al., 2000, Zhang et al., 2009).

The emergence of other vertebrate FGFs and their similar requirements for HSPG, as well as the discovery of the first non-vertebrate FGF, Drosophila's ortholog Branchless, bolstered this hypothesis; however it was still unclear how FGFs physically interacted with the negatively charged heparan sulfate (Lin et. al., 1999; Sutherland et. al., 1996). Crystal structures of the acidic and basic FGFs in the presence of heparin were able to show that several discontinuous, positively-charged amino acid residues, Lys-26, Arg-44, Lys-119, Arg-120, Lys-125, Lys-129, and Lys-135 on basic FGF and Asn-18, Lys-113, and Lys-118 on acidic FGF, were displayed on the protein surface most prominently in the third sheet of the β-trefoil domain and entered into extensive hydrogen bond networks with heparin (Eriksson et.al., 1991; Zhang et. al, 1991; Zhu et. al., 1991). Deletion of this portion of the β-trefoil domain from basic FGF severely reduced the ability of the protein to bind heparin-Sepharose, but did not appear to affect receptor affinity in BALB/c3T3 cells (Seno et. al., 1990). A biochemical analysis using site-directed mutations of basic FGF showed that in addition to the residues initially identified in the crystal structure analysis, Asn-27, Arg-81, Thr-121, Gln-123 and Gln-134, also contributed significantly to heparin binding *in vitro* (Thompson et. al., 1994). The identification of these four polar, neutral amino acids involved in heparin binding suggests that in addition to electrostatic

interactions, there are important non-ionic interactions that help to stabilize heparin-FGF complexes perhaps explaining the exclusion of other negatively charged substrates such as chondroitin sulfate as binding partners. The divergence in sequence of this core region, among the paracrine-acting FGFs at least, also helps to explain their differing affinities for both FGF receptor isotypes and differentially sulfated HSPGs (Guilmond and Turnbull, 1999; Moy et. al., 1997; Plotnikov et. al., 1999; Venkataraman et. al., 1999).

The discovery of a group of autocrine-acting FGFs (FGF 19, FGF 21 and FGF 23) further illustrated the importance of these amino acid residues in binding HSPGs. Each of these FGF subfamily members can interact with heparin although with a significantly lower affinity compared to the paracrine-acting FGFs (Goetz et. al., 2007; Harmer et. al., 2004). The lower binding affinity allows for these FGFs to migrate away from their primary areas of production, intestinal epithelial cells, hepatocytes or bone osteocytes, to interact with FGF receptors expressed on distant tissues (Kurosu and Kuro-o, 2009). Because of their autocrine-like nature and low affinity for HSPGs, these FGFs also require a tissue specific co-receptor to stimulate an appropriate FGF receptor. For FGFs 19, 21 and 23, this co-receptor has been identified as β-Klotho, a single-pass; transmembrane protein expressed primarily in liver, kidney and mature adipocytes cells (Kurosu et. al., 2006; Ogawa et. al., 2007; Wu et. al., 2007). Comparison of the crystal structures of FGF 19 and FGF 23 with paracrine-acting FGFs, notably FGF 4, have shown the core architecture is largely intact, although there is a significant remodeling of the third β-sheet (β10 through β12 loops) with the β11 strand adopting a helical conformation and distorting the β-trefoil at the c-terminus end (Goetz et. al., 2007; Harmer et. al., 2004). In paracrine-acting FGFs, this area is essential for the specificity of HSPG binding and overall stabilization of the specific FGF-FGF receptor complexes; although in autocrine-acting FGFs this region may help to stabilize the interaction of the C terminus with β-Klotho (Mohammadi et. al., 2005).

### *The FGF Receptor*

Another difference identified from comparing structures of the various FGFs involved their respective FGF receptor binding domains. Before we can begin this discussion however, we first need to understand the key characteristics of this class of receptors. All of the vertebrate fibroblast growth factors studied to date, with the exception of the FGF homologous factors (FGFs 11-14); interact with at least one of four distinct classes of tyrosine kinase receptor

molecules. Each of these fibroblast growth factor receptors (FGFRs 1-4) exist as monomers and are composed of three basic elements: an extra-cellular FGF binding domain, a trans-membrane domain, and a cellular tyrosine kinase domain (Coulier et.al., 1997; Jaye et. al., 1992; Mohammadi et.al., 2005). Sequence analysis of the full length products show these receptors are highly conserved with sequence identities between 55 and 72% at the protein level (Johnson and Williams, 1993; Itoh and Ornitz, 2004). The greatest diversion in sequence among the receptors occurs in the extra-cellular domain which gives each class certain structurally identifying characteristics as well as differing affinities for each of the FGF signal ligands. Still, even with this diversity, a major question arises on how signal specificity can occur given a large number of signal ligands and a small number of cognizant receptors.

To answer this question, research has focused on the first tyrosine kinase receptor identified as the interacting partner of an FGF signal ligand: FGFR-1. FGFR-1 is considered the prototypical FGF receptor, having first been identified as a binding partner with basic FGF during a chemical cross-linking study involving baby hamster kidney cells (Neufeld and Gospodarowicz, 1985). The sequence for this receptor was deduced during a subsequent screen of phosphorylated tyrosine kinases from a cDNA library constructed from mRNA of chicken embryos and from humans in a screen of a cDNA library derived from human placenta and umbilical vein endothelial cells (Johnson et. al, 1990; Pasquale and Singer, 1989). Since this initial work however, FGFR-1 has been shown to bind nearly all secreted forms of FGFs although with markedly differing affinities (Groth and Lardelli, 2002; Zhang et. al., 2006).

Structural analysis of human FGFR-1 has shown that the full length receptor (FGFR1-IIIc) is composed of an extracellular domain, amino acids 40-359, formed into three immunoglobulin-like loops labeled D1-D3 (Groth and Lardelli, 2002; Kiselyov et. al., 2006). Each of these loops is separated by a short 10-12 amino acid linker sequence; however the linker sequence between D1 and D2 is somewhat longer and contains seven consecutive glutamic acid residues forming an “acid box” which is critical for binding to cell adhesion molecules such as N-cadherin and preventing heparin sulfate from binding to the receptor in the absence of FGF (Groth and Lardelli, 2002; Olsen et. al., 2004; Sanchez-Heras et. al., 2004). The intermediate transmembrane domain, amino acids 377-462, is well conserved among FGFRs and anchors the receptor to the cell membrane. Its α-helical arrangement allows for effective dimerization of receptors upon stimulation (Weng et. al., 2008). This dimerization is thought to be essential for

receptor signaling because it allows for close association and subsequent trans-phosphorylation of the intracellular domain. With human FGFR-1, this intracellular domain, amino acids 462-822, is composed of 2 consensus tyrosine kinase domains separated by a short linker sequence (Johnson and Williams, 1993; Groth and Lardelli, 2002). Mutational analysis has shown that there are six auto-phosphorylation sites within the two FGFR-1 kinase domains (Y-463, Y-583, Y-585, Y-653, Y-654, Y-730) and one just outside of the terminal kinase domain (Y-766) which are instrumental for growth factor induced signaling either through the Ras/mitogen activated protein kinase (Ras/MAPK) pathway or the phospholipase Cγ (PLCγ) pathway. Interestingly, of the seven auto-phosphorylation sites, only two (Y-653 and Y-654) are conserved among the other three FGFR classes and are considered essential for *in vivo* phosphorylation for intracellular substrates (Mohammadi et. al., 1996).

In addition to full-length FGFR-1, there are also twelve known receptor isoforms corresponding to alternative splice products identified from human, mouse, frog and fish sources (Groth and Lardelli, 2002). The human *fgfr-1*, for example, is organized into seventeen exons which encode the full length FGFR-1-IIIc (described previously) as well as two other additional receptor isoforms arising from alternative splicing. One of these isoforms, FGFR1-IIIb, is a structurally similar to the full-length receptor but lacks the D3 loop of the Ig-like domain due to exon skipping (Johnson et. al., 1991). The lack of the D3 loop dramatically alters the affinity of the two isoforms for certain specific FGFs with FGFR-1-IIIc preferentially binding to FGF-2,-4,-6, and -9 while FGFR-1-IIIB binds preferentially to FGF-3, -7, and -10 (Beer et. al., 2000; Mathieu et. al., 1995; Miki et.al. 1992; Mohammadi et. al., 1996; Ornitz et. al., 1996). In addition to preferential binding of FGFs, the two FGFR-1 isoforms also appear to be expressed differentially in tissues with FGFR-1-IIIc being produced primarily in the epidermis, brain, kidney, lung, liver and adipocytes while the truncated form is expressed preferentially in the brain, pancreas, epidermis, skeletal muscle, testis, and intestine (Beer et. al. 1999; Liu et.al. 2007).

Furthering increasing the complexity of this receptor type, the third human isoform, FGFR-1-IIIa, is a truncated product lacking both the D3 loop as well as the transmembrane and intracellular kinase domain (Johnson et al. 1990; Johnson et. al., 1991). This soluble form of the receptor binds to both acidic and basic FGFs, although its affinity for the basic FGF ligand is greater than 10 fold higher than for the acidic ligand (Duan et. al., 1992). FGFR-1-IIIa has been

detected in blood and retinal fluid and is thought to be an inhibitor of normal FGF signaling, specifically basic FGF, by acting as a sink for the ligand preventing it from binding to membrane associated FGFR-1 which may help to regulate errant FGF signaling *in vivo* (Guillonneau et. al., 1998; Guillonneau et. al., 2000; Hanneken et.al., 1994).

A quick review of the other three FGFR classes show much of the same variation as FGFR-1 including multiple isoforms and localized, tissue specific expression. The two predominant human FGFR-2 isoforms, for example, develop from alternative splicing of exons eight and nine resulting in a full-length receptor (FGFR2-IIIc) and one missing part of the D3 loop (FGFR2-IIIb). FGRF2-IIIc appears to be preferentially expressed in epithelial cells and binds FGF-1, FGF-2, FGF-4, FGF-6, FGF-9, FGF-16 and FGF-20. Conversely, FGFR2-IIIb is predominantly expressed in smooth muscle, bone and kidney tissue and tightly binds FGF-1, FGF-3, FGF-7, FGF-10 and FGF-22 (Dell and Williams, 1992; Ornitz et. al., 1996; Zhang et. al., 2006). Similarly, FGFR3 has three isoforms as well; a full-length FGFR3-IIIc, a smaller FGFR3-IIIb variant, and a soluble variant FGFR3-IIIS lacking both the transmembrane and kinase domains. Each of these appear to be differentially expressed in various tissues and have differing affinities similar to FGFR1 and FGFR2 variants (Ornitz et. al., 1996) Interestingly, FGFR4 has only two isoforms; a full-length variant FGFR4 and a soluble variant, sFGFR4, lacking the transmembrane and kinase domains (Ornitz et. al., 1996; Shigeo et. al., 2000).

### *The FGF Receptor Binding Site*

With an understanding of the basics of FGFR structure, we can now turn our attention back to the initial question of what structural features are present on FGFs that allow them to interact with and stimulate target receptors. The first rudimentary structural analysis of an FGF binding to a target receptor was done with basic FGF modeled onto the extracellular fragment of FGFR1 lacking the D1 domain (Plotnikov et. al., 1999). As mentioned previously, the D2 and D3 domains of FGFR1 have been shown to be critical for FGF mediated signaling, while D1 is considered non-essential.

The primary interaction between the receptor's D2 domain and the ligand was mostly derived from hydrophobic interactions between discontinuous residues spaced throughout the beta-trefoil domain and several well conserved hydrophobic residues of the receptor. A sequence alignment of human FGFs shows that these discontinuous residues essential for binding for FGF-2 are not well conserved with the exception of two tyrosine residues (Tyr-24 and Tyr-103) and a

leucine residue (Leu-140) which are present in all FGFs known to interact with FGFR1 (Mohammadi et. al., 2005a). In addition to the hydrophobic interaction with D2, a tyrosine residue (Tyr-33) within FGF-2 engages in hydrogen bond formation with the receptor (Leu-165) which helps to orient the D2 domain to maximize the hydrophobic interactions. A sequence alignment of the human FGFs shows that only three FGFs (FGFs 7, 10, and 22) lack this tyrosine residue which may help to explain itheir lower affinity with respect to FGFR1 (Yeh et al., 2003).

Interaction of FGF-2 with the linker sequence between D2 and D3 also requires hydrogen bond formation with three invariant bonds being formed. Two of these are formed between the amide side chain of an asparagine residue (Asn-104) interacting directly with a highly conserved arginine residue (Arg-250) of the linker region. A third bond is formed between this same residue and the backbone carbonyl oxygen residue (Plotnikov et. al., 1999). The formation of these hydrogen bonds appears to be very important considering all FGFs have residues capable of forming 3 hydrogen bonds with the FGFR1 linker sequence with the exception of the four FGF homologous factors. In place of asparagine, these FGFs encode a non-polar valine residue which is incapable of hydrogen bond formation. This single amino acid change appears to be one of the reasons why these factors cannot stimulate any of the know isoforms of FGFRs (Mohammadi et. al., 2005a).

While the interaction between FGF-2 and the D2 domain appears to be quite flexible in nature, the opposite is true for its interaction with D3 of FGFR-1. This is due to the extensive hydrogen bond formation that occurs between four discontinuous residues of the ligand with the receptor. The rigid structural nature of this interface allows for a more traditional “lock and key” interaction between the FGFR and the cleft formed at the base of the FGF beta trefoil “barrel” (Plotnikov et. al., 1999). A sequence analysis shows that three of the four residues involved in the hydrogen bond formation are variable, however a glutamic acid residue (Glu-96) involved in hydrogen bond formation with an invariant glutamine residue (Gln-285) of D3 is highly conserved among FGFs (Mohammadi et. al., 2005a). The importance of this residue is further illustrated by an early work which showed when Glu-96 of FGF-2 was replaced with a non-polar alanine residue; there was a subsequent 1600-fold loss of binding affinity to FGFR-1. Subsequent replacement of Glu-96 with the polar residue glutamine ameliorated this loss of binding significantly with only a 10-fold reduction in binding affinity compared to wildtype (Zhu et.al., 1995).

Subsequent comparisons of models including FGF-2 complexed with FGFR-2, as well as FGF-10 complexed with FGFR2-IIIb, have shown many of the same interactions seen with FGF-2 and FGFR-1 (Plotnikov et. al., 2000; Yeh et. al., 2003). Interestingly, the models suggest the interaction between FGF and D3 domain of the FGFR is one of the key determinants for ligand-receptor specificity despite the fact that several prominent isoforms of FGFRs lack the full-length D3 domain. This is due to the interplay of the variable regions of FGFR which, along with the various residues of the FGF core domain including Glu-96, help to establish the hydrophobic network which facilitate the lock and key binding of the ligand to specific receptors. The limited number of models however, makes any conclusions highly speculative at this time.

## Putting It All Together: FGF Signaling in Brief

Fibroblast growth factor signaling typically begins with the secretion of mature growth factors to the extracellular matrix. To accomplish this, most *fgf*s encode a bipartite signal sequence which targets the nascent protein to the endoplasmic reticulum-Golgi transport pathways for efficient secretion (Coulier et. al., 1997). As in most cases, however, there are several important exceptions found among the various FGF homologs. For example, vertebrate FGFs 9, 16, and 20 all lack definable signal sequences but are still efficiently secreted utilizing the endoplasmic reticulum-Golgi transport pathways (Jeffers et.al., 2001; Miyakawa and Imamura, 2003; Revest et.al., 2000). In addition, both the prototypical vertebrate FGFs-1 (acidic FGF) and 2 (basic FGF) have a nuclear localization sequence instead of a bipartite signal sequence but are still exported to the extracellular matrix under certain conditions with the aid of cellular cargo proteins (Nickel, 2004; Prudovsky et. al., 2003; Schäfer et. al., 2004).

Independent of how they are secreted, all FGFs bind to exogenous heparin with near equal affinity (Harmer, 2006; Ornitz, 2000). Structurally, this is accomplished through hydrogen bond formation between basic amino acid residues, primarily lysine and arginine, on the protein surface and the negatively charged sulfate groups on the glycan chains (Baird et.al., 1988; Nagendra et.al, 2001; Pellegrini et.al., 2000). The secretion and binding of FGFs to HSPGs on the cell surface, besides providing a rapidly-releasable pool of paracrine signaling molecules, also provides an additional level of signal complexity to the stimulation of FGF receptors. This is accomplished due to the subtle differences in sulfation patterns of the sugar side chains which preferentially interact with not only the FGFs but also with the D3 domains of certain FGFR isoforms.

Once localized to the extracellular matrix, FGF signaling complexes are biologically inactive unless they are released from the cell surface. In mammalian systems, this is accomplished through either enzymatic cleavage of the HSPG-FGF complex through the actions of either cellular heparanase or matrix metalloprotease or the activity of the fibroblast growth factor-binding protein (Ardi et. al., 2009; Matzner et. al., 1985; Vlodavsky et. al., 1990; Wu et. al., 1991). Once released, the biologically active complex can interact with nearby cells expressing specialized FGF receptors (Supplementary Figure 1). Specific interactions between the FGF- HSPG signaling complexes and the various FGFR isoforms are determined by several factors including the spatial arrangement of several highly conserved residues within both the FGF beta trefoil domains and the invariant D2/D3 loops of the FGFRs as well as interactions with the receptor and the variably sulfated HSPGs. The role of the HSPG here is essential for signaling because it allows for the localization of multiple FGFs in a finite space, as well as helping to mediate the homo-dimerization of two FGFRs which begins the essential phosphorylation cascade.

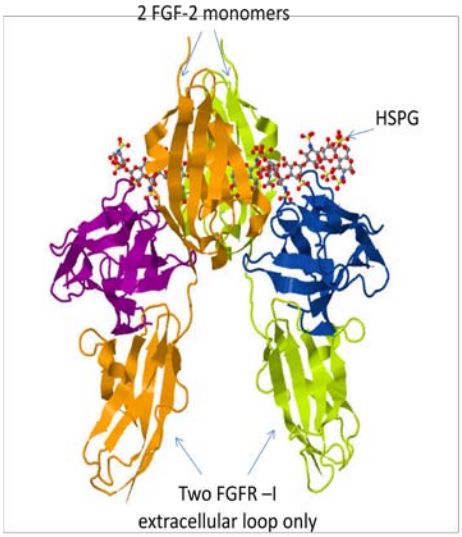


**Supplementary Figure 1**: Crystal structure (PDB code: 1FQ9) of two FGF-2 monomers complexed with HSPG and two monomers of the FGFR-1 receptor, extracellular loop only. Binding to HSPG is essential for the binding and dimerization of the cognizant receptors and is mediated by a number of positively charged amino acid residues spaced along the surface of the FGF. Binding to the receptor is mediated by interaction between the D2/3 domains of the FGFR and certain residues of the FGF. Differences in the amino acid profile responsible for interacting with the FGFR confer specificity to certain receptors.

# CHAPTER 2 - FGFs in Action, the Insect Model

The complexity of the mammalian FGF signaling systems, as well as their redundancy in certain biological processes, made, at least early on, the *in vivo* study of FGFs very difficult even within the well established mouse and zebrafish model systems. Further compounding the problem was the lack of any potential FGF-like signal ligands in the single-celled bacterial and yeast models. Thankfully for the field, the discovery of a limited number of potential FGF homologs in *Drosophila melanogaster* seemed tailor-made for researchers to be able to study basic FGF functions in detail, which could then be potentially translated into the more complex signaling systems seen in mammals. The first step in this process, however, was to prove that the insect proteins were indeed FGF homologs.

## The Discovery of Branchless

Like most good scientific discoveries, the finding of a fibroblast growth factor homolog in *D. melanogaster* was precipitated by careful observation and a bit of luck. It was known, prior to the isolation of the *Drosophila* FGF homolog (dFGF) that there was at least one tyrosine kinase receptor present with enough sequence identity to be considered a potential FGFR (Glazer and Shiloh, 1991; Shishido et. al., 1993). This receptor was found through a low stringency hybridization screen using the mouse FGFR-1 sequence as a probe. Only a partial sequence was isolated, however, but it predicted a protein structurally comparable to mammalian FGFRs with an extracellular Ig-like domain along with its corresponding acidic box, a transmembrane region and two distinct intercellular kinase domains. Using embryos at different developmental stages, it was also demonstrated that expression of this gene was limited primarily to terminal tracheal cells, midline glial cells of the endoderm, and to cells surrounding the wing and genital imaginal discs. Furthermore, embryos lacking both copies of this gene showed the formation of tracheal pits but lacked any significant branching (Glazer and Shiloh, 1991).

Subsequent work was able to isolate the full-length mRNA of this potential insect FGFR and somewhat surprisingly it encoded not the typical two or three Ig-like loops found in the typical mammalian extracellular domains, but five discernible Ig-loops. In addition, there did not appear to be any splice variants present in their screen which were seen with the mammalian FGFRs. Loss of function mutations of this dFGFR were embryonic lethal with embryos failing to develop main tracheal branches from the six progenitor tracheal pits. In addition to the tracheal

defects, midline glial cells, which also normally express high levels of the FGFR, did not migrate from their anterior starting point to the posterior side of the developing embryo in the mutant dFGFR-1 strains (Klämbt et.al., 1992). Because of the loss of branching observed in the trachea of the dFGFR mutants, the dFGFR-1 gene was given the name *breathless (btl*) and work was focused on how *btl* activation was able to coordinate tracheal branching and glial cell migration.

The first line of evidence to determine how the *Drosophila* FGFR was functioning was done by examining embryos expressing either a dominant negative allele of *btl* or ones expressing a constitutively active form of *btl*. In embryos expressing the dominant negative form, the phenotype was less severe than the complete loss of function *btl* mutants with the six primary tracheal branches forming from the tracheal progenitor cells, but then failing to develop any secondary or tertiary tracheal branching. Secondary and tertiary branches could be marginally restored in the presence of the dominant negative form of Breathless by co-expressing a constitutively active form of Ras. This restoration suggested the activation of the *Drosophila* FGF receptor utilized the downstream Ras/MAPK pathway in the same manner as its mammalian counterparts (Reichman-Fried et. al., 1994).

Interestingly, in the embryos expressing the constitutively active form of *btl*, there was also a loss of main branch formation similar to the effect of expressing the dominant negative form of *btl*. If the main tracheal branches were allowed to form prior to the expression of the constituitively active form of *btl*, however, there was a hyper-formation of secondary and terminal tracheal branches well beyond what is typically seen in developing embryos (Lee. et al., 1996). Taken together, this data showed that the function of this growth factor pathway was to direct tracheal main tracheal branch formation early in embryogenesis and then direct secondary and tertiary tracheal cell migration at later stages. Furthermore, because the number of progenitor tracheal cells remained constant even with expression of the constituitively active form of *breathless*, it did not appear that tracheal cell proliferation was under FGF control.

To answer the question of what was acting as a stimulant for dFGFR activation, researchers began looking for potential receptor ligands by inducing genome mutations in *Drosophila* and then screening progeny embryos for the loss-of-function *breathless* mutant phenotype. The results of this screen identified a potential gene target which was appropriately named *branchless* (*Bnl*) due to the complete loss of normal tracheal development. The predicted Branchless protein, based on the nucleotide sequence, was 770 residues in length with a

molecular mass of 84 kilodaltons, significantly larger than any known mammalian FGF. The expression profile of *Bnl* showed that it was expressed as early as 1.5 hours into embryonic development, peaked between 5-11 hours, and then dissipated until it was undetectable at 16 hours post fertilization. In situ-hybridization of embryos at different stages showed high levels of gene expression in the cells surrounding the tracheal pits where branch points form during development. A closer examination showed most of the epidermal cells expressing this protein were in direct contact with tracheal cells, and that protein expression pre-dated tracheal branch formation in every instance. In several cases however, the *branchless*-expressing epidermal cells were separated from the nearby *btl*-expressing tracheal cells by short distances suggesting that the ligand was secreted and could also act in a gradient-like manner to induce branching (Sutherland et. al., 1996).

The two striking conclusions based on this early work were the relative size of this potential FGF ligand in *Drosophila,* at least compared to known mammalian FGFs, and the possible gradient-like manner it could induce motility. A homology search using the *bnl* nucleotide sequence showed there was ~400 nucleotide segment stretching through the middle of *bnl* which corresponded to a beta-trefoil coding sequence similar to the one seen with mammalian FGFs. In addition to having a similar internal domain, the nucleotide sequence also revealed a clearly defined bipartite signal sequence suggesting that Bnl is a secreted protein similar to most mammalian FGFs which is vital for any paracrine-like signal ligand. At the protein level, an alignment of just the Branchless core domain with the core domains of the prototypical mammalian basic and acidic FGFs showed between 31 and 37% sequence identity respectively (Sutherland et. al., 1996).

### *The Role of HSPGs in Branchless-mediated Signaling*

Still, with large undefined N- and C-terminal domains, it was not clear whether Branchless was a classical FGF or a multi-function chimeric protein which happened to have a segment that was structurally similar to mammalian FGFs. One potential way to differentiate between these possibilities was to see if Branchless utilized heparan sulfate comparable to mammalian FGFs. To assess the role of heparan sulfate in Branchless-mediated signaling, researchers used two established fly lines, each with a mutation which inhibits the normal formation of HSPGs. One of these mutations, called *sugarless,* prevents UDP-D-glucose dehydrogenase function and results in a complete lack of glucuronic acid, a key intermediate to

the formation of not only heparan sulfate but also chondroitin sulfate and dermatan sulfate (Häcker et. al., 1997). The second mutation, called *sulfateless*, lacks a functional N-deacetylase/N-sulfotransferase. In this mutant, heparan side chains form but lack normal 2-O and 6-O sulfation patterns (Lin and Perrimon, 1999). Embryos, with loss-of-function mutations in either *sugarless* or *sulfateless*, were examined for deficiencies in tracheal branch formation similar to those seen in *btl* and *bnl* mutants. In both cases, there appeared to be a severe loss of tracheal branch formation similar to, but not quite as severe as, that observed with either deletions of *Bnl* or *Btl* (Lin et. al., 1999). Thus, with a βeta-trefoil domain core structure and reliance on negatively charged heparan sulfate proteoglycans for activity, even with the large undefined N- and C-terminal regions, Branchless appeared to be a *bona fide* member of the FGF family.

Having already established the role of heparan sulfate in Branchless-mediated signaling, the next step was to determine first if a single type of HSPG was involved and second if the sulfation patterns of the heparan affected signaling. Fortunately, in *Drosophila*, there are only four genes which have been identified as encoding distinct heparan sulfate proteoglycans: two encode glycipans, one a perlecan and the fourth a syndecan (Perrimon and Bernfield, 2000). One of the genes encoding a glycipan was discovered in a screen for cell patterning and division defects in *Drosophila's* neural development and was called *division abnormally delayed*, or *Dally* (Nakato et.al., 1995). The other glycipan gene, *Dally-like (Dlp)*, was discovered in a screen of Wingless signaling mutants similar in nature to the screen that identified *sugarless* and *sulfateless* (Khare and Baumgartner, 2000). The other two HSPG genes, *dsyndecan* and *terribly reduced optic lobes (trol)*, were initially identified based on their sequence similarity to mammalian homologs and are the least characterized of *Drosophila*'s HSPGs (Friedrich et. al., 2000; Spring et. al., 1994). Of these four, only *Dally-like* appears to be involved with Branchless-mediated tracheal migration, but surprisingly, it does not need to be expressed in the epithelial cells producing Branchless but in the tracheal cells expressing the Breathless receptor (Yan and Lin, 2007). This suggests Dlp is acting as a low affinity receptor for secreted Branchless in the tracheal buds prior to the stimulation of Breathless and in part, explains how Branchless can act in a gradient-like manner to determine fine tracheal branching.

The next step was to determine if the discrete sulfation patterns of the heparan side chains of Dally-like affected Branchless-mediated signaling. In mammals, an examination of the

structural relationship between receptors and heparan side chains suggested the binding affinity of various FGFs to specific FGFRs could be altered by changing the sulfation patterns of the HSPGs (Chellaiah et. al., 1999; Mohammadi et. al., 2005b; Pye et. al., 2000; Sanderson et. al., 2005). To study the role of differential sulfation on the activity of Branchless, two mutant fly lines were created which deleted either one or both of the predominant sulpho-transferases in *Drosophila*. Single deletions of either the *HS 2-O sulfotransferase* (*Hs2st*) or *HS 6-O sulfotransferase* (*Hs6st*) genes did not appear to affect development and embryos survived through to adulthood. An examination of tracheal branching showed defects in 39% of the *Hs6st* mutant embryos, but only 9% of *Hs2st* mutants. These defects were significantly less severe than those seen with either the deletion of *breathless/branchless* or *sugarless/sulfateless* with the most obvious deficiency being small breaks in the main dorsal trunk (Kamimura et. al., 2006).

To try to explain the differences in phenotype between the *Hs2st/Hs6st* single mutants and the *sugarless/ sulfateless*-mutants, researchers next focused on the sulfation patterns of the HSPGs isolated from the adult flies. As expected, the HSPGs isolated in the *Hs2st* mutants completely lacked 2-O sulfation, but there was a concurrent increase in 6-O sulfation which restored the net negative charge of the HSPGs to 99.2% of wildtype levels. A similar increase in 2-O sulfation was also seen in the *Hs6st* mutant HSPGs suggesting that each of the enzymes could increase their activity in the absence of the other. To confirm the compensatory effect of the two enzymes, *Hs2st/Hs6st* double mutants were created but the effects of losing both primary sulpho-transferases proved to be embryonic lethal with a complete failure to develop tracheal branches. In addition, ectopic expression of the *Drosophila* dual sulphatase, *Sulf1*, resulted in an overall reduction of charge on HSPGs in adult flies and a significant loss of tracheal branching in embryos compared to that seen in the *Hs2st* or *Hs6st* single mutants (Kamimura et. al., 2006). Interestingly, the same compensatory effect with respect to increased 6-O sulfation patterns has been seen in HSPGs of *Hs2st*-deficient mice. The loss of the 2-O sulfation in mice does reduces HSPG binding affinity for both FGF-1 and FGF-2 *in vitro* by ~30%, but this reduction does not appear to significantly reduce FGF-mediated signaling *in vivo* (Merry et. al., 2000). Similarly, in *Xenopus* larvae, over-expression of *QSulf1*, a 6-O specific sulphatase, results in an overall reduction in HSPG charge and a concurrent reduction, but not complete loss of, FGFR-1/FGF-2-mediated signaling (Wang et. al., 2004). These results, taken together, suggest that the loss of single sulpho-transferases may be functionally compensated for in FGF-mediated signaling

through the activity of the other enzymes, but a complete loss of sulfation of HSPGs dramatically reduces the ability of FGFs such as Branchless to stimulate a cellular response.

### *Branchless-mediated Signaling Outside of Embryogenesis*

As discussed in the previous chapter, many of the mammalian FGFs have roles outside of embryogenesis, but it was unknown whether Branchless functioned outside of a very strict time frame (1.5 to 16 hours post fertilization) during early development (Sutherland et. al., 1996). Work by Sato and Kornberg, however was able to detect low levels of *branchless* expression in wing imaginal discs early during the third instar stage of pupae development. These discs are composed of four distinct cell types: squamous peripodial cells, columnar epithelial cells, adepithilial cells and stalk cells. The peripodial cells undergo a contraction during differentiation and give rise to tissues in the mesothorax of the adult fly while the columnar epithelial cells expand and give rise to the major wing structures such as the hinge, scutum and notum. The adepithilial cells develop into the flight muscles for the wing and make direct contact with other epidermal structures including the main tracheal branch. Stalk cells, which are lost during maturation, initially serve to hold imaginal disc in place during early development (reviewed by Maves and Schubiger, 1999). Expression of *bnl* appeared to be restricted to the columnar epithelial cells of the disc and gradually increased from early to late instar development. Expression of the *breathless* receptor was also detected in the tissues of the wing imaginal disc, although not in the columnar epithelial tissues or the surrounding peripodial cells, but in the adepithelial tissue directly adjacent to the main tracheal branch. These adepithelial cells remain distinct from trachea by not forming a luminal cuticle, the defining characteristic of traditional trachea, and instead develop into three adult air sac tracheoblasts (Sato and Kornberg, 2002).

The formation of the adult air sac tracheoblasts begins during third instar maturation when clusters of *btl*-expressing cells migrate from the area where the wing hinge forms first dorsally, then anteriorally until three distinct clusters form. The migration of these immature tracheoblasts in the wing disc is, at least in part, directed by columnar cells expressing *branchless*. Indeed, the expression of an inactive form of Branchless in the wing imaginal disc, or ectopic expression of *Bnl* in tissues surrounding the imaginal disc seriously perturbed the proper migration of the *Btl*-expressing adepithelial cells. Quite surprisingly however, expression of a dominant-negative form of *breathless* in the wing imaginal disc not only resulted in a loss of migration, but also a dramatic decrease in the overall number of adepithelial cells. Conversely,

expression of the constituitively active form of *breathless*, or ectopic expression of Breathless in the surrounding tissues, resulted in hyper-proliferation of these cells with the end result being the formation of additional air sacs tracheoblasts (Sato and Kornberg, 2002). This suggests that in the adult, Branchless/Breathless not only provides cues to direct proper cell migration, but also acts as a powerful mitogen directing cell proliferation.

In addition to the formation of adult tracheoblasts, Branchless-mediated signaling has also been linked to the proliferation and differentiation of adult neuroblast cells in the second instar developmental stage (Barrett et. al., 2008; Park et. al., 2003). The progenitor cells which form the adult neuroblast become quiescent during embryogenesis and only proliferate and mature during adulthood when levels of the signal ligand Sonic Hedgehog reach a certain threshold (reviewed by Datta, 1995). Work with mutant fly strains where *branchless* expression is perturbed in the neuroblast precursor cells has shown a dramatic decrease in Hedgehog levels and a lack of neuroblast maturation. Conversely, increasing the amount of Hedgehog in immature neuroblasts leads to a concurrent increase in Branchless, and hyper-proliferation of neuroblast cells suggesting that the formation of adult neuroblasts works through a positive feedback loop involving both *branchless* and *hedgehog* expression (Barrett et. al., 2008). Interestingly, neuroblast proliferation is greatly decreased when the perlecan-encoding *trol* gene is mutated although it is still unclear whether Branchless or Sonic Hedgehog utilize this type of HSPG for signaling (Lindner et. al., 2007; Park et. al., 2003; Voight et. al., 2002).

Lastly, Branchless-mediated signaling has also been implicated in the formation of the male reproductive organ in adult flies. The precursor cells for the male and female sex organs are found primarily in the genital imaginal disc and are formed from cells originating in four contiguous abdominal segments (AS). The cells of AS-8 give rise to the female genital primordium, while AS-9 gives rise to the male genital primordium. Cells of the imaginal disc from AS-10 and AS-11 give rise to male- or female-specific analia (reviewed in Sánchez and Guerrero, 2001). Some cells which develop into the male organ, however, are not part of the imaginal disc but part of the surrounding mesoderm. These cells migrate to the imaginal disc filling a space between the anterior and posterior portions during the second and third instar stages and form a novel intermediate structure. The migrating cells were shown to be expressing *breathless*, and were migrating in response to *branchless* expression from cells of AS-9 lineage. Upon contact with the imaginal disc, the *breathless* expressing cells underwent an

uncharacteristic differentiation pattern to become epithelial-like forming the paragonia and vas deferens structures of the male reproductive organ. In female flies, *branchless*-expression is directly repressed by Dsx-F, which prevents the migration of mesodermal cells to the imaginal disc. Indeed, ectopic expression of *branchless* in the AS-8 primordium of female flies results in reproductive organs developing multiple male paragonia, an observation first noted by Hildreth in his observation of *dsx* mutant flies (Ahmad and Baker, 2002).

### *The Emergence of Heartless, Pyramus, and Thisbe*

As work with Breathless/Branchless-mediated cell signaling was occurring, researchers had successfully identified three other FGF family members with active roles both during *Drosophila* embryonic development as well as during later larval maturation. The first of the "other" FGF genes isolated from *Drosophila* was a tyrosine kinase receptor, DFGFR-2, found exclusively in tissues of mesodermal origin (Klämbt et.al., 1992). DFGFR-2 is structurally similar to the mammalian FGFR1-IIIb ortholog with two only Ig-like extracellular loops compared to the five Ig-like domains seen with Breathless, a transmembrane domain and two discrete tyrosine kinase domains (Shishido et. al., 1993). In embryos, defects in this receptor resulted in a loss of mesodermal cell migration in the dorsolateral direction and a failure to develop several cell lineages includes those of the visceral mesoderm, somatic muscles and the heart. The failure to develop these tissues could be overcome with the ectopic expression of *decapentaplegic* (*dpp*) suggesting that the receptor, called Heartless due to the mutant phenotype, was solely responsible for the loss of cell migration and not cellular differentiation (Gisselbrecht et. al., 1996; Bieman et. al., 1996).

Subsequent work with *heartless* however, showed that in addition to inducing cell migration, the receptor, working through activation of the Ras/MAPK pathway, was also responsible for the specification of certain muscle founder cells of the ventral mesoderm (Dutta et. al., 2005; Michelson et. al., 1998). These founder cells, which first appear ~7 hours into development, are part of the mesoderm that does not migrate over the endoderm during development and give rise to specific muscle groups including the lateral somatic muscles (Bate, 1990). In mutants lacking *heartless*, the differentiation of these founder cells into somatic muscle could be accomplished by either ectopic expression of wildtype Heartless or a constituitively active form of Ras (Michelson et. al., 1998).

The identification of this second FGFR in *Drosophila* precipitated the search for additional signal ligands since there appeared to be little overlap in the expression patterns of *heartless* and the only known signal ligand in Drosophila, *branchless.* Using a microarray assay to examine gene expression during embryonic development of the neurogenic ectoderm, researchers were able to identify two putative FGF-like genes in close proximity with each other. Named *pyramus* and *thisbe* in reference to the heartbroken lovers of Ovid's *Metamorphoses,* these two signal ligands are both predicted to have the traditional β-trefoil core domain, with sequence identity closest to that of the mammalian FGF 8 subfamily, and a N-terminal signal sequence designating them for secretion (Stathopoulus et. al., 2004). *In situ* hybridization of embryos at various stages show broad, overlapping expression patterns of these two signal ligands early during embryogenesis, but a discrete expression pattern after germ-band elongation is completed. At this time, *pyramus* appears to be primarily expressed in cells adjacent to nascent pericardial cells while *thisbe* is expressed in the founder cells of the visceral muscle. A large chromosomal deletion containing both *pyramus* and *thisbe* results in embryos with severe gastrulation defects similar to those seen in *heartless* mutants, but these effects can be partially overcome through either the ectopic expression of *thisbe* or a constituitively-active form of *heartless* (Gryzik and Müller, 2004; Stathopoulus et. al., 2004). Interestingly, single deletion mutants of either *pyramus* or *thisbe* could be not be generated suggesting perhaps that their function, with respect to mesodermal migration during early embryogenesis, is redundant.

## Putting it all together: FGF signaling in *Drosophila melanogaster*

To date, there have been three ligands and two receptors identified in *Drosophila* involved with FGF-mediated signaling. Empirical evidence suggests Branchless is the primary ligand involved with stimulating the Breathless receptor, while both Pyramus and Thisbe ligands interact and stimulate the Heartless receptor. The spacial and temporal expression of the FGF genes suggests there is very little overlap in terms of which cells and tissues they control, although activation of both Heartless and Breathless appear to both drive cell migration at least during the early stages of embryogenesis. Of the three ligands, Pyramus and Thisbe are structurally similar to the mammalian FGF-8 subfamily, while the Branchless core domain is structurally similar to that of the mammalian FGF-10 subfamily. Unlike any of the mammalian FGFs or even Pyramus and Thisbe, Branchless has very bulky N- and C-terminal domains flanking the β-trefoil core domain making it by far the largest FGF identified to date. The size of

the flanking domains in Branchless may add specificity to the interaction with the abnormally large extracellular domain of Breathless.

Early in embryogenesis, Branchless-mediated stimulation of the Breathless receptor in the epithelial cells of the tracheal pits results in the proper migration of these cells to form the main tracheal branches. At later stages, after these branches are formed, the same signal cascade leads to the formation of secondary and tertiary tracheal branches. Outside of tracheal branch formation, Branchless-mediated signaling has also been implicated in the formation of adult tracheoblasts from the wing imaginal disc, adult neuralblasts from glial progenitor cells, and the male appendage from the genital imaginal disc. In each of these cases, Branchless-mediated cell migration plays a significant role in their development, however, in some cases cell proliferation has also been observed. It is not clear, however, whether Branchless signaling is driving proliferation or another signaling pathway that is tied to the FGF pathways.

Pyramus- and Thisbe-mediated stimulation of the Heartless receptor early during embryogenesis leads to the proper migration of mesodermal cells during embryogenesis. Once in the proper position, these cells differentiate into the visceral mesoderm, somatic muscles and the heart via the activation of other developmental signaling pathways including Dpp and Sonic Hedgehog. The loss of both Pyramus and Thisbe leads to a failure for the mesoderm to migrate properly, but this defect could be rescued through the ectopic expression of *thisbe* alone suggesting that Pyramus and Thisbe share redundant functions with respect to mesodermal migration patterns. Since single *pyramus* and *thisbe* mutants have not been successfully created, it is unclear whether they have other unique functions which cannot be complemented.

# CHAPTER 3 - Baculovirus Fibroblast Growth Factors

The initial discovery of fibroblast growth factor orthologs outside of multicellular organisms was noted with the annotation of the genome sequence of *Autographa californica M* Nucleopolyhedrovirus (Ac*M*NPV), the first baculovirus genome to be completely sequenced and often considered to be the prototypical virus of this family (Ayres, et. al., 1994). This putative viral FGF (Ac-vFGF) was predicted to be 181 amino acids in length with a cleavable N-terminal signal sequence ( amino acids 1-18) targeting it for secretion and an internal β-trefoil core domain (amino acids 26-153) with architecture similar to that of the mammalian FGF 9, 16, and 20 subfamily as well as *Drosophila*'s Branchless core domain. Subsequent work to demonstrate that Ac-vFGF was a *bona fide* member of the fibroblast growth factor family showed that Ac-vFGF was indeed a secreted protein capable of binding to heparin and when added to various insect cell lines, capable of stimulating cell motility (Detvisitsakun et. al., 2005).

A second virus genome, *Bombyx mori* Nucleopolyhedrovirus (BmNPV), sequenced shortly after Ac*M*NPV, was also predicted to encode a FGF (Bm-vFGF) ortholog with the same architecture and physical properties as Ac-vFGF suggesting the protein is potentially well conserved among baculovirus (Gomi et. al., 1996; Katsuma et.al., 2004). Indeed, forty-eight of the fifty-three currently sequenced baculovirus genomes in the National Center for Biotechnology Database (NCBI) database encode at least one putatively identified FGF ortholog. Of the five exceptions, four are viruses which infect either Diptera or Hymenoptera and are limited to replication in the midgut epithelial cells. The fifth virus, *Maruca vitrata* M Nucleopolyhedrovirus (MaviNPV) is the smallest in terms of nucleic acid content of the Lepidoptera-infecting baculoviruses and does not encode homologs of a number of highly conserved baculovirus genes including *vfgf, odv-e66,* and *hcf-1* (Chen et. al., 2008). An alignment of the vFGF orthologs present in the remaining forty-eight Lepidoptera-infecting baculoviruses shows a sequence identity of between 30 and 70 percent. This high degree of conservation with respect to viral FGFs seen among these viruses suggests a critical role or roles during the infection process. To hypothesize what these potential roles could be, however, requires us to step back and first understand about how baculoviruses typically replicate in their host organisms.

## Baculoviruses in Nature

Baculoviruses are double-stranded DNA, enveloped viruses which infect Arthropods, primarily in the order Lepidoptera although other members of this virus family, infecting both Diptera and Hymenoptera species, have been studied with several of their genomes sequenced (Afonso et.al., 2001; Duffy et. al., 2006; Garcia-Maruniak et. al., 2004; Lauzon et. al., 2004). Within the family of baculoviruses, members are divided into four major genera: Lepidoptera-infecting Nucleopolyhedrovirus (NPVs), Lepidoptera-infecting Granuloviruses (GVs), Hymenoptera-infecting NPVs and Diptera-infecting NPVs (Jehle et. al., 2006) The distinction between these two Lepidoptera-infecting genera is based on the major protein component of their occlusion bodies (OBs), although there are other cytopathological differences which can also be used to distinguish them such as whether the nuclear membrane remains intact upon infection (NPVs) or dissociates (GVs) (Federici, 1997). Within the Lepidoptera-infecting NPVs, there is often an additional subdivision based on whether the virus encodes a homolog of the envelope protein GP64 (Group I NPVs) or a homolog of the envelope F protein (Group II NPVs) (Herniou et. al., 2003).

Within these classifications, there appears to be an extensive amount of diversity between the baculovirus with only thirty highly conserved "core" genes common to all (reviewed by Herniou and Jehle, 2007; McCarthy and Theilmann, 2008). Analysis of the viral genomes using bioinformatic tools shows the greatest sequence divergence present in the genomes of Hymenoptera- and Diptera-infecting NPVs, while most conservation occurs among the Group I NPVs (reviewed by Harrison, 2009). The ample diversity seen among the genomes of the various baculovirus may in part be due to the co-evolution of the pathogen with its arthropod host (Herniou et. al., 2004). This hypothesis helps to explain the functional specialization of certain viral proteins as well as the narrow host range of the majority of baculovirus studied to date (Miller and Lu, 1997). Unfortunately, this hypothesis also makes it difficult to formulate broad assumptions about baculovirus, particularly when it comes to examining host-pathogen interactions. Still, despite these limitations, we can look at overall patterns of infectivity and come to some idea of how baculoviruses function in nature.

### *The Beginning of the End: Ingestion of the Occluded Virus*

The Lepidoptera-infecting baculoviruses traditionally have a bi-phasic replication cycle with one phase devoted to the production of a budded virus (BV) which systemically spreads the infection throughout a single host, and a second phase devoted to the creation of an

environmentally-stable occluded virus form (reviewed in Cheng and Lynn, 2009 and Federici, 1997). baculoviruses infecting species of Hymenoptera and Diptera are somewhat atypical because there does not appear to be a sustained budded virus phase and virus spread is limited to the insect midguts, the initial site of infection. Due to this atypical nature, for the remainder of the discussion, we will focus solely on Lepidoptera-infecting baculoviruses unless otherwise noted.

Among Lepidoptera-infecting baculoviruses, the occluded form of the viruses is characterized by small cuboidal bodies composed of infectious occlusion-derived virus (ODV) embedded in a para-crystalline protein matrix and surrounded by an outer calyx sheath. The protein component of this matrix can be composed primarily of either polyhedrin or granulin, and while these proteins share several significant characteristics such as relative size and amino acid composition, they are functionally divergent (Summers and Smith, 1975). This divergence is easily seen in the morphology of the two occlusion bodies with polyhedrin-based occlusions having a variable number of ODVs per occlusion, while the occlusions composed of granulin contained only a single encapsulated virion (reviewed by Hilton, 2008 and Theilman and Blissard, 2008). These morphological differences attributed to the matrix proteins may in part be explained by their ability (or inability) to interact with other viral proteins required for efficient occlusion body formation. For example, attempts to pseudotype the *polyhedrin* gene in Ac*M*NPV with the *granulin* gene from *Trichoplusia ni* granulosis virus (TnGV) resulted in a few large, ill-defined occlusions virtually devoid of ODV (Eason et. al., 1998). Interestingly, a similar attempt to pseudotype the *polyhedrin* gene in Ac*M*NPV with the nearly identical *polyhedrin* gene (97% identity) from *Spodoptera frugiperda M* Nucleopolyhedrovirus (Sf*M*NPV) met with a similar, albeit less severe, phenotype suggesting that even subtle differences in the structure of polyhedrin can lead to significant defects in occluded virus assembly (Gonzalez et. al., 1989).

Typically, viral occlusions deposited on foliage from previously infected hosts are ingested by Lepidoptera larva inadvertently during feeding. These occlusions pass through the foregut of the insect and enter into the insect midgut. Unlike other holometabolous insects, the midgut environment of Lepidoptera larva is alkaline with a pH range between 8 and 12 depending upon larval stage and diet (Chapman, 2007). This basic pH causes the polyhedrin or granulin matrix to dissociate releasing the embedded ODV, which can then infect the epithelial and regenerative cells lining the midgut of the insect (Granados and Lawler, 1981; Ji et. al.,

2010). In order for this to occur, however, the ODV first must bypass the insect's protective peritrophic membrane.

The peritrophic membrane of most Lepidoptera species is a semi permeable barrier surrounding the nutrient-absorbing epithelial cells of the insect midgut and extending posteriorly into the insect hindgut. It is composed of various proteins, glycoproteins, proteoglycans, and poly-(1,4)-N-acetyl-D-glucosamine (insect chitin), although the exact make-up and distribution of these components widely varies between insect species. Specialized cells forming the cardia or proventriculus of the anterior midgut secrete the peritrophic membrane as a continuous sheet so that it appears sieve-like with openings just 2-6 nanometers (nm) in diameter (reviewed in Lehane, 1997). Since the diameter of a single, typical baculovirus capsid is significantly larger (50-100 nm) than the openings of the peritrophic membrane, simple diffusion across the membrane is considered impossible so alternative methods of entry must be employed (Khosaka et.al., 1971; Tweeten et. al., 1977).

One alternative method to bypass the peritrophic membrane employed by a number of Baculoviruses, most notably the *Lymantria dispar M* Nucleopolyhedrovirus (Ld*M*NPV) and *Trichoplusia ni* granulosis virus (TnGV), is to produce a modified matrix metalloprotease similar in structure to bacterial enhancin proteins. These viral enhancins are incorporated into the envelope of the occlusion-derived virus and work to degrade the peritrophic membrane immediately prior to midgut infection (Lepore et. al., 1996; Slavicek and Popham, 2005). Sequence analysis of the baculovirus genomes however, shows that a large number (40 out of 53) do not encode a suitable metalloprotease, but work with Ac*M*NPV, which does not encode an enhancing protein, suggests that other unknown viral factors may also help to degrade the peritrophic membrane (Derksen and Granados, 1988). In addition, it has also been hypothesized that viruses lacking metalloproteases may use small breaks in the peritrophic membrane arising naturally from the feeding of course plant materials although more study of this subject needs to be done at this time (Plymale et. al., 2008).

Once past the peritrophic membrane, the baculovirus ODV attaches to the brush boarder membrane of the epithelial midgut cells via the interaction of an unknown cellular receptor. The close proximity of the viral and cellular membranes allows them to fuse, internalizing the capsids and establishing the primary site of infection (Granados, 1978; Granados and Lawler, 1981; Horton and Burand, 1992). Studies of Ac*M*NPV infections of various susceptible hosts have

demonstrated the initial attachment of the virus particle to the midgut epithelial cell is mediated by three highly conserved *per os* infectivity factors (Pif): P74, Pif-1 (Ac119) and Pif-2 (Ac022). These three factors are found on the envelope of the ODV particle and mediate both attachment and entry into the target cells (Haas-Stapleton et. al., 2004; Ohkawa et. al., 2005). Two other *per os* infectivity factors, Pif-3 (Ac115) and Pif-4 (Ac096) have also been shown to affect the initial establishment of infection in the midgut epithelial cells, but their exact roles have not been determined to date (Fang et. al., 2009; Ohkawa et. al., 2005).

Once internalized into cells, viral capsids are trafficked to the cytoplasmic side of the nuclear envelope via interaction of the major capsid protein, VP39, with the host's filamentous actin (Charlton and Volkman, 1993; Lanier and Volkman, 1998; Lu et. al., 2002). To start the infection process however, the genetic material inside the capsid must somehow either exit the capsid and transverse the nuclear membrane, or the capsid itself must be transported across the nuclear envelope, perhaps through nuclear pores, prior to uncoating and DNA release. Which of these two alternatives occurs with baculovirus infections is not currently known although the limited amount of evidence suggests the latter hypothesis may be correct since empty capsids have been detected in the nuclei of newly infected cells (Granados and Lawler, 1981). Certainly, before this hypothesis is widely accepted though, much more work needs to be done in this area.

Not all capsids internalized into cells share the same fate, however. Several studies examining the initial stages of infectivity of Ac*M*NPV, which contain multiple capsids within a single envelope, and *Helicoverpa zea* single Nucleopolyhedrovirus (HzSNPV), which consists of a single enveloped capsid, suggests when multiple capsids are present in the cell not all of them will be transported to the nucleus. Instead, many will be quickly repackaged as budded virus to establish secondary infections in the surrounding epithelial cells within two hours of the establishment of the primary foci (Flipsen et. al, 1995; Washburn et. al., 1999; Washburn et. al., 2003). Rapid establishment of the infection throughout the midgut and subsequent escape to the hemocoel is thought to be beneficial to the virus since many Lepidoptera species routinely slough their midgut cells prior to pupation and in some cases in response to viral or bacterial infection (Engelhard and Volkman, 1995; Hakim et. al., 2010; Washburn et. al., 2003). What factors determine whether a virus capsid will enter the nucleus or become repackaged is not well understood at this time.

### *The Second Phase: Production of Budded Virus*

The dissociation of the capsid and release of the genome into the nucleus begins the process of virus replication and the production of budded virus. To achieve the initial burst of budded virus production prior to a potential host response, the patterned expression of viral genes is temporally regulated at the transcription level. This ensures that adequate levels of necessary viral proteins are available to quickly produce BV prior to the production of proteins required for ODV formation (Friesen, 1997). Extensive work temporally mapping viral RNA transcripts showed three distinct phases of gene expression, with only a small number of viral genes, such as the GP64 gene from Ac*M*NPV, expressed through multiple phases (Friesen and Miller, 1988; Lübbert and Doerfler, 1988; Wood, 1980; Zhou et. al., 2003).

The immediate early and early phases of viral gene expression begins upon the release of the viral DNA in the nucleus and lasts for roughly four to six hours until the onset of viral genome replication. During these phases, gene transcription is α-amanitin sensitive suggesting the virus exclusively utilizes the host's DNA-dependent RNA polymerase II to produce viral mRNAs (Huh and Weaver, 1990; Theilmann and Stewart, 1991). Analysis of the upstream sequences of early transcribed genes show genetic elements that are remarkably similar to known arthropod promoter sequences including a TATA binding protein site (TATAA motif) 25 to 31 nucleotides upstream of the +1 initiator start site (consensus CAGT) as well as downstream activating region elements (consensus CACNG) (Blissard et. al., 1992; Cherbas and Cherbas, 1993; Kogan et. al., 1995; Pullen and Friesen, 1995). Together, these cis-acting elements provide a high basal level of transcription for viral genes which must be synthesized prior to viral DNA replication and late gene expression.

Examples of viral products from Ac*M*NPV infections produced during this early phase include the major trans-activating proteins IE1 and IE2, the four subunits for a novel DNA-dependent RNA polymerase, and the anti-apoptotic factor p35. In addition to these proteins, there are at potentially twelve other viral products, termed late expression factors (lefs), which must be expressed during the early phases in order for efficient late gene expression to occur (Todd et. al., 1995; Rapp et. al., 1998). The expression of either the F protein or GP64, the two major budded virus envelope proteins, also begins during this phase and may be required for efficient repackaging of the capsids derived from ODV.

The late phase of gene transcription begins with the synthesis of viral DNA within the nucleus of infected cells and persists for roughly eighteen hours. During this phase, host gene

and early viral transcription declines while late viral gene transcription under the control of a promoter element with the common initiator site, (A/G/T) TAAG, increases. This initiator site is not recognized by the host polymerase, but by the novel, virally-encoded DNA-dependent RNA polymerase II (reviewed by Passarelli and Guarino, 2007). The exact mechanism for the switch from host polymerase to viral polymerase is not completely understood, but several reports suggest that a number of the late replication factors responsible for viral DNA replication also trigger a cellular reaction similar to the DNA damage response in vertebrates (Du and Thiem, 1997; Schultz and Friesen, 2009).

In insect cells, this DNA damage response leads to an arrest of the cell cycle at the G2 phase along with a noticeable enlargement of the nuclei of infected cells coinciding with the displacement of the cellular genomic material to the periphery of the nucleus (Braunagle et. al., 1998; Knudson and Harrap, 1975). Along with these obvious morphological changes, there is a concurrent reduction in global host protein synthesis and in some cases, with the absence of the viral anti-apoptotic *p35* gene, eventual cell death (Schultz and Friesen, 2009). One interesting avenue of speculation is that the induction of the DNA damage response by baculovirus infection was an early anti-viral response designed to limit the spread of the virus. This anti-viral response was later circumvented by the virus's acquisition and adaptation of a DNA-dependent polymerase and anti-apoptotic factors which allowed the virus to maintain high levels of protein synthesis despite the loss of the cellular transcription machinery.

Examples of genes expressed during the late phase of Ac*M*NPV infections include the nine virus structural genes such as *VP39* and *vp80* as well as genes encoding viral proteins essential for assembly of the mature budded virions (Thiem and Miller, 1989; Wu et. al., 2008). With sufficient copies of the viral genome present, assembly of the complete viral capsids begins during this phase as well. Thin-section micrographs of infected cells during this time frame have shown that this assembly takes place in an electron dense, sub-nuclear compartment called the virogenic stroma (Frasier, 1986).

Early work on the structure of this sub-nuclear compartment showed it was composed primarily of filamentous proteins but extracted stroma proved to be sensitive to treatment with both DNAse and RNAse suggesting a nucleic acid component as well (Frasier, 1986; Young et. al., 1993). Further studies of cells infected with *Bombyx mori* Nucleopolyhedrovirus (BmNPV) demonstrated that in addition to the filamentous proteins, several viral structural proteins as well

as a number of proteins associated with genomic replication co-localize in the virogenic stroma. These proteins include the major structural protein, VP39, the major trans-activation protein IE1, the single-stranded binding protein (LEF-3), and the DNA helicase P143 (Kawasaki et. al., 2004; Nagamine et. al., 2006). Because of these studies, is now thought that the virogenic stroma is the site of both DNA replication and capsid assembly and that the lattice-like structure of the stroma provides a unique scaffold for the rapid and efficient assembly and packaging of virus capsids (Charlton and Volkman, 1991; Kawasaki et. al., 2004)

Once capsids are assembled and packaged during this late phase, they must exit out of the nucleus to start the process of becoming infectious BV. Electron micrographs of infected cells during this phase suggest capsids assembled in the virogenic stroma migrate to the periphery of the nucleus. There, the capsids orientate themselves perpendicular to the nuclear membrane and egress occurs through a budding process similar to the one seen upon exit from the cell even to the extent that the capsid acquires a nuclear membrane-derived envelope which is subsequently shed (Granados and Lawler, 1981). An early study done with a temperature sensitive mutant of Ac*M*NPV, defective in BV production at higher temperatures, suggested that the capsid egress is mediated by a nuclear membrane-associated protein, GP41 (Olszewski and Miller, 1997). Since then, subsequent studies of Ac*M*NPV deletion mutants have suggested that a variety of other highly conserved, structural proteins including Ac66, Ac98, and Ac141 also play a significant role in efficient virus egress out of the nucleus, perhaps by directing the association of the capsids with cellular transport proteins and/or microtubules (Fang et. al., 2007; Fang et. al., 2009; Ke et. al., 2008; Wu et. al, 2008).

Capsids move through the cytoplasm to locations along the interior of the surface cell membrane where they will eventually exit the cell. In Ac*M*NPV-infected midgut epithelial cells of *Trichoplusia ni* larva, BV egress appears to directed almost exclusively to the basal and lateral surfaces of the cells which are highly enriched in the viral envelope proteins GP64 and F protein. Studies using other tissues such as fat body and in cell culture, however, have noted GP64 localization appears to uniform across the entire cell surface suggesting BV egress is only directed in columnar epithelial cells of midgut lineage (Blissard and Rohrman, 1989; Keddie et. al., 1989; Pearson et. al., 2001). The tissue specific differences in BV egress sites may provide a proliferative advantage for the virus since any BV released from the apical surface of midgut epithelial cells would be released into the alkaline environment of the midgut lumen where it

would quickly be inactivated. By directing a baso-lateral exit, the virus is increasing the likelihood that the BV produced in this early phase would be used to establish secondary foci

The exact mechanism which allows the capsid to exit the cell and acquire a cellular-derived envelope is not well understood, however the major envelope protein GP64 has been shown to play a significant role in the process. In Ac*M*NPV, GP64 is an abundantly expressed transmembrane protein with a heavily glycosylated extracellular domain and a very short, seven-amino acid, cytoplasmic domain. An early study with a virus having an insertional mutation in *gp64* demonstrated a lack of cell to cell virus transmission both *in vitro* and *in vivo* (Monsma et. al., 1996). This result was somewhat expected considering a previous work had already demonstrated GP64 was essential for membrane fusion under low pH conditions, a step necessary for BV entry into cells via absorptive endocytosis (Blissard and Wenz, 1992; reviewed by Marsh and Helenius, 2006). What was unexpected however was an inability to detect non-infectious budded virus progeny in the supernatant of primary infected cells. This result suggested that GP64 had another important function in addition to membrane fusion related to virus egress out of the cell.

A subsequent study using a *gp64* deletion mutant showed virus capsids were able to exit the nucleus and enter into the in the cytoplasm of infected cells, but were then unable to egress from the cell without GP64. A comparison of a series of C-terminal GP64 truncation mutants showed that the BV egress-function involved the cytoplasmic domain and at least a portion (seven amino acids) of the transmembrane domain (Oomens and Blissard, 1999). A more recent study has further refined this work and in addition to this essential C-terminal region, four conserved amino acids of the extracellular domain (T463, G460, G462, and G474) were also needed for efficient virus egress (Li and Blissard, 2009). How these various domains and amino acids direct the budding and acquisition of the viral envelope is still unknown, although it has been speculated that the amino acids of the C-terminal domain make direct contact with viral capsid proteins and through a conformation change work to pull the capsid through the membrane (Westenberg and Vlak, 2008).

### *The Third Phase: Dissemination of Budded Virus and Systemic Infection*

In the pathway of infection of a permissive Lepidoptera host, the production of budded virus is first detected with the establishment of secondary infections of midgut columnar and goblet cells as well as the pluripotent midgut stem cells. Depending upon both the host's developmental stage and virus used, the advancement of virus infection throughout the midgut occurs between four and eight hours post inoculation with ODV (Barrett et. al., 1998; Hass-Stapleton et. al., 2003; Washburn et al., 1995). This initial spread of infection is driven by the release of budded virus from the basolateral surface of the infected epithelial cells which is then able to spread laterally to infect nearby cells. The process of infecting these cells by BV is similar to the initial infection of the cells by ODV, however there are some subtle differences.

**Budded Virus Attachment**

To establish the primary infection, ODV attach to the surface of epithelial cells via an unknown cellular receptor. The same is true for BV. An early study of Ac*M*NPV using several permissive and non-permissive cell culture lines showed that the attachment of BV could be inhibited by pre-treating the cells with Proteinase K or trypsin immediately prior to infection. In addition, kinetic studies showed virus attachment was saturable for both cell lines permissive for AcMNPV infection (6,000 and 13,700 binding sites per cell), and non-permissive for infection (600 binding sites per cell) (Wickham et. al., 1992). The large difference in the number of available binding sites on cells suggests receptor mediated attachment may be one of limiting steps for the establishment of baculovirus infections among various hosts.

To identify the viral components responsible for Ac*M*NPV attachment, research initially focused on the major glycoprotein found on the virus envelope, GP64. Early work using a monoclonal antibody (AcV1) against an undefined epitope of GP64 demonstrated that it could interfere in a dose dependent manner with the attachment of Ac*M*NPV to permissive cells (Volkman and Goldsmith, 1984). The follow up study using the same antibody under more controlled conditions, however, suggested that the neutralizing effects of the antibody were primarily due to its interfering with the membrane fusion activity of GP64 and not its role in receptor-mediated attachment (Volkman and Goldsmith, 1985) Subsequently, a more refined approach was utilized with antibodies against specific segments of the extracellular domain of GP64. This work showed the N-terminal region of GP64 (amino acids 21-159) was essential for receptor-mediated attachment. Still, even with this refined approach, roughly 30% of virions in

this study still bound to the cell surface suggesting additional viral proteins could be involved in attachment (Zhou and Blissard, 2008).

In Ac*M*NPV, as well as a number of other Lepidoptera-infecting baculoviruses sequenced to date (Group I NPVs), the other major viral protein present on the BV envelope is the F protein. Several studies have demonstrated that Ac*M*NPV's F protein homolog, Ac23, is a non-essential protein which cannot functionally substitute for GP64 primarily because a mutation in its furin-cleavage site makes it unable to induce membrane fusion (Long et. al., 2008; Monsma et. al., 1996; Pearson et. al., 2000). That is not to say however that the F protein from Group I NPVs is completely non-functional or incapable of receptor interaction. In fact, a study has shown that the deletion of *ac23*, while not having an effect on BV production in cell culture, does delay host mortality (~24 hours) during a *per os* infection (Lung et. al., 2003). In addition, work with BV of a mutant Ac*M*NPV lacking *ac23* showed a much more significant decrease in attachment in the presence of the anti-GP64 neutralizing antibodies than the wildtype BV suggesting that it also functions as a viral attachment protein similar to, but not with the same efficacy as, GP64 (Zhou and Blissard, 2008).

This finding is supported by evidence from the other class of NPVs (Group II) as well as Granuloviruses (GVs) which do not encode a *gp64* homolog but instead have a single copy of *F protein*. Several studies have demonstrated F proteins from Group II NPVs are localized to the BV envelope and facilitate attachment of the virus particles to cell membranes, although from competition experiments it is clear that the F protein utilizes a cellular receptor distinct from that employed by GP64 (Pearson et. al., 2000; Wickham et. al., 1992; Westenberg et. al., 2007). In addition to attachment, the F protein homologs from Group II NPVs and GVs all appear to have intact furin-cleavage sites which would allow them to retain their function as membrane fusion proteins (IJkel et.al., 2000; Long et. al., 2007;; Westenberg et. al., 2004). Similar to the phenotype observed with the deletion *gp64*, the deletion of the *F protein* from Group II NPVs results in a complete lack infectious BV production although it is unknown at this time whether this phenotype is due to a loss of BV egress out of the cell or the inability of the BV lacking F protein to attach to cells or uncoat after internalization (Westenberg and Vlak, 2008). Interestingly while the effects of *gp64* deletion in Ac*M*NPV can be somewhat rescued by the expression of several Group II *F proteins*, the converse is not the case since the expression of *gp64* is completely unable to compensate for the loss of *F protein* in a Group II virus (Lung

et.al., 2002; Westenberg and Vlak, 2008). This result makes it tempting to speculate that Group II NPV F proteins have additional essential functions or unique interacting partners which GP64-expressing viruses do not have or need.

**Budded Virus Entry**

After the process of attachment, BV need to enter into the cell to establish an infection. One potential pathway of entry for BV, receptor-mediated endocytosis, was discovered initially by Volkman and Goldsmith with their work with Ac*M*NPV and the α-GP64 antibody, AcV1. In their experiments, however, there appeared to be a small fraction of neutralized BV that attached to cells but then still entered through a process involving membrane fusion, similar to that seen with ODV mediated entry (Volkman and Goldsmith, 1985; Volkman et. al., 1986). Concurrent with these experiments, work with another Group I NPV closely related to Ac*M*NPV, *Trichoplusia ni M* Nucleopolyhedrovirus (Tn*M*NPV), seemed to support membrane fusion as the primary entry mechanism for BV, and not receptor-mediated endocytosis. This membrane fusion peaked 30 minutes post incubation of BV with permissive *Spodoptera frugiperda* (Sf9) cells and appeared to be pH dependent. In addition, the fusion could be significantly increased in the presence of the enhancin protein, a metalloprotease, from *Pseudaletia unipuncta* granulosis virus in a manner similar to what was seen with ODV entry (Kozuma and Hukuhara, 1994). Together, these two differing results suggested that entry of BV into permissive cells could occur through either a membrane fusion process or a receptor-mediated endocytosis process, or a combination of both.

To resolve the issue, researchers first looked at Ac*M*NPV BV entry into permissive cells in the presence of chloroquin and sodium azide, two adsorptive endocytosis inhibitors which would not affect membrane fusion. As was the case with neutralizing antibody AcV1, there was a decrease (~50%) in BV entry when chloroquine was applied to cells and a significant decrease (<95%) when sodium azide was applied. There also appeared to be no visual evidence of membrane fusion and, unlike the previous study by Kozuma and Hukuhara, the addition of the enhancin protein from TnGV did not improve BV entry (Wang et. al., 1997). Subsequent studies on the kinetics of entry demonstrated BV were internalized into Sf9 cells within 20 minutes after attachment via clatharin-mediated endocytosis. The periodic addition of ammonium chloride to Sf9 cells to prevent the acidification of the endosomes showed that release of virus from these vesicles occurred 15 to 30 minutes after initial internalization (Hefferon et. al., 1999; Long et.

al., 2006). The process of membrane fusion between the viral envelope and the endosome, a step essential for the eventual release of the capsid into the cell, was shown to be mediated by either homo-trimeric GP64 complexes or proteolytically active F protein complexes under low pH conditions (Long et. al., 2008; Markovic et. al., 1998). After BV are released from the endosome, they are trafficked to the nucleus in the same process as capsids derived from ODV and the infection cycle begins anew.

**Escape from the Midgut**

As mentioned previously, the rapid establishment secondary infections in the midgut epithelial cells of a susceptible host is essential for a successful baculovirus infection, but it cannot be the only tissue susceptible to BV attachment and entry. Somehow, during the course of infection, the virus must move beyond the tissues of the midgut into the hemocoel of the host in order to avoid being shed when the midgut is sloughed. Inhibiting the movement of virus into the hemocoel is a natural physical barrier, the basal lamina, which serves to exclude large particles such as virions by both size and charge (Lieleg et.al., 2009; Reddy and Locke, 1990; Summers, 1971). It is secreted by virtually all epithelial cells as a continuous sheet with two visually distinct layers. The uppermost layer, the lamina lucida, is primarily composed of the glycoproteins laminin and entactin, and minor components such as integrins. The lower layer, the lamina densa, forms a mesh like layer consisting of type IV collagen coated by perlecan (Chapman, 1998; Hynes and Zhou, 2000). Together, these layers form a continuous mesh-like structure which effectively prevents the virus from budding out of the infected midgut epithelia and directly entering the insect hemocoel. Much like the case with the other physical barrier, the peritrophic membrane, Lepidoptera-infecting NPVs may have developed a rather effective means of bypassing the restrictions of the midgut basal lamina; they simply utilize the gas exchange conduit which transverses the entirety of the host, the insect tracheal system (Engelhard et. al., 1994).

Similar to the tracheal system briefly described earlier for *Drosophila melanogaster* larva, the tracheal network of Lepidoptera larvae originates from the cuticle of the insect. It begins with a series of external openings called spiracles arranged along the side of the insect which can be manually opened and closed to allow for gas exchange. Among Lepidoptera species, there are typically ten pairs of spiracles, two on meso- and meta-thoracic segments and eight on the abdominal segments. The spiracles are joined by two main tracheal conduits, the

dorsal and ventral tracheal trunks. Each of these trunks is composed of a chitin and protein matrix forming a tube-like structure that is supported by spirals of thickened chitin called taenidium. The inner chitin tube is encased completely by tracheal epithelial cells arising from the ectoderm. From these main tracheal branches, there is an extensive network of secondary and tertiary tracheal branches which are similar in structure to the main tracheal branches. Eventually, the fine tertiary tracheal branches terminate in very thin (less than 1µm in diameter) fluid-filled tubes called tracheoles which are capped by a single cells called a tracheoblasts. These tracheoles/tracheoblasts bypass the midgut basal lamina and intercalate into and between the epithelial cells to facilitate gas exchange via simple diffusion (Chapman, 1997; Klowden, 2007).

Engelhard and others were able to demonstrate the utilization of this tracheal network to establish baculovirus infection in the hemocoel by feeding permissive 4$^{th}$ instar *Trichoplusia ni* larvae with ODV from a recombinant Ac*M*NPV expressing a reporter gene *lacZ.* As previously noted, the initial infection by ODV was detected as early as 4 hours post inoculation in midgut epithelial cells and a small number of regenerative cells. By 12 hours post inoculation, multiple foci of infection were detected throughout the midgut epithelial cells, and by 16 hours, the infection of the tracheoblasts servicing the midgut epithelial was also noted. At 24 hours post inoculation, the infection had spread throughout the entirety of the midgut. In addition, infection could be detected in the tracheolar epithelial cells entering the midgut. 12 hours later, the first infection outside the confines of the midgut was observed with distal tracheal branches and hemocytes both expressing lacZ. By 48 hours post inoculation, extensive infection of secondary and tertiary trachea was noted as well as infection of hemocytes and fat body. Concurrently, the lacZ expression of the midgut decreased dramatically with the sloughing of the midgut and the clearing of virus infection. By 72 hours post inoculation, virus infection was evident throughout the hemocoel and in all the distal tissues serviced by trachea including salivary glands, muscle tissue, malpighian tubules, gonads and the cuticular epidermis (Engelhard et al., 1994). Subsequent work examining viral pathogenesis in a variety of hosts has supported the conclusions made by Engelhard concerning the importance of infecting tracheal tissue to disseminate virus infection throughout the hemocoel (Barrett et. al., 1998 Rahman and Gopinathan, 2004). Clearly, based on this body of work, the utilization of the tracheal conduit is essential for the systemic spread of a successful baculovirus infection.

This finding, in itself, creates a significant problem because tracheal epithelial cells secrete their own basal lamina similar in structure to the one surrounding the midgut epithelia. How then can BV penetrate this protective coating but not the one between the midgut and the hemocoel? There have been two theories advanced to explain this dichotomy. The first, outlined by Engelhard and others, suggested that the tracheoblasts are the initial site of tracheal infection because these cells lack basal lamina and make direct cell-to-cell contact with midgut epithelial cells (Adams et. al., 1978; Engelhard et. al., 1994; Maina, 1989). The infection then proceeds along the tracheal epithelial cells by utilizing the unique lateral lymph system and epidermal feet of the tracheoles until it bypasses the basal lamina barriers of the midgut (Locke 1985). Once in the hemocoel, the infection proceeds to other tissues rapidly through the infection of circulating hemocytes which make direct contact with tracheal epithelial at branch nodes (Locke 1997; Trudeau et. at 2001).

An alternative hypothesis to the one offered by Engelhard was presented by Federici who proposed that BV makes use of either thin spots in the basal lamina (>20 μm thickness) or carry an as-yet-undefined enzyme which degrades the basal lamina to allow for the establishment of a virus infection in tissues protected by this barrier (Federici 1997). This alternative hypothesis was based on several lines of indirect evidence. First, an early report on the pathogenesis of an Ac*M*NPV infection in a permissive host showed that presumably repackaged BV could be detected in the hemocoel of infected larvae within 30 minutes of a very high dose ($10^6$ occulsion bodies per larvae) feeding suggesting that the virus could penetrate the basal lamina barrier independent of tracheal infection (Granados and Lawler, 1981). Second, a report on baculovirus infection of ovarian tissue demonstrated that the co-injection of clostridial collagenase, a basal lamina-specific protease, with BV into the follicular cells of *Bombyx mori* larvae dramatically increased the spread of infection into the hemocoel compared to injection of BV alone (Smith-Johannsen et. al., 1986). And last, reports by both Flipsen and Knebel-Mörsdorf showed the infection of early second instar *Spodoptera exigua* midgut tracheoles and circulating hemocytes occurred simultaneously and not in the linear progression pattern of infection noted by Engelhard (Flipsen et.al., 1995; Knebel-Mörsdorf et.al., 1996).

Despite the Engelhard- hypothesis having garnered limited supporting evidence since it was formulated, a recent report by Means and Passarelli tracking the pathogenesis of a recombinant Ac*M*NPV infection has offered more conclusive proof that basal laminae

degradation is the correct one hypothesis for the route of infection. In their work, they demonstrated the basal lamina covering of tracheal cells is transiently degraded during a *per os* infection. This degradation is mediated by a viral protein (vFGF) that initiates a cascade of activated host metalloproteases and effector caspases and is specific for basal lamina (Means and Passarelli, 2010). Thus, based on this evidence, it is clear that the viral-mediated degradation of the basal lamina plays a significant role in the secondary infection of trachea and the systemic infection of the host.

**The Final Barrier to Infection: the Insect Cellular-mediated Immune Response**

The infection of tissues in the hemocoel and beyond is essential if the virus is to produce sufficient numbers of occlusion bodies to infect additional host organisms. To oppose this, various Lepidoptera species have developed complex humoral and cellular defense responses including the production of potent anti-microbial peptides, phagocytosis of foreign bodies and melanization of infected cells followed by encapsulation (reviewed by Lavine and Strand, 2002). While much of the research in this area indicates these responses are effective against bacterial challenges, a growing body of work suggests that certain insect species can utilize their cellular defense network against viral challenge as well.

The cells most often associated with insect immune response in Lepidoptera are granulocytes and plasmatocytes, two specific types of circulating hemocytes which increase in number during later larval stages until they compromise nearly half of all hemocytes present in the hemocoel (Chapman, 1998). Granulocytes are responsible for the phagocytosis of small amounts of foreign material as well as apoptotic or necrotic cells and are also associated in the very early stages with the recruitment of plasmatocytes to damaged tissues too large to be phagocytized. Plasmatocytes are adherent cells responsible for the encapsulation of large foreign bodies or necrotic tissue (reviewed by Ribeiro and Brehélin 2002). Together, these cells provide a potent method of preventing the spread of pathogens into and throughout the hemocoel.

Some of the most compelling evidence that circulating hemocytes also function during the course of baculovirus infections was seen with work examining the susceptibility of 4$^{th}$ instar *Spodoptera littoralis* larvae to infection by Ac*M*NPV. When fed *per os*, these larvae are highly resistant to infection even with doses as high as 100,000 occlusions per insect. Inspection of the insect midguts after infection with Ac*M*NPV show a large number of melanized, encapsulated nodes around tracheal tissues servicing these tissues suggesting a cellular mediated immune

response was able to prevent the systemic spread of the virus into the hemocoel. Direct intrahemocoelic injection of $2x10^4$ BV or suppression of the immune response resulted in efficient systemic spread of the virus infection and subsequent mortality of the host (Rivkin et. al., 2006). Other Lepidoptera species have also demonstrated varying degrees of resistance to oral infection due to a cellular mediated immune response suggesting an effective immune response may be another limitation in the host range of certain baculoviruses (McNeil et. al., 2010; Trudeau et. al., 2001).

To counter the immune response, some researchers have suggested baculovirus "target" the host immune cells preferentially to remove them as a protective barrier as well as to spread the infection throughout the hemocoel (Barrett et. al., 1998; Hass-Stapleton et. al., 2003). A recent report using the cotton bollworm, *Helicoverpa armigera*, reinforced this assertion by demonstrating that Ac*M*NPV could infect all five types of circulating hemocytes including granulocytes and plasmatocytes within 36 hours of intrahemocoelic injection. In addition, the presence of Ac*M*NPV in the hemocoel marginally triggered the up-regulation of two of twenty known immune-related genes, *gloverin-like* and *lysozyme,* but it is not known whether either of these have anti-viral activities (Wang et. al., 2010).

It is also important to note at this time that the preferential infection of hemocytes is by no means universal even in permissive infections where the host is fully infected. Several reports have shown that in certain species, circulating hemocytes are highly resistant to infection, but do little to prevent the systemic infection process from occurring (Chikhalya et. al., 2009; Clarke and Clem, 2002). In the work by Clarke and Clem, for example, they demonstrated that hemocytes of $4^{th}$ instar *Spodoptera frugiperda* larvae were highly resistant to infection compared to other tissues such as fat body and trachea even when the virus was delivered through intrahemocoelic injection. Indeed, at the highest dosages used, only 52 percent of the circulating hemocytes recovered from the hemocoel showed signs of infection as late as 120 hours post injection. At the same dosage however, 100% host mortality was observed suggesting that even though nearly half of the circulating hemocytes present were functional, they could not counter the progression of the virus infection. Interestingly, in the same report, 90 percent of the hemocytes recovered from *Trichoplusia ni* larvae injected in the same manner with Ac*M*NPV BV showed obvious signs of infection perhaps indicating the susceptibility of hemocytes to infection is species specific (Clarke and Clem, 2002).

Based on these results, it is therefore quite likely that the cellular mediated immune response elicited by hemocytes only provides a barrier to systemic virus infection in a limited number of cases. In those cases where the immune response is not effective, the virus may preferentially infect circulating hemocytes to remove them as an effective barrier but this is not a general mechanism employed by all baculoviruses to circumvent the immune response. Finally, even in the cases where hemocytes are effective at preventing one virus strain from entering the hemocoel of a host, e.g. Ac*M*NPV and *Spodoptera littoralis*, they may be completely ineffective at preventing other baculovirus strains from replicating in the hemocoel (Simón et. al., 2004).

***The Final Phase: Production and Release of Occlusion-derived Virus***

After the amplification of BV and systemic infection of various host tissues, the next phase of the virus replication cycle is primed to begin. During this phase, there is an abrupt transition from BV production to ODV as capsids formed in the nucleus no longer egress but instead accumulate in the periphery of the nucleus called the ring zone. Here, either singly or in the case of MNPVs bundled together, the capsids acquire the viral envelope necessary to become mature infectious ODV. The cause for this transition is not completely understood but it could be coupled either to a depletion of early viral proteins required for egress out of the nucleus or the accumulation of late viral products essential for ODV formation. In either case, the build-up of capsids in the ring zone of the nucleus is the first cytopathological evidence for the very late phase of viral gene transcription.

Two examples of Ac*M*NPV genes expressed at high levels during this timeframe include the occlusion matrix protein gene *polyhedrin* as well as the cytoskeleton-associative protein gene *p10*. Both of these viral transcripts can be detected as early as 12 hours post infection (pi) but unlike late gene transcripts whose levels slowly decline after DNA replication has ended, the level of *p10* and *polyhedrin* transcripts rise dramatically beginning 18 hours pi. By 48 hours pi, these very late gene products become by far the dominant message present in infected cells (Rohel et. al., 1983). Promoter analysis of the *polyhedrin* and *p10* genes has shown that similar to the late gene transcription, this phase of viral gene expression requires the consensus initiator site, (A/G/T) TAAG and utilizes the virally encoded DNA-dependent RNA polymerase for transcription (Rankin et. al., 1988; Wyler and Possee, 1989; Weyer et al., 1990). In addition, for maximal expression of *polyhedrin*, the promoter element consists of an auxiliary 20 nucleotide sequence upstream of the initiator site and 49 base pair non-coding leader sequence (Rankin et.

al., 1988). Interestingly, the *p10* promoter element is significantly larger than that of *polyhedrin* promoter with a 30 nucleotide upstream sequence and a 71 base pair non-coding leader sequence involved (Wyler and Possee, 1989). Alignment of the two promoter elements shows that outside of a 12 base sequence encompassing the initiator site, there is very little sequence homology present between the two elements.

The lack of sequence homology between the two promoters suggested that more than one viral factor was responsible for enhancing expression of these two very late viral genes. An analysis however of a temperature sensitive Ac*M*NPV mutant defective in polyhedra formation at higher temperatures showed that the expression of both *polyhedrin* and *p10* was affected by a single viral protein, very late expression factor-1 (VLF-1). A sequence homology search suggested VLF-1 was a member of the integrase family of proteins involved in site-specific DNA recombination as well as variety of other functions including gene regulation (McLachin and Miller, 1994; reviewed by Grainge and Jayaram, 1999). Gel shift and in vitro transcription assays using purified, recombinant VLF-1 showed that it bound DNA and stimulated the transcription of the *polyhedrin* gene but not the late gene product VP39 (Mikhailov and Rohrmann, 2002; Mistretta and Guarino, 2005). The ability of VLF-1 to bind to the promoters of *polyhedrin* and *p10* was mapped to the non-coding leader sequences between the consensus initiator site and the start codon but there does not appear to be any direct competition between these elements for VLF-1 binding (Chaabihi et. al., 1993; Mistretta and Guarino, 2005; Yang and Miller, 1999). Deletion of *vlf-1* from Ac*M*NPV, as expected, resulted in the dramatic reduction of both *polyhedrin* and *p10* expression, but unexpectedly resulted in the inability of the virus to propagate. This deficiency was subsequently linked to the defective formation of mature capsids suggesting VLF-1's transactivation of polyhedrin and p10 promoters may be a secondary function which occurs after capsid assembly is completed (Vanarsdall et. al., 2004, Vanarsdall et. al., 2006).

The rapid accumulation of polyhedrin or granulin is a primary step in the process of forming occlusion bodies required for the host to host transmission of infection discussed earlier. Equally important is the capsid acquisition of an occlusion-derived viral envelope (reviewed by Braunagel and Summers, 2007). The proper formation of these envelopes begins with the production of major ODV envelope proteins E-66 and E-25 which are integrated into the endoplasmic reticular (ER) membrane during translation. Mutational analysis of these proteins

has demonstrated they are targeted to the ER by short, hydrophobic N-terminal signal sequences roughly 33 amino acids in length (Hong et. al., 1997). In addition to targeting the viral protein to the ER, several positively charged amino acids near the C-terminal end of this signal sequence have been shown to associate with a cellular protein, *Spodoptera frugiperda's* importin-α-16, which helps translocate the viral protein through the nuclear pore where it becomes integrated into the intranuclear membrane (INM) surrounding the ring zone (Braunagel et. al., 2008; Saksena et. al., 2006). In the absence of viral infection however, ODV E-66 and ODV-E25 do not translocate to the INM, but instead become embedded in the outer nuclear membrane suggesting that importin-α-16 itself is insufficient to direct viral proteins to the ODV envelope (Hong et. al., 1997). Several studies with mutant Ac*M*NPV have indicated that at least two additional viral proteins, FP25k and Ac141, are required for the proper targeting of essential ODV proteins, perhaps by working to stabilize the importin-α-16 complex (Braunagel et. al., 1999; Braunagel et al., 2009; Fang et. al. 2006).

Once essential viral proteins are localized to the intranuclear membrane, microvesicles incorporating these proteins need to be formed which will eventually form the ODV envelope (reviewed in Braunagel and Summers, 2007). It is unclear whether these vesicles are *de novo* synthesized or derived directly from blebbing of the inner nuclear membrane, however recent evidence suggests that a highly conserved viral protein, Ac76, plays an integral role in the process (Williams and Faulkner, 1997; Hu et. al., 2010). Interestingly, deletion of *ac76* from Ac*M*NPV results in not only a lack of microvesicles and enveloped ODV, but a loss in infectious BV production (Hu et. al., 2010). Since capsid formation, DNA replication, and packaging all appear to be largely unaffected by the deletion of *ac76*, it is possible that this viral protein also plays a significant role in the BV acquisition of the nuclear envelope prior to its egress out of the nucleus.

After acquiring its microvesicular-derived envelope, ODV become randomly embedded in the polyhedrin or granulin protein matrix and occlusion bodies (OBs) are formed. OBs can be viewed in infected cells with light microscopy as early as 24 hours post infection and are fully formed between 60 and 72 hours. At these later stages, the very late viral protein p10 helps to organize a protective calyx sheath around the OBs (Lee et.al., 1996). This calyx is composed of bilamellar sheets forming a lattice like structure with porous openings which is fused to the polyhedrin matrix by thiol bonds (Whitt and Manning 1988). Substitution of *granulin* for

*polyhedrin* in Ac*M*NPV, while dramatically reducing the number of ODV embedded in the matrix, does not affect calyx formation suggesting that it occurs independently of ODV (Eason et. al., 1998).

The release of the mature calyx sheathed occlusion bodies from infected cells occurs when the cell is ruptured through the action of a combination of cellular and viral proteins. It is this loss of cellular integrity in an infected host that subsequently results in the liquefaction of the body mass and release of mature OBs into the environment. A genome analysis of Ac*M*NPV identified two potential viral proteins which may be involved in this process, chitinase A (Ac-ChiA) and cathepsin (Ac-vCath). In cell culture studies, both Ac-ChiA and Ac-vCath were shown to be late viral gene products with proteolytic functions that could be inhibited with either aprotinin or leupeptin (Hawtin et. al., 1985; Slack et. al., 1998). *In vivo* studies with infected *Trichoplusia ni* larvae demonstrated that the deletion of either *ac-ChiA* or *ac-vcath* resulted in host mortality but a failure for the insect body to liquefy and release OBs (Hawtin et. al., 1997). Intriguingly, the deletion of the anti-apoptotic gene *p35* from Ac*M*NPV also resulted in a loss of liquefaction for infected *Trichoplusia ni* larvae, independent of either of Ac-ChiA and Ac-vCath (Clem et. al., 1994). It has not been demonstrated however whether p35 is directly involved in host liquefaction or indirectly involved, perhaps by increasing the levels or efficacy of Ac-ChiA or Ac-vCath in infected cells.

### *Putting It All Together: Baculovirus Infection from A to Z*

A typical baculovirus infection cycle begins with a permissive larva inadvertently ingesting occlusion bodies deposited by a previously infected host. The alkaline environment of the insect midgut dissolves the protein matrix of the OB, releasing the occlusion-derived virus to infect the nearby midgut epithelial cells. Once infected, these cells become mini-factories for the production of budded virus which serves to extend the infection, first throughout the midgut and then into the adjacent tracheal network. The secondary infection of the tracheal tissues allows the virus to escape the physical barriers of the midgut and enter into the hemocoel where it can freely infect the entirety of the host. Once the systemic spread of the infection has occurred, the production of budded virus diminishes and occluded virus production begins. This phase is marked by the accumulation of enveloped capsids in the nucleus and the rapid production of matrix proteins which eventually engulf the enveloped capsids forming environmentally

protected occlusion bodies. The release of these occlusion bodies from the infected host occurs through a liquefaction process involving viral proteolytic proteins.

## Baculovirus FGFs in the Process of Infection

With this understanding of the baculovirus infection process, we can now return to the discussion of virally encoded FGFs. In Ac*M*NPV infections, the putatively identified Ac-vFGF was shown to be an early gene product appearing as early as 3 hours post infection and peaking by 12 hours pi. Surprisingly, low levels of v*fgf* transcript were present at later time points in the infection time course along with what appears to be significantly higher levels of a bicistronic message corresponding to v*fgf* and its directly upstream open reading frame, the virally encoded *superoxide dismutase* gene (Detvisitsakun et. al, 2005). In BmNPV infections, the same expression pattern was noted with Bm-vFGF appearing as early as 2 hours post infection and persisting throughout, although because of the method of detection, it is not know whether the expression levels of Bm-v*fgf* are affected by the presence of a bicistronic message at the later time points (Katsuma et. al., 2004).

### *The Effects of vFGF in Cell Culture*

Surprisingly, despite the high degree of conservation initially suggesting an essential role for vFGF during infection, deletion of v*fgf* from the Ac*M*NPV genome showed no apparent defects when used to infect SF-21 cells. BV production, viral protein synthesis, and viral DNA replication were all comparable between the deletion and wild type viruses. Furthermore, co-infection followed by the serial passaging of the deletion and wild type viruses demonstrated there was no proliferative advantage gained by the presence of vFGF (Detvisitsakun et. al., 2006). Contrastingly, the deletion of Bm-vFGF from the genome, in BmN5 cell culture studies, did show significant defects in BV production, viral DNA replication and late viral protein synthesis, but these effects were mostly transient in nature and by late times p.i. the deletion vFGF levels were comparable to wildtype (Katsuma et. al., 2006a).

The subtle differences in phenotypes between the two deletion mutants suggested there were functional variations between Ac- and Bm-vFGF. In order to determine what these could be, researchers initially compared the two protein sequences looking for structural alterations. As expected from Group I NPVs, the two protein sequences were markedly conserved with only nineteen amino acid differences between them. Four of these differences, however, occurred specifically in the locations of the two N-glycosylation sites which are present in the Bm-vFGF

and conserved among other baculovirus FGFs (Katsuma et. al., 2004; Katsuma et. al., 2006c). The amino acid changes in Ac-vFGF at these sites removed the necessary sequence required for N-glycosylation, and a Eukaryotic Linear Motif (ELM) scan of the remaining Ac-vFGF sequence suggests the protein is devoid of this particular modification (Hunt and Dayoff, 1970; Puntervoll et.al., 2003). Western blot analysis of recombinant Ac-vFGF and Bm-vFGF, expressed in the presence of an inhibitor of N-glycosylation tunicamycin, further supported this *in silica* finding (Katsuma et. al., 2006c). Certainly, based on the preponderance of evidence, Ac-vFGF is an unglycosylated viral protein.

It has been put forth by Katsuma and others that the natural lack of N-glycosylation for Ac-vFGF has significant negative consequences with respect to vFGF function (Katsuma et. al., 2006c). The basis for this hypothesis came from several sources. First, deletion of Ac-v*fgf* from Ac*M*NPV did not result in any apparent defects in cell culture work whereas a similar deletion of Bm-v*fgf* from BmNPV resulted in significant replication defects (Detvisitsakun et. al., 2006; Katsuma et. al., 2006a). Additionally, only Bm-vFGF and not Ac-vFGF could be detected in the supernatant of Sf9 cells infected with recombinant Ac*M*NPVs expressing either Ac- or Bm-v*fgf* from the *ie-2* promoter element (Katsuma et. al., 2006c). Because of the high degree of sequence similarity between Ac-vFGF and Bm-vFGF, it was surmised that the lack of N-glycosylation directly affected the secretion of the vFGF. This conclusion was supported with the lack of secretion of several Bm-v*fgf* mutants which altered the N-glycosylation sites to resemble the Ac-v*fgf* sequence (Katsuma et. al., 2006c).

Additionally, several examples of the critical nature of N-glycosylation for FGF function have been noted for mammalian FGFs. For example, FGF-9 and -16, both of which lack a bipartite signal sequence, require N-glycosylation for efficient movement through the ER-Golgi network to the cell surface and subsequent release from the EM (Miyakawa et. al., 1999; Miyakawa and Imamura, 2003). Moreover, N-glycosylation of FGF-6, was shown to be required for the efficient stimulation of cell proliferation (Asada et. al., 1999). Because Ac-vFGF naturally lacks N-glycosylation and its deletion results in no apparent defects in cell culture, it was suggested that the viral protein is non-functional, an artifact of evolutionary changes in the Ac*M*NPV genome.

If this is indeed true and N-glycosylation is essential for vFGF function, we would expect that Ac-vFGF would not be secreted from cells or it were secreted, it would not be functional.

Based on the evidence beginning with the initial work with Ac-vFGF by Detvisitsakun and others, neither of these conditions actually applies. Recombinant Ac-vFGF, expressed from *Drosophila's heat shock protein 70* (*hsp70*) promoter element, was clearly detected in the supernatant of transfected SF-21 cells independent of N-glycosylation (Detvisitsakun et. al., 2005). Additionally, similar results were obtained from infected SF-21 cells when Ac-vFGF was expressed from the *polyhedrin* promoter using a recombinant Ac*M*NPV (Detvisitsakun et. al., 2007). The presence of Ac-vFGF in the supernatant is somewhat expected considering that unlike the mammalian FGF-9 and -16, Ac-vFGF has a well defined bipartite signal sequence. This sequence targets the nascent protein to the endoplasmic reticular pathway and eventual secretion independent of the presence of the hydrophobic N-glycosylation sequence. Interestingly, the work by Katsuma and others exploring the role of N-glycosylation for vFGF utilized a recombinant BmNPV to express mammalian FGF-9. Their work demonstrated that neither the bipartite signal sequence nor N-glycosylation was absolutely required for the efficient secretion of the FGF  further diminishing the claim that Ac-vFGF is ineffectively secreted due to the lack of this post translational modification (Katsuma et. al., 2006c).

In addition to being secreted, unglycosylated Ac-vFGF also appears to be functional even when used in cell culture. Work with partially purified, recombinant Ac-vFGF from transfected SF-21 cell supernatant was able to stimulate cell migration in a dose dependent manner (Detvisitsakun et. al., 2005). This chemokinetic activity was similar to the one observed with partially purified, recombinant Bm-vFGF which was also able stimulate BmN5 cell motility in a dose dependent manner (Katsuma et. al., 2006b). The ability to function as a chemo-attractant strongly suggests that the vFGFs from both viruses can interact with cellular receptors and function as a "traditional" FGF independent of N-glycosylation. It is therefore quite likely that the discrepancy between the phenotypes of the two deletion viruses in cell culture was not due to a loss of vFGF function, but perhaps due to the alteration of another, unknown viral factor during the construction of the recombinant BmNPV virus. Alternatively, it is also possible that the more subtle defects seen in cell culture with the deletion of Bm-v*fgf* were masked during the studies of the deletion Ac-v*fgf* virus either by the presence of endogenous growth factors secreted by the SF-21 cells or exogenous growth factors (fetal bovine serum) added to the media.

### *The Lepidoptera (v)FGF Receptor*

Perhaps the most interesting aspect of the cell culture work involving Ac-vFGF and Bm-vFGF was the identification of cellular FGFR for both *Bombyx mori* and *Spodoptera frugiperda*. It was clear from the chemotactic work with Ac-vFGF and Bm-vFGF that cellular FGF receptors were involved in viral growth factor signaling, but the sequences of these receptors was largely unknown. To fish them out, researchers turned to the closest known homolog of an insect FGFR, the Breathless receptor from *Drosophila*. Using this sequence as bait, the *Bombyx mori* Expressed Sequence Tag (EST) database was probed and a putative FGFR sequence was identified. The full length Breathless homolog from *Bombyx mori* (Bmbtl) is predicted to be 856 amino acids in length with a molecular weight of 97.3 kDa. Similar to *breathless*, *Bmbtl* is expressed in a variety of host tissues including the insect midgut, trachea and hemocytes, but not the fat body or posterior silk glands. In addition, recombinant *Bmbtl* expressed from a plasmid in Sf9 cells could be phosphorylated in a dose dependent manner with Bm-vFGF, ensuring that the receptor is indeed responsive to vFGF. Not surprisingly, high concentrations of Bm-vFGF could also lead to the phosphorylation of a *Spodoptera frugiperda*-specific FGFR (Sfbtl), probably due to the high degree of conservation between Ac-vFGF and Bm-vFGF. The exact sequence of this *Spodoptera frugiperda*- receptor was identified in the same manner as *Bmbtl* and it is predicted to encode an 847 amino acid protein with a molecular weight of 96.1 kDa (Katsuma et. al., 2006b).

An alignment of the three insect FGFRs show they are remarkably conserved with Bmbtl sharing 70 percent identity with Sfbtl and 42 percent identity with Breathless (Katsuma et. al., 2006b). Interestingly, a Blast search showed that the other Drosophila FGF receptor, Heartless, had a higher sequence identity (45%) to the Lepidoptera FGFRs compared to Breathless. This finding is supported by the fact that an ELM search predicts each of the Lepidoptera FGFRs to have the three Ig-like extracellular domains typical of most FGFRs including Heartless instead of the five Ig-like domains found in Breathless. Beside the number of extracellular Ig-like domains, Bmbtl, Sfbtl, Breathless and Heartless all share the same C-terminal architecture including a transmembrane domain and two discrete tyrosine kinase domains. It is not known at this time if there are any additional Lepidoptera FGFRs, or whether these receptors can be stimulated by other virally-encoded FGFs outside of the two tested here.

### *The Effects of Deleting Viral FGFs During a Host Infection*

The presence of the Lepidoptera FGFR in the host midgut, trachea and hemocytes suggested there could be multiple points during the normal course of infection in which vFGF could impact viral pathogenicity. To determine which of these points were actually relevant, it was necessary to examine permissive hosts infected either *per os* or through intrahemocoelic injection with a recombinant virus deficient in v*fgf* expression. The outcome of these treatments could then be compared to the outcomes of similar infections using a recombinant virus expressing normal levels of v*fgf*.

These host mortality assays were able to demonstrate the deletion of Ac-vFGF from the Ac*M*NPV genome did not affect the lethal concentration ($LC_{50}$) of the virus when given orally or delivered through intrahemocoelic injection. *Per os* infection did however increased the lethal time ($LT_{50}$) by roughly eleven hours in *Spodoptera frugiperda* neonates and *Trichoplusia ni* neonates as well as 4$^{th}$ instar *Spodoptera frugiperda* larvae. This delay in $LT_{50}$ could be circumvented through intrahemocoelic injection of BV, suggesting Ac-vFGF functioned primarily in the midgut of the host and was perhaps responsible for the virus escape into the hemocoel (Detvisitsakun et. al., 2008).

If the deletion of the Ac-v*fgf* slowed the escape of recombinant Ac*M*NPV from the midgut, it stands to reason that expressing higher levels of Ac-v*fgf* would have the opposite effect. To see if this was the case, another recombinant Ac*M*NPV was constructed which expressed *vfgf* from the *polyhedrin* promoter element. The direct effect of placing Ac-v*fgf* under *polyhedrin* control was a temporal shift in the expression pattern of this gene from early to very late in the infection cycle, as well as a dramatic increase in vFGF production. In cell culture, these changes resulted in a significantly lower BV titers and increased levels of cell death suggesting either the temporal shift or the heightened expression of Ac-v*fgf* was not totally beneficial for the propagation of the virus. However, when insects were infected *per os w*ith this Ac-v*fgf* over-expressing virus, there was a significant decrease in both the $LC_{50}$ and $LT_{50}$ in *Spodoptera frugiperda* neonates and *Trichoplusia ni* neonates as well as 4$^{th}$ instar *Spodoptera frugiperda* larvae. Unlike with the deletion Ac-v*fgf* virus, a similar significant decrease of both the $LC_{50}$ and $LT_{50}$ could also be seen when the recombinant BV was injected intrahemocoelically suggesting Ac-vFGF could have a function outside of the midgut environment. Visually, the effects of the over-expression of Ac-v*fgf* were evident in the *per os* infected hosts beginning with

the rapid melanization of the insect cuticle followed by its subsequent liquefaction nearly 24 hours before the same effects were seen with Ac*M*NPV infections (Detvisitsakun et. al., 2008).

Based on this evidence alone, the heightened expression of vFGF had a significant impact on the health of the host in the context of a virus infection. Furthermore, it is tempting to speculate that the reduction in both the $LC_{50}$ and $LT_{50}$ was due to the rapid, vFGF-mediated escape of the virus from the midgut and the establishment of tertiary infections in the hemocoel. The effects of this virus in cell culture suggest an alternative hypothesis however. It is equally plausible to think that the reduction in both $LC_{50}$ and $LT_{50}$ was due to vFGF-induced toxicity which destroyed host tissues independent of infection. Clearly, more work with this virus is needed to determine which speculation is correct.

Similar host mortality assays done with a recombinant BmNPV lacking v*fgf* in 4$^{th}$ instar *Bombyx mori* larvae also showed no significant differences in the $LC_{50}$ when given orally or delivered through intrahemocoelic injection. There was, however, a significantly longer delay in $LT_{50}$ (~20 hours) evident with the *per os* infection using the deletion Bm-v*fgf* virus. Unlike the outcome seen with the deletion Ac-v*fgf* virus, the intrahemocoelic injection of the recombinant BV into 5$^{th}$ instar *Bombyx mori* larvae could not circumvent the effects seen with *per os* infections resulting in an identical 20 hour delay in the $LT_{50}$. This finding suggested that Bm-vFGF functioned during the course of infection in the hemocoel of the host and not in the midgut. This conclusion was further refined by evidence that there was a significant decrease in circulating BV in the hemolymph when intrahemocoelic injection was used to introduce deletion Bm-v*fgf* virus into the host, an effect markedly similar to the one seen in cell culture studies of the same deletion Bm-v*fgf* virus (Katsuma et. al., 2006a).

To better understand these results, researchers next modified the deletion Bm-v*fgf* virus and wildtype BmNPV by introducing the jellyfish *green fluorescent protein* (*gfp*) gene under *ie1* promoter control into the viral genomes. This reporter product allowed the researchers to visually track the progress of infection from both oral feeding of OBs and intrahemocoelic injection of BV. For *per os* infections, the deletion of Bm-v*fgf* did not appear to impact either the primary infection of midgut epithelial cells or the secondary infection of tracheal cells and fat body but did impact the infection of hemocytes as there appeared to be significantly fewer infected at late times (<96 hours) pi. Intrahemocoelic injections of the deletion Bm-v*fgf* virus showed a similar defect in the hemocyte infection, but only within 6 hours pi. At later times, the number of

infected hemocytes was consistent between the deletion Bm-v*fgf* virus and wildtype BmNPV (Katsuma et. al., 2008).

It has been suggested by Katsuma and others, based on this evidence, that Bm-vFGF is acting as a chemotactic factor which preferentially targets circulating hemocytes for infection, perhaps to help disseminate the virus infection throughout the hemocoel or prevent a host immune response. This explanation is unlikely, however for several reasons. First, we would expect that in the absence of Bm-vFGF and the corresponding infection of hemocytes, there would be a delay in the dissemination of the virus which would be evident in fat body and distal tracheal tissues. In the reported work, these tissues were infected at the same time, independent of the presence of Bm-vFGF. Secondly, with the intrahemocoelic injection of BV, the numbers of infected hemocytes were the roughly the same as early as 12 hours post injection, yet there was still a significant decrease in BV in the hemocoel as well as a 20 hour delay in the $LT_{50}$ of infected hosts. If the role of Bm-vFGF was limited to chemotaxis and the infection of circulating hemocytes, this result makes little sense. It is therefore quite likely that there are additional roles for Bm-vFGF during the course of a virus infection of *Bombyx mori* larvae which have not been identified to date.

### *Virally-encoded FGFs in Brief*

Virally encoded FGFs have been putatively identified in 48 of the 53 sequenced baculovirus genomes. Two of these vFGFs, one from Ac*M*NPV and the other from BmNPV, have been somewhat characterized both biochemically as well as *in vivo* during the course of host infections. It has been shown that both are secreted signal ligands which can bind to Heparin-Sepharose as well as induce cell motility, presumably through the stimulation of cellular FGFR. Neither of these vFGFs is an essential gene, but deletions of Ac-vFGF and Bm-vFGF result in a delay in host mortality when the virus is introduced *per os*.

Aside from these somewhat superficial attributes, Ac-vFGF and Bm-vFGF appear to contribute to several different viral outcomes. Deletion of Bm-v*fgf*, for example, results in decrease production of BV in the hemocoel as well as a number of cell culture defects, none of which are seen with the deletion of Ac-v*fgf*. In addition, Bm-vFGF appears to function in the spread of virus after it has escaped the midgut, whereas Ac-vFGF works specifically to help the virus escape the midgut, perhaps by causing the de-lamination of trachea.

The discrepancies in the results of the cell culture studies as well as the bioassays are somewhat perplexing considering the degree of conservation between the two vFGF ligands. One possible explanation is the effects of vFGFs are host specific and dependent upon a variety of cellular factors. These factors may include receptor availability, the mechanism of release for the sequestered ligand, or the overall context in which the vFGF signaling is occurring. Alternatively, Ac-vFGF and Bm-vFGF may have similar functions during the course of infection, but these functions are masked either through the action of other viral genes or by technical deficiencies which makes it appear as if these two proteins are responsible for wholly different processes.

# CHAPTER 4 - Virion-associated vFGF

Despite the significant amount of data generated by the biochemical and *in vivo* studies of the two baculovirus FGFs, there were still several important questions which had yet to be answered, Chief among them was to determine both the timing and levels of vFGF production during the course of infection. In the previous works with both Ac- and Bm-vFGF, detection of the protein was only accomplished using a variety of heterologous promoter elements including *Drosophila's heat shock 70* and the viral *polyhedrin* promoter. Based on transcript analysis, however, neither of these promoter elements drive the expression of vFGF to the same level or in the same temporal time frame as the native promoter element.

In addition to determining the protein expression levels, it was also important to determine the cellular localization of Ac-vFGF during infection. In the various mammalian models discussed earlier, FGFs are either localized intracellularly or secreted and retained to the extracellular matrix via HSPGs until subsequent release. It has been suggested that the lack of N-

glycosylation in Ac-vFGF results in a deficiency in secretion and *de facto* intracellular localization. However, indirect evidence from a variety of sources suggests that non-glycosylated Ac-vFGF is a still efficiently secreted. Determining whether Ac-vFGF was localized to the cell surface would certainly resolve any lingering questions on this subject.

Another question which was developed during the course of doing a literature review involved a potential role for vFGF in virus attachment. In the early days of baculovirus research, a great deal of emphasis was placed on utilizing viral OBs, specifically Ac*M*NPV, as an alternative to traditional chemical pesticides in managing crop pests (reviewed by Szewczyk et. al. 2006). In order to prove the safety of this type of application, several researchers began to examine the effects of baculovirus exposure to mammalian systems. Perhaps much to their surprise, high concentrations of BV could efficiently transduce a variety of mammalian and Dipteran cell lines (Carbonell et. al., 1985; McIntosh and Shamy, 1980; Volkman and Goldsmith, 1983). Neither the cell lines tested nor the direct infection of a mammalian host could support baculovirus DNA replication however, although a limited number of early viral transcripts were detected including the viral trans-activating protein IE1 (Carbonell et. al., 1985; Döller et. al., 1983; Murges et. al., 1997). The expression of these viral genes does not appear to affect host cellular function which makes recombinant Ac*M*NPV an ideal platform to transiently introduce heterologous proteins into a variety of mammalian cell lines and tissues, perhaps even in a therapeutic manner (reviewed in Hu, 2008; Kenoutis et. al., 2006).

Basic research into the process of transduction demonstrated BV entry was temperature dependent and occurred via absorptive endocytosis (Duiset et. al., 1999). Subsequent work was further able to show the major envelope protein GP64 was sufficient to mediate viral entry into mammalian cells much like with entry into insect cells (Tani et. al., 2001). Conversely, attachment of BV to mammalian cells was non-saturatable even when a multiplicity of infection (MOI) of 5000 plaque forming units (PFU) per cell was employed. It was therefore unlikely that cellular surface proteins were acting as receptors for attachment as is the case with insect cells.

Non-specific, electrostatic interactions were the next likely target considering both Adenovirus and Herpes Simplex Virus (HSV-1) had previously been shown to attach to mammalian cells in a similar manner (Fuller and Lee, 1995; Summerford and Samulski, 1998). To demonstrate this, Duiset and others co-incubated HEK 293 cells and BV in the presence of the cationic compound polybrene. Virus transduction of the cells was dramatically inhibited

(<90%) over a range of polybrene concentrations suggesting negatively-charged cell surface components were responsible for attachment. To determine if there was any specificity to this interaction, they attempted competition assays with soluble forms of chondroitin sulfate, dermatan sulfate and heparan sulfate. Of the three, only soluble heparan sulfate was capable of interfering with BV transduction. In vitro assays with Heparin-Sepharose beads subsequently confirmed that BV had a significant affinity for this specific proteoglycans, and removal of the HSPG from HEK 293 cells using heparinase inhibited transduction by nearly 50 percent (Duiset et. al., 1999). Together, this evidence strongly supported the conclusion that the interaction of heparan sulfate proteoglycans with Ac*M*NPV BV is the major mode of attachment in the transduction of mammalian cells.

These results, in light of the intimate relationship between FGFs and HSPGs, prompted us to ask the question whether vFGF played any role in BV attachment to cells. Certainly, for this to be the case, we would first have to answer two very important questions: 1) Whether the *in vitro* interaction of BV with heparin-Sepharose reported by Duiset and others is mediated by Ac-vFGF and 2) Is Ac-vFGF retained on the envelope of BV upon egress from the cell? In addition to potentially affecting BV attachment, the presence of Ac-vFGF on the BV envelope opens up another interesting avenue of research; specifically whether the BV-associated Ac-vFGF could interact with and stimulate the cellular FGFR.

And finally, the *in vivo* and *in vitro* results with the virus expressing Ac-v*fgf* from the *polyhedrin* promoter element were intriguing, but it was difficult to determine if the observed phenotypes were due to an increased pathogenicity of the recombinant virus or heightened toxicity in response to such high levels of vFGF. Additionally, the very late temporal expression of Ac-vFGF was problematic with respect to deducing the role of vFGF on the BV particle. To address these concerns, a second recombinant Ac*M*NPV was constructed with Ac-v*fgf* under *Drosophila*'s *heat shock 70 protein* promoter control. As noted earlier, this promoter element was previously used to drive the high level transient expression of Ac-v*fgf* in transfected SF-21 cells as early as 12 hours post transfection without any discernible cell death. It was hoped by incorporating the *hsp70-vfgf* cassette into the virus, an increased level of Ac-vFGF would be achieved while more closely mirroring the timing of expression of the native promoter.

## Effects of Virion-associated vFGF

Transcription of *vfgf* has been previously examined; *vfgf* was classified as an early gene since transcription was evident at early times post infection (p.i.) and in the presence of cycloheximide (Detvisitsakun et al., 2005; Katsuma, et al., 2004). However, protein production kinetics have not been reported during the infection cycle. To examine vFGF accumulation during infection, we constructed an Ac*M*NPV-based bacmid expressing *vfgf* with a hemagglutinin (HA) tag at the C terminus to facilitate immunodetection. Briefly, 448 base pairs of v*fgf* (~82% from the N terminus) were replaced via homologous recombination with the zeocin resistance gene using the commercially available bacmid bMON14272. The enhanced green fluorescent protein gene (*egfp*) under the *Drosophila heat shock protein 70* promoter control, a high-level inducible promoter in insect cells, and the *polyhedrin* (*polh*) gene under *polh* promoter control were introduced into the *polh* locus of bMON14272, resulting in AcBAC–v*fgf*KO (Detvisitsakun et al., 2006). To construct AcBAC-vfgfHARep virus, *egfp* and *polh* cassettes, and the HA-tagged v*fgf* under the control of its own promoter was inserted in AcBAC-vfgfKO, so that only one copy of the gene was present (Fig.1A). The *vfgf* promoter, a 207 base pair fragment, has been previously shown to support *vfgf* expression (Detvisitsakun et al., 2006). To construct a virus carrying *vfgf* driven by the *Drosophila hsp70* promoter, AcBAC-HSP70v*fgf*HA, the 207 base pair *vfgf* promoter fragment was replaced with the *hsp70* promoter. The presence of v*fgf* and its correct insertion location within the viral genome was confirmed using PCR (results not shown). RT-PCR was used to ensure that *vfgf* was expressed in AcBAC-v*fgf*HARep. We detected *vfgf* transcripts at 6, 12, 24 and 48 h p.i. (Fig. 1B); AcBAC-v*fgf*Rep virus, expressing untagged *vfgf* from the same promoter, also expressed *vfgf* transcripts (Detvisitsakun et al., 2006). Although it is possible that *vfgf* is better expressed at its native locus, this 207 base pair *vfgf* promoter region was sufficient to repair phenotypic defects in AcBAC-v*fgf*KO (Detvisitsakun et al., 2006).

To evaluate whether insertion of *vfgf* under either native or *hsp70* promoter control in AcBAC-v*fgf*HARep and AcBAC-HSP70v*fgf*HA, respectively, affected virus replication, we performed single-step growth curve analyses. SF-21 cells were infected with either AcBAC-v*fgf*HARep, AcBAC-HSP70v*fgf*HA or AcBAC, a virus in which v*fgf* has not been perturbed, at a multiplicity of infection (MOI) of 5 plaque forming units (PFU)/cell, supernatant was collected

at several times p.i., and the titer determined by $TCID_{50}$. We did not detect any significant growth differences between the viruses throughout the time courses of infections (Fig. 1C). We determined accumulation of vFGF driven by its native promoter by infecting TN-368 cultured cells at an MOI of 5 PFU/cell with either AcBAC-v*fgf*HARep or AcBAC-HSP70v*fgf*HA and immunodetection. vFGF steady-state levels were observed in immunoblots with whole cell lysates prepared from AcBAC-v*fgf*HARep-infected cells at 24 and 48 h p.i. but not at 12 h p.i. or earlier (Fig. 2A and results not shown). Despite numerous attempts, vFGF could not be detected in the supernatant of AcBAC-v*fgf*HARep-infected cells (Fig. 2B). AcBAC-HSP70vfgfHA-infected cells, as expected, exhibited much higher levels of vFGF accumulation starting at 12 h p.i., peaking at 24 h p.i. and continuing at 48 h p.i., even though 25-fold less total protein was loaded per lane than in the AcBAC-v*fgf*HARep cell lysate (Fig. 2A). vFGF was also detected in the supernatant of AcBAC-HSP70v*fgf*HA-infected cells, suggesting vFGF was efficiently secreted and released from cells (Fig. 2B). It is possible that the inability to detect vFGF in the medium of AcBAC-v*fgf*HARep-infected cells, where *vfgf* expression is lower than from AcBAC-HSP70-vfgfHA-infected cells, was due to protein detection sensitivity levels. As a signaling molecule, the necessary levels of vFGF for efficient function do not need to be high.

We detected vFGF in whole cell lysates and in cell culture media when expressed at high enough levels. When expressed at lower levels, vFGF secretion may be hard to detect. In addition, the presence of vFGF in whole cell lysates could be due to secreted vFGF tethered to the surface of cells by heparan sulfate proteoglycan interactions or its presence intracellularly. To validate that vFGF was cell surface-bound, SF-21 cells were infected with AcBAC-HSP70v*fgf*HA and harvested 24 h p.i. Infected cells were fixed and immunolabeled with anti-HA antibody followed by a gold-labeled secondary antibody prior to embedding in resin. Dense pockets of gold-labeled antibodies, corresponding to cell surface-bound vFGF, were evident on cells, confirming that vFGF was indeed secreted and retained on the surface of cells (Fig. 3A). To further strengthen the observation that vFGF binds to cell membranes and have a quantitative comparison of cell bound-vFGF from each virus construct, TN-368 cells were infected with AcBAC-HSP70v*fgf*HA, AcBAC-v*fgf*HARep, or AcBAC-v*fgf*KO and harvested at 12, 24 and 48 h p.i. After harvesting, cell surfaces were immunolabeled with anti-HA primary antibody and an allophycocyanin (APC)-conjugated secondary antibody, and labeled cells were analyzed using

fluorescence-based flow cytometry. The number of vFGF positive cells was considerably higher in AcBAC-HSP70v*fgf*HA- than AcBAC-v*fgf*HARep-infected cells at all time points examined although with both AcBAC-HSP70v*fgf*HA and AcBAC-v*fgf*HARep infections, the number of vFGF positive cells increased approximately 5.4 to 6-fold between 12 and 24 h p.i., respectively (Fig. 4). Only background levels of antibody were bound to the cell surfaces of AcBAC-v*fgf*KO-infected cells at all time points.

We predicted that if vFGF was secreted from cells and bound to heparan sulfate proteoglycans on cell membranes, virions budding from cells would acquire heparan sulfate-bound vFGF on their envelopes. To examine if budded virions incorporated vFGF on the virus particle, budded virions from AcBAC-v*fgf*KO-, AcBAC-v*fgf*HARep-, or AcBAC-HSP70v*fgf*HA-infected SF-21 cells were purified by gradient centrifugation, fixed onto Nickel Formvar/Carbon 200 mesh grids, and vFGF was detected using immunoelectron microscopy. Gold-labeled particles specific to HA-tagged vFGF were detected on AcBAC-v*fgf*HARep virions (Fig. 3B); however, these were absent in AcBAC-v*fgf*KO virions, indicating specificity (Fig. 3D). In the majority of experiments, we could only detect three or less gold-labeled particles on individual vFGF-HA carrying virions. In contrast, there were over 10-fold more gold-labeled particles conjugated to anti-GP64 that associated with GP64, an envelope associated viral protein essential for virus entry (Fig. 3C). Interestingly, the gold-labeled vFGF-HA particles were usually localized at one end of the virion. Virions derived from the AcBAC-HSP70v*fgf*HA-infected cells showed increased gold-labeled particles also at the bulbous end of the virion, reaffirming the polarization of virions and vFGF (Fig. 3E).

Since FGFs, including vFGF, have high affinity to heparin-Sepharose, we next compared the affinity of AcBAC-v*fgf*HARep, AcBAC-v*fgf*KO and AcBAC-HSP70v*fgf*HA purified virions to heparin-Sepharose and determined whether the presence or absence of vFGF on the virus surface affected this property. Equal numbers of infectious virions, calculated prior to use by $TCID_{50}$, were incubated with heparin-Sepharose beads, sulfated and carboxylated glucosaminoglycans on Sepharose that yield an overall negative charge and serve as a cation exchangers. To reduce non-specific interactions, the beads were washed with 125 mM NaCl to disrupt ionic interactions prior to eluting the bound proteins with a 1.25 M NaCl solution. All fractions were dialyzed against TC-100 incomplete media and virus solutions titered. We found that dialysis was necessary since high salt concentrations used during washes and elution

interfered with infections (Lehiy and Passarelli, unpublished results). AcBAC-v*fgf*KO virions had less affinity to heparin-Sepharose than either AcBAC-v*fgf*HARep or AcBAC-HSP70v*fgf*HA virions, with the majority of virions eluting in the unbound fraction, flow through, and wash fractions. In contrast, virions with vFGF on the surface had higher affinity to heparin beads, eluting mainly in the presence of high salt concentrations (Fig. 5). Non-specific virus binding to heparin-Sepharose can be attributed to either cellular FGFs incorporated on the viral envelopes, FGFs from the serum containing media, or other ionic interactions.

It has previously been demonstrated that heparin-Sepharose purified vFGF stimulates motility of insect cells by stimulating an FGFR and ensuing a subsequent signaling cascade (Detvisitsakun et al., 2004; Katsuma et al., 2006); thus, we asked whether virions containing vFGF could stimulate cell motility. Using transwells with polycarbonate membrane inserts, 2 x $10^4$ SF-21 cells were placed in the upper chamber while 1 x $10^5$ to 1 x $10^7$ infectious purified AcBAC-HSP70v*fgf*HA or AcBAC-v*fgf*KO virions were placed in the lower chamber. After four hours, the transwell inserts were removed and cells that migrated to the lower chamber were quantified using CellTiter-Glo luminescent substrate that measures ATP production and is indicative of live cells. The amount of cell migration to the lower chamber increased in proportion to virus titer with 1 x $10^7$virions producing statistically significant differences between the three viruses used in the assay (Fig. 6A). At this point, however, we were concerned that the amount of migration we were observing at the higher virion concentrations could be due to overwhelming virus infection and not to vFGF specifically. To address this, we treated 1 x $10^7$purified AcBAC-HSP70v*fgf*HA virions with 1U of Heparinase III, an enzyme known to cleave heparin sulfate proteoglycans from the cellular surface. After treatment, the virion and supernatant fractions were isolated using centrifugation and used in the same migration experiment outlined above. The amount of migration induced from virions decreased dramatically after Heparinase III treatment, while the supernatant containing the vFGF was still capable of inducing significant cell motility (Fig. 6B).

vFGFs is a membrane-associated protein that interacts with other membrane proteins, including heparan sulfate proteoglycans and the FGFR. In addition, a number of viruses belonging to several virus families, use heparan sulfate molecules as their receptors (Flint, et al., 2005). Thus, we were interested in evaluating whether the presence or absence of vFGF on the surface of the virions affected virus attachment to and/or entry into permissive insect cells. To

this end, virions from AcBAC-v*fgf*HARep, AcBAC-v*fgf*KO, and AcBAC-HSP70v*fgf*HA were radiolabed with $^{35}$S-methionine and partially purified to remove unbound radioactivity. Radiolabeled AcBAC-v*fgf*HARep, AcBAC-v*fgf*KO, or AcBAC-HSP70v*fgf*HA was added at an MOI of 1 PFU/cell to chilled SF-21 or TN-368 cells. At specific times post attachment, the virus supernatant (*i.e.*, unattached virions) was removed and the cells washed three times with cold PBS. After washing, the cells were lysed and the radioactivity determined in a scintillation counter. SF-21 cells treated with AcBAC-v*fgf*KO bound less radioactive particles than AcBAC-HSP70v*fgf*HA and AcBAC-v*fgf*HARep at every time point measured (Fig. 7A). Similar defects were observed using TN-368, although the binding defects of AcBAC-v*fgf*KO compared to viruses encoding *vfgf* were not as marked as those in SF-21 cells, and differences were not significant 30 minute post attachment (Fig. 7B). We repeated the binding assay at 25 °C using SF-21 cells and also observed a defect in attachment at this temperature, which was more prominent at early times (Fig. 7C).

To determine whether the presence of vFGF on the budded virus envelope affected entry, we inhibited endosomal acidification, a step required for endosomal membrane fusion, with ammonium chloride at several time points after AcBAC-v*fgf*Rep or AcBAC-v*fgf*KO attachment to SF-21 cells (Hefferon et al., 1999). At early times post attachment (0 through 20 minutes), treatment of cells with ammonium chloride resulted in an entry defect ranging between 24.6 and 34.5% for AcBAC-v*fgf*KO-compared to AcBAC-v*fgf*HARep-infected cells (Fig. 7D). At 30 and 60 minutes post attachment, treatment of AcBAC-v*fgf*KO-infected cells with ammonium chloride resulted in an entry defect of 15.9 and 14.1%, respectively, compared to AcBAC-v*fgf*HARep. AcBAC-v*fgf*Rep- and AcBAC-v*fgf*KO-infected but ammonium chloride-untreated cells showed no significant differences (Fig. 7D, control column). Although we observed entry differences between AcBAC-v*fgf*HARep and AcBAC-v*fgf*KO, they were too small to infer any significance during the normal virus attachment phase.

## Future Work

In this current study, we observed that AcBAC-v*fgf*HARep-infected TN-368 cells produced low, detectable levels of HA-tagged Ac-vFGF at 24 and 48 h p.i, but not at the earlier time points assayed. This is somewhat inconsistent with previous results which showed Ac-*vfgf* as an early gene product, with message present as early as 3 hours p.i., but persisting throughout the course of infection. The persistence of the message may indicate that Ac-vFGF accumulates

to detectable levels slowly over the course of infection, which explains the detection pattern seen here (Detvisitsakun et al., 2005). We were also able to establish that the Ac-vFGF detected in the cell lysate fraction was localized to the cell surface, consistent with the expected model of secretion followed by subsequent binding to the EM.

The inability to detect Ac-vFGF in the supernatant of AcBAC-v*fgf*HARep-infected cells has been attributed by Katsuma and others to be due to a lack of N-glycosylation which inhibits efficient secretion. The detection of Ac-vFGF in the supernatant from AcBAC-HSP70v*fgf*HA-infected cells suggests this is not the case. Instead, we think that Ac-vFGF is expressed at low levels from its native promoter and released from the cell in concentrations under 5 ng/ml, well below the detectable limits of our assays, but still quite capable of inducing chemotaxis (Detvistsakun, Wu, and Passarelli, unpublished results; Katsuma et al., 2006a). Additionally, any of the Ac-vFGF-HSPG complex released from the cell would likely interact with cellular receptors and quickly become internalized in the signaling process, further removing it from the supernatant fraction.

The detection of membrane-associated Ac-vFGF during BV production was intriguing, so we investigated and were able to detect Ac-vFGF on the envelope of budded virions. We then tested the effects of BV-associated Ac-vFGF, first by measuring the affinity of virions to bind heparin-Sepharose *in vitro* and then by measuring attachment to cells *in vivo*. In both cases, the presence of Ac-vFGF on the virus envelope played a role in mediating attachment, but a closer examination of the *in vivo* results suggests the effects are highly transient particularly at temperatures more closely resembling the physiological conditions for infection. This observation is consistent with the lack of any observable cell culture defects in attachment from deleting Ac-v*fgf*. It is therefore quite likely that Ac-vFGF only plays a minor role, compared to perhaps GP64 and F protein, at mediating attachment to the insect cells. This is not to say that vFGFs, in general, are not significantly involved in attachment under certain conditions. In mammalian systems, for example, the role of vFGF in attachment has not been ascertained and it is quite possible that it plays a significant role in this process. Additionally, Group II viruses and Granuloviruses, which lack GP64, may rely more heavily on vFGFs to mediate attachment prior to entry.

The ability for BV-associated Ac-vFGF to stimulate motility was also intriguing, not because it was able to stimulate motility, but because it could be an additional method for the

release of the functional Ac-vFGF-HSPG signaling complex from the cell. Recent work by Means and Passarelli has demonstrated that metalloproteases are activated in the context of infection, but only presumably after vFGF release. It is not clear what factor is responsible for the initial cleavage of the signaling complex, but the egress of BV with vFGF would accomplish this during the course of infection. Certainly, before this hypothesis is accepted, more work would have to be placed into understanding what factors if any are responsible for the initial release of Ac-vFGF.

## Virion Associated vFGF: Figure and Legends

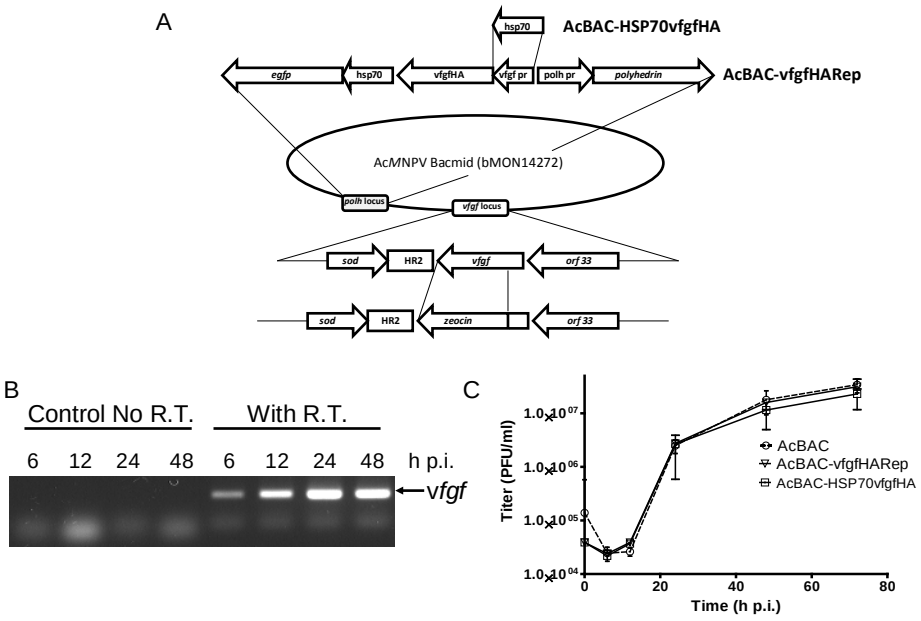


**Figure 1:** Construction of two recombinant baculoviruses expressing a hemagglutin (HA) tagged *vfgf*. A) Using an Ac*M*NPV bacmid template lacking a functional *vfgf* gene, an HA-tagged *vfgf* under the control a 207-base pair native promoter element was inserted into the polyhedrin (*polh*) locus along with an enhanced green fluorescent protein (*egfp*) gene and the *polh* gene. To construct a recombinant virus with *vfgf* under heat shock protein (*hsp*) 70 promoter control, the 207-base pair promoter element was replaced with the *Drosophila hsp* 70 protein promoter. Confirmation of the transposition site was verified by PCR (results not shown). B) Transcription of *vfgf* under its native promoter control was confirmed using RT-PCR at various hours (h) post infection (p.i.) and *vfgf* specific primers. C) One-step growth curve analysis of AcBAC-vfgfHARep and AcBAC-HSP70vfgfHA. SF-21 cells were infected with AcBAC, AcBAC–vfgfHARep or AcBAC-HSP70vfgfHA at an MOI of 5 PFU/cell. At indicated h p.i., the supernatant was collected and the amount of infectious virus present was determined.

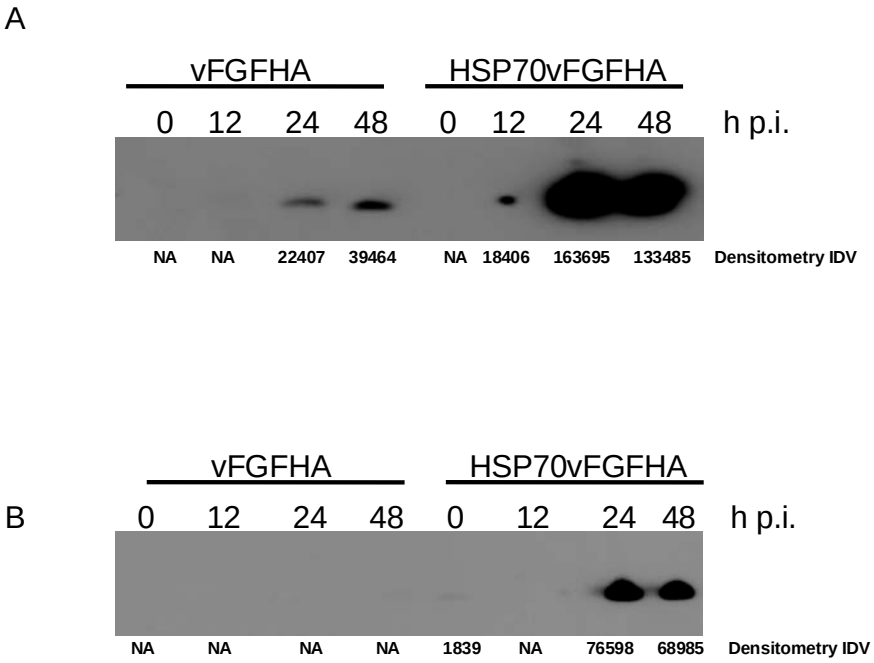


**Figure 2:** Production of vFGF during virus infection. Intracellular (A) and extracellular (B) production of vFGF from TN-368 cells infected with AcBAC-v*fgf*HA (vFGFHA) or AcBAC–HSP70v*fgf*HA (HSP70 VFGFHA) at an MOI of 10 PFU/cell. Cells were lysed at the times (hours, h) post infection (p.i.) indicated at the top and total protein levels were quantified. Lanes with vFGFHA lysates have 25-fold more total protein compared to HSP70 vFGFHA lanes. After transfer to a PVDF membrane, the samples were immunoblotted using anti-HA antibody. Integrated Densitometry Values (IDV) for each lane, normalized to background levels reported at the bottom of each panel. NA, not applicable, equivalent to background levels

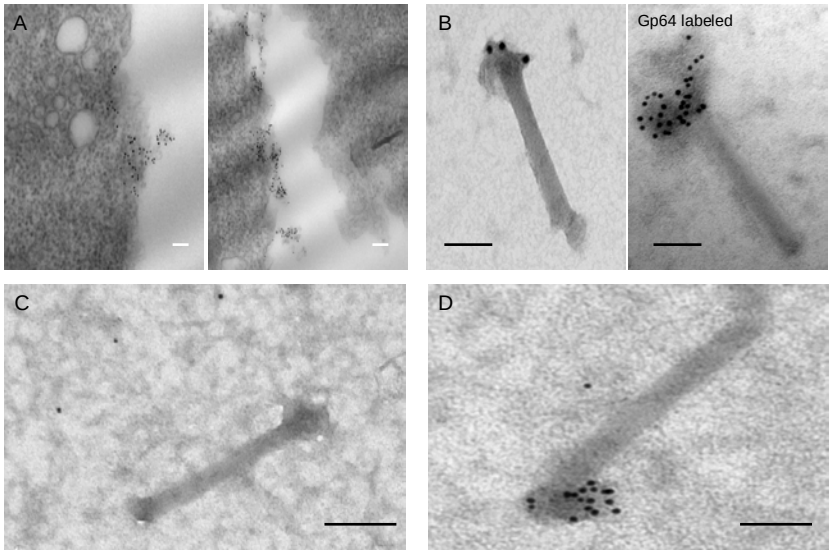


**Figure 3:** Presence of vFGF on the surface of cells and budded virions. (A) SF-21 cells were infected with AcBAC-HSP70v*fgf*HA at a MOI of 5 PFU/cell. At 24 hours post infection, cells were fixed and immunolabeled with anti-HA.11 primary antibody and a gold-conjugated secondary antibody. After embedding, cells were examined for the presence of vFGF on the cell surface. vFGFHA was detected in dense pockets denoted by the dark label. (B-D) SF-21 cells were infected with AcBAC-v*fgf*HARep (B, C), AcBAC-v*fgf*KO (D), or AcBAC-HSP70v*fgf*HARep (E) at an MOI of 0.1 PFU/cell and virions isolated by high speed centrifugation using either sucrose or NycoPrep TM gradients. Virus particles were labeled with anti-HA.11 antibody (B, D, E) or anti-GP64 antibody (C) and a gold-conjugated secondary antibody. Individual virions were visualized using a Philips MC-100 transmission electron microscope. The images are representative of the findings from three independent experiments. Bars represent 0.1 μM.

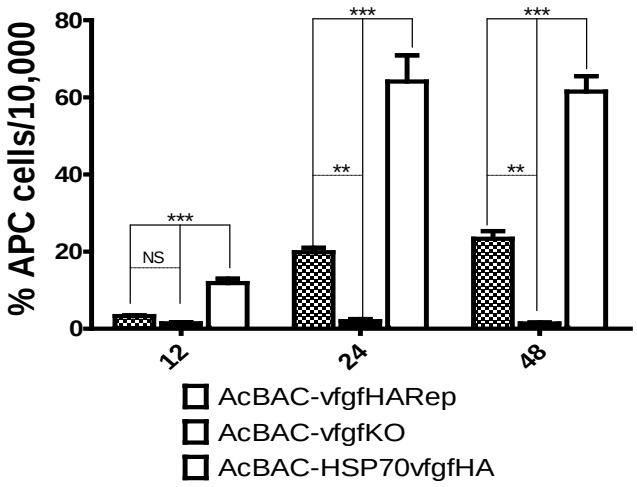


**Figure 4:** TN-368 cells were infected at a MOI of 5 PFU/cell with either AcBAC-v*fgf*HARep, AcBAC-v*fgf*KO, or AcBAC-HSP70v*fgf*HA. At 24 and 48 hours post infection (h p.i.), the cells were harvested and resuspended in PBS, pH 6.2. The surface of cells was labeled with anti-HA and an APC-conjugated secondary antibody. Labeled cells were analyzed for APC fluorescence using a FACSCalibur flow cytometer. The number of cells reported as APC positive are from a total of 10,000 cells counted. (*** $p < 0.05$, ** $p<0.01$).

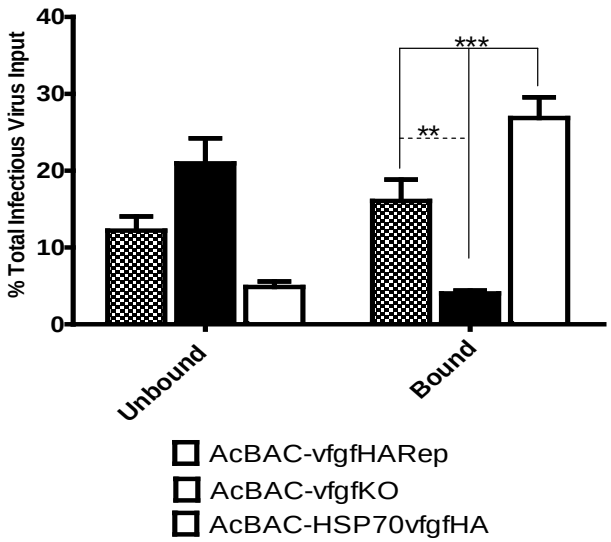


**Figure 5:** Binding of budded virions to heparin-Sepharose beads. Purified virions from either AcBAC-v*fgf*HARep, AcBAC-v*fgf*KO, or AcBAC-HSP70v*fgf*HA-infected SF-21 cells were incubated with heparin-Sepharose beads. The beads were washed with a salt-containing solution to remove non-specific binding and then with a 1.25 M NaCl solution. After dialysis, the flow-through, wash and elution fractions were dialyzed to remove excess salt and the infectious virus titered. Virus in the flow-through and wash fractions was combined and is represented in the unbound columns. The elution fraction represents the amount of virus that remained bound to the column after washing. (*** $p<0.05$, ** $p< 0.01$).

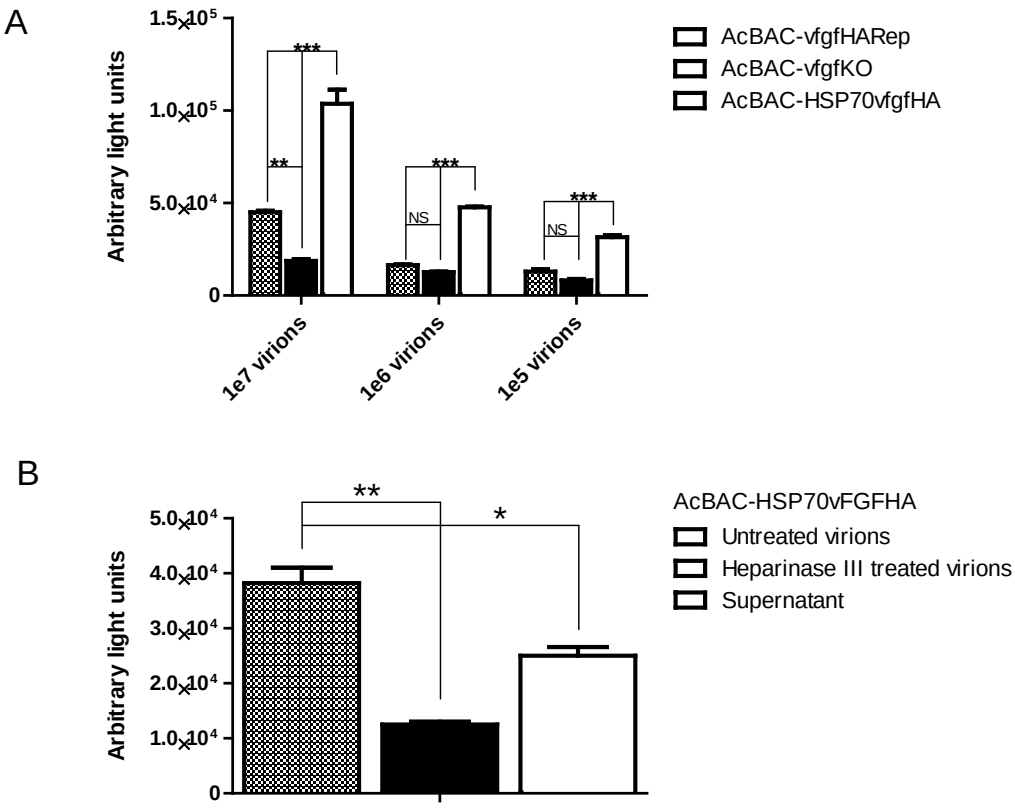


**Figure 6:** Virus induced cell migration. (A) SF-21 cells (2 x $10^4$) were placed in the upper chamber of a migration chamber with an 8 µM pore size and purified infectious virions from AcBAC-v*fgf*HARep, AcBAC-v*fgf*KO, or AcBAC-HSP70v*fgf*HA, were placed in the lower chamber. After 4 hours of incubation at 27C, the upper chamber was removed and the number of cells that migrated to the lower chamber was determined using Cell Titer Glo Luminescent Assay. (B) AcBAC-HSP70vFGFHA virions were treated with Heparinase III to liberate vFGF-heparin complexes from the virus envelop. Virions were then isolated and reconstituted using centrifugation and used in a motility assay along with the supernatant containing vFGF. (*** $p< 0.05$, ** $p<0.01$, * $p<0.5$)

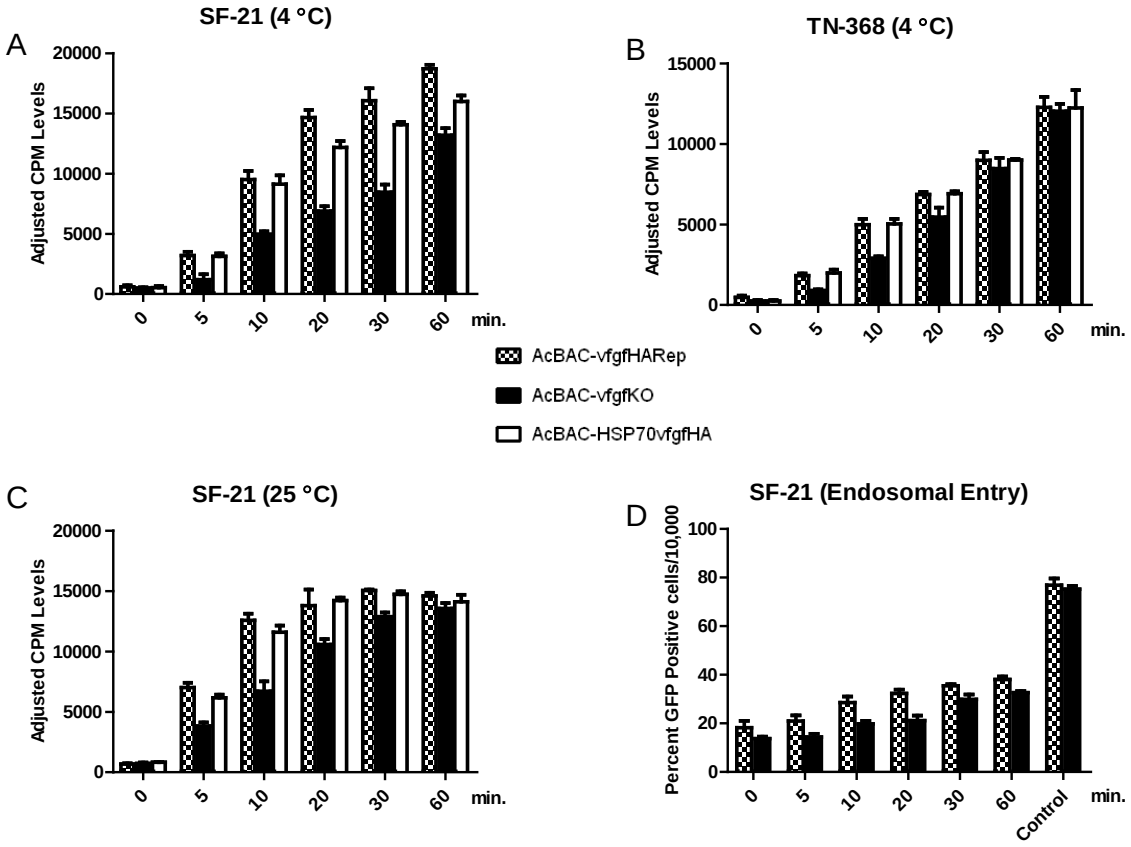


**Figure 7:** Virus attachment and entry into SF-21 and TN-368 cells. $^{35}$S-methionine radiolabeled AcBAC-v*fgf*HARep, AcBAC-v*fgf*KO, or AcBAC-HSP70v*fgf*HA virions (MOI of 1 PFU/cell) were allowed to attach to SF-21 (A, C) or TN-368 (B) cells at either 4C (A, B) or 25C (C) for the specific times (in minutes) indicated at the bottom of each graph. After attachment, the virus supernatant was removed and cells washed 3 times prior to harvesting. Radioactivity (CPM) in the cell lysate was determined in a scintillation counter. To normalize all samples, the CPM counts on all samples were adjusted relative to initial CPM counts. D) To determine vFGF effects on virus entry, AcBAC-v*fgf*HARep or AcBAC-v*fgf*KO virions (MOI of 1 PFU/cell) were allowed to attach to SF-21 cells for 60 minutes at 4C. Virus supernatant was removed, cells washed, and resuspended in TC-100 complete media. Exit from the endosome was inhibited by the addition of ammonium chloride at specific times post attachment (in minutes) or left untreated (Control) as indicated at the bottom of the graph. At 24 h post attachment, eGFP expression was determined using flow cytometry.

# CHAPTER 5 - Baculovirus Core Gene Ac-orf109

Over the course of our examination of Ac-vFGF, we became interested in the functions of several baculovirus core genes. Currently, there are 31 genes identified among all the baculovirus genomes sequenced to date (reviewed by Herniou and Jehle, 2007; McCarthy and Theilmann, 2008). These are divided, based on function, into five broad categories: viral transcription, replication, structural proteins, auxiliary proteins, and proteins of unknown function. Among the core genes of unknown function which we were interested in characterizing was Ac-*orf109*. Initially identified in the *Autographa californica* M Nucleopolyhedrovirus genome between position 94721 and 95893, Ac-*orf109* is predicted to encode a 390 amino acid protein with a molecular mass of 44.8 kDa (Ayers 1994). Component analysis of the ODV form of Ac*M*NPV has indicated Ac-orf109 is one of 22 proteins associated with the nucleocapsid although work with a homolog of Ac-orf109 found in *Helicoverpa armigera* S Nucleopolyhedrovirus (64.6% consensus with Ac-orf109) determined it was also a component of both the envelope and capsid components of BV (Fang et.al., 2003 Braunagel, 2003). A BLAST search using the protein sequence of Ac-orf109 showed no homologous proteins outside of baculovirus and an ELM search revealed no known functional motifs were present (Puntervoll et.al., 2003).

Recently, two independent reports were published on the characterization of Ac*M*NPV lacking Ac-*orf109*. The first of these reports, by Fang and collegues (2009), used homologous recombination in *Escherichia coli to* delete 1142 nucleotides of the open reading frame of Ac-*orf109* from the commercially available Ac*M*NPV-bacmid, leaving only 43 nucleotides of the C-terminus to act as a promoter element for the downstream open reading frame, Ac-*orf108.* The deletion Ac-*orf109* construct was then transfected into *Spodoptera frugiperda* cells (Sf9) and monitored for the production of BV and ODV. Over the course of 96 hours post transfection (pt), only the cells initially transfected showed obvious signs of virus infection including enlarged nuclei and the presence of occlusion bodies. The lack of virus spread was not due to deficiencies in either viral DNA synthesis or late gene expression, and capsid structures were evident in the supernatant of transfected cells (Fang et. al., 2009). Based on these observations, they concluded the deletion of Ac-*orf109* resulted in the production of non-infectious BV.

To bolster these observations, Fang and others generated a recombinant virus expressing an epitope tagged version of Ac-orf109. Immunoblots of isolated BV and ODV produced from infections with this virus showed the protein was present in both structures making Ac-orf109 one of only eleven baculovirus proteins known to be associated with both virus forms (McCarthy et. al., 2007). Fractionation of the infected cells into nuclear and cytoplasmic fractions showed Ac-orf109 was equally distributed between the two, congruent with its role in both BV and ODV formation (Fang et. al., 2009).

The second of these reports, by Lin and collegues (2009), used the same recombination method to construct their deletion Ac-*orf109* construct, but unlike the earlier report, they only deleted a 278 nucleotide internal fragment (102-380) from Ac-*orf109,* leaving a large N-terminal fragment unperturbed. The results of this deletion were similar to the ones observed by Fang and others with respect to a lack of systemic spread of the virus. Viral DNA replication of the deletion Ac-*orf109* virus was equivalent to that of the controls through 48 hours pt, but was at least 600- to 1000 fold- less at later time points, most likely due to the lack of virus spread to nearby cells. Other than enlarged nuclei and electron dense bodies associated with virogenic stroma, no other obvious signs of virus infection were noted in the deletion Ac-*orf109* virus-transfected cells including the formation of occlusion bodies or the presence of intact capsids (Lin et. al., 2009). The effects of deleting Ac-*orf109,* in their hands at least, seemed to be much more severe than those reported by Fang and others.

To resolve the discrepancies between these two reports, we constructed a number of recombinant viruses (Fig. 8A) using the method outlined by Bideshi and Federici (2000). The first of these deleted 94% of Ac-*orf109* including the start codon from the commercially available Ac*M*NPV bacmid bMON14272 leaving only a 69 nucleotide C-terminal fragment to act as the promoter element for Ac-*orf108*. Since this bacmid virus lacks the *polyhedrin* (*polh*) gene, we used the translocation method previously described by Detvisitsakun to introduce *polh* controlled by its native promoter as well as the enhanced *green fluorescent protein* gene (eGFP) under Drosophila *heat shock protein 70* promoter control to produce the final product AcBAC-*orf109*KO (Detvisitsakun, et. al., 2006). To ensure that the phenotype observed from deleting Ac-*orf109* were specific and not due to inadvertent mutations or deletions in other areas of the bacmid, we also constructed a repair virus, AcBAC-*orf109*Rep, using the deletion backbone and translocation. In this case, along with eGFP and polh, Ac-*orf109* driven by a 49 nucleotide

upstream region acting as the promoter element was reintroduced into the genome at the *polyhedrin* locus. After construction of AcBAC-*orf109*KO and AcBAC-*orf109*Rep, PCR was used to confirm that recombination and translocation occurred as designed (Fig. 8B). In order to determine protein levels and temporal expression patterns of Ac-orf109 during an infection, a third virus which introduced a C-terminal hemagglutinin epitope (HA) tagged form of Ac-*orf109* into the deletion background was created (AcBAC-*orf109*glyHA). Each of these viruses was then transfected into SF-21 cells and the effects observed with respect to virus replication.

## Results of Deleting Ac-*orf109*

Ac-orf109 homologs are predicted in all baculoviruses sequenced to date including those viruses infecting members of the orders Diptera and Hymenoptera (Fig. 9). Protein sequence alignments of the 53 predicted homologs using ClustalW software suggest a high degree of conservation with over 47% consensus, but a BLAST search shows no significant sequence identity with non-baculovirus proteins. Analysis of the promoter element of Ac-*orf109* shows a TATA element at +8 nucleotides upstream of the start codon and a consensus late gene initiator site (G)TAAG at +14 nucelotides. Consistent with this finding, a Northern blot analysis of total RNA extracted from SF-21 cells infected with Ac*M*NPV hybridized with an RNA-specific probe derived from Ac-*orf109* identifies a ~1.6 kb message first evident at 9 h p.i. and continuing through 48 h p.i. (Fig. 10A). The transcript was markedly reduced in infected cells treated with aphidicholine, a viral DNA synthesis inhibitor, consistent with the expression profile of late viral genes, but surprisingly was not affected in the presence of cyclohexamide. Consistent with these results, Ac-orf109 was detected in SF-21 cells infected with AcBAC-*orf109*glyHA as early as 12 hours p.i., and the levels of protein remained consistent throughout the remainder of the time course (Fig. 10B)

To determine the role of Ac-orf109, viral DNA from both AcBAC-*orf109*KO and AcBAC-*orf109*Rep were transfected into SF-21 cells and then these cells were observed for signs of infection. At 24 h post transfection (p.t.), between 10 and 25% of the AcBAC-*orf109*KO and AcBAC-*orf109*Rep transfected cells were expressing e*gfp* corresponding to the cells initially transfected with bacmid DNA (Fig. 11 A and C, respectively). By 48 h p.t., 100% of the AcBAC-*orf109*Rep transfected cells expressed e*gfp*, whereas in AcBAC-*orf109*KO transfected cells, the number of fluorescent cells remained relatively constant (Fig 11 B and D). The lack of cell to cell virus transmission seen with the AcBAC-*orf109*KO- transfected cells strongly

suggests a defect in infectious BV production. By 96 h p.t., however, AcBAC-*orf109*KO-transfected cells showed the presence of occlusion bodies suggesting that the viral replication cycle was not completely stalled with Ac-*orf109* deletion (Figure 11M).

To test for the presence of infectious budded virus, supernatant from AcBAC-*orf109*KO- or AcBAC-*orf109*Rep-transfected cells was used to treat naïve SF-21 cells. By 48 h p.i. all the cells incubated with AcBAC-*orf109*Rep supernatant (Fig 11J) showed obvious signs of infection (fluorescent cells with occlusions), whereas none of the cells treated with AcBAC-*orf109*KO supernatant were infected (Fig 11I). To rule out the possibility that this phenotype was due to errors generated during bacmid construction, we utilized plasmids containing either Ac-*orf109* or a frame-shift mutant to trans-complement the deletion virus. The plasmids p109 (containing Ac-*orf109* and Ac-*orf110*) and p109FS (which introduced a premature stop codon truncating Ac-*orf109* by 40%) were co-transfected with AcBAC-*orf109*KO into SF-21 cells. At 24 h.p.t., the number of *egfp*-expressing cells were similar to the those observed with the AcBAC-*orf109*KO- or AcBAC-*orf109*Rep-transfected cells (Fig 11 E and G) By 48 h p.t., nearly 100% of the cells co-transfected with p109 showed obvious signs of infection while the percentage of those co-transfected with the frame-shift mutant of Ac-orf109 remained constant (~15%) (Fig 11 F and H). As before, supernatant from these transfections was used to treat naïve SF-21 cells, but only the supernatant from AcBAC-*orf109*KO co-transfected with p109 produced new rounds of infection (Fig. 11 K and L).

The absence of budded virus production in AcBAC-*orf109*KO-infected cells could be attributed to many factors including lack of viral DNA replication, late viral gene expression, packaging of the capsids, or even shuttling of the intact capsids to the cell surface. To account for some of these possibilities, we looked at genome replication and late viral gene expression. Using the method outlined by Vanarsdall, SF-21 cells were transfected with 1 µg of AcBAC, AcBAC-*orf109*KO, AcBAC-*orf109*Rep, or vAc$^{gp64-}$, a *gp64* null mutant capable of replicating viral DNA genome, but unable to produce infectious BV (Oomens and Blissard, 1999; Vanarsdall et. al., 2006). At specific times p.t., genomic DNA from infected cells was harvested and the Ac*M*NPV genomic copy number was determined for all the samples taken. As expected, AcBAC- and AcBAC-*orf109*Rep-infected cells, produced significantly more copies of viral DNA at the late time points compared to AcBAC-*orf109*KO, attributable to the spread of these viruses systemically (Fig. 12A). Interestingly, both AcBAC-*orf109*KO- and vAcgp64-transfected

cells appeared to have more copies of viral DNA at earlier time points (24 and 36 h p.t.) compared to either cells transfected with the control virus or AcBAC-*orf109*Rep. One possible explanation for this is both AcBAC and AcBAC-*orf109*Rep produce infectious BV which exits the cell and reduces the total genome copy number at the early time points. Alternatively, the disparity in genome copy numbers at the early time points could be attributable to subtle differences in the transfection efficiencies of the various bacmids, although the consistency of the results over three independent experiments suggests this is unlikely.

To determine the ability of viruses to express late viral genes, we used Reverse Transcriptase (RT)-PCR and gene specific primer sets to identify the presence of early (*lef-1*), early and late (*gp64*) and very late (*polh*) viral transcripts from SF-21 cells transfected with either AcBAC-*orf109*KO or AcBAC-*orf109*Rep. Viral message from each of the target genes could be detected at 12, 24, and 48 h p.t, suggesting that Ac-*orf109* deletion did not adversely affect transcription of these genes and probably gene transcription at different stages p.i. (Fig. 12B). In addition, a western blot using cell lysates from SF-21 cells transfected with AcBAC-*orf 109*Rep or AcBAC-*orf109*KO and immuno-probed for GP64, an early to late viral product, showed the protein was present in both transfected cell lysates at 24 h p.t. In supernatants collected at 24, 48, and 72 h p.t., however GP64 could only be detected from AcBAC-*orf109*Rep transfected cells which produce infectious budded virus (Fig. 13).

Since AcBAC-*orf109*KO was able to express representative genes in the three temporal phases and replicated its genome, the lack of spread for infection coupled with the absence of GP64 in the supernatant strongly suggested a failure to produce BV in the deletion mutant. We considered that the inability of AcBAC-*orf109*KO to produce BV was at the assembly stage where capsids are packaged with DNA and then shuttled out of the nucleus. To test this hypothesis, SF-21 cells were transfected with AcBAC-*orf109*KO or AcBAC-*orf109*Rep DNA and at set intervals the cells were harvested, fixed in 2% para-formaldehyde and embedded in resin. Thin sections of embedded cells were examined for the presence of budded and occluded virus. Cells transfected with AcBAC-*orf109*Rep DNA showed virions in the nucleus (Fig. 14 C and D), cytoplasm (Fig. 14C) and BV in the supernatant (data not shown) at 24 h p.t. In cells transfected with AcBAC-*orf109*KO, however, virions could only be detected in the nucleus and not the cell periphery or supernatant suggesting an inability for the capsids to egress from the nucleus (Fig. 14 A and B).

At late times post transfection, capsids were clearly aligned in the ring zone in both AcBAC-*orf109*Rep- or Ac-BAC-*orf109*KO-transfected cells (Fig. 15 A and C). The capsids in the AcBAC-*orf109*KO-transfected cells however were devoid of the characteristic ODV envelope (Fig. 15 A and B) seen in AcBAC-*orf109*Rep-transfected cells (Fig. 15 C and D). The lack of encapsulation appeared to affect the number of ODV embedded in the polyhedrin-based occlusion bodies formed in cells transfected with Ac-BAC-*orf109*KO (Fig. 16B), but not in the cells transfected with AcBAC-*orf109*Rep (Fig. 16A).

A recent study involving *Helicoverpa armigera* Nucleopolyhedrovirus (HearNPV) demonstrated interactions of ODV proteins utilizing a yeast two-hybrid screening method. The results of this screen indicated Ha-EC43, a homolog of Ac-orf109, interacted with HA9, the homolog of Ac-142 (Peng et. al., 2010). Since the results of two-hybrid studies are sometimes mis-leading, we performed interaction studies using plasmids expressing either an HA- or FLAG-epitope tagged version of Ac-*orf109* or a FLAG-epitope tag version of Ac-142. In these studies, Ac-orf109 could be immuno-precipitated with Ac-142 as well as itself suggesting they formed a complex during infection (Fig. 17). Interestingly, the deletion of Ac-142, another baculovirus core gene of unknown function, from the genome of Ac*M*NPV results in a phenotype identical to the one observed with the Ac-*orf109* deletion (Vanarsdall et. al., 2007; McCarthy et. al. 2008). It is tempting to speculate based on the interaction of the two proteins, as well as the similar phenotypes of the deletion mutants, that Ac-orf109 and Ac-142 form a functional complex during the course of infection which is essential for the egress of capsids from the nucleus for BV formation, as well as the encapsulation of capsids for the proper formation of ODV.

## Future Work

Based on observations here, Ac-*orf109* is an essential baculovirus core gene. It is expressed as a late viral gene product with detectable levels of protein produced as early as 12 hours post infection. Deletion of Ac-orf109 from the genome of Ac*M*NPV results in an inability of the virus to spread. This defect can be recovered though either through the re-introduction of Ac-*orf109* into the genome or the expression of the protein *in trans* from a plasmid.

Closer examination of cells transfected with the deletion Ac-*orf109* virus showed an absence of BV production was responsible for the defect. Viral DNA replication, late gene expression, and capsid formation in the nucleus all appeared to be normal. At late times post

transfection, multiple occlusion bodies could be detected in the cell suggesting the infection cycle continued in the absence of Ac-*orf109.*

Of the two previous studies on Ac-*orf109*, our results most closely mirror those of Fang and others, but with one important distinction. In their report, they were capable of detecting non-infectious BV in the supernatant of cells transfected with their deletion Ac-*orf109* virus (Fang et. al., 2009). Despite numerous attempts, we were not able to detect any evidence of BV in the supernatant of cells transfected with Ac-BAC-*orf109*KO, nor were we able to visually detect virions exiting the nucleus. There are several potential explanations for this.

First, our transfection efficiency with our recombinant viruses using SF-21 cells was only between 20 and 35 percent across all of the experiments. A lower transfection efficiency, compared to the ones achieved by Fang and others, could reduce the amount of non-infectious BV in the supernatant to below a detectable threshold. Second, in our attempts to isolate BV, we examined supernatant at 72 hours post transfection whereas Fang and others, in their experiments, collected supernatant at 96 hours post transfection. The additional 24 hours may have allowed for the accumulation of BV to accumulate to detectable levels.

While both of these explanations are plausible, they are not likely. To begin with, based on the data provided, our transfection efficiencies appeared to be roughly equivalent to the ones achieved by Fang and others. With similar transfection efficiencies, it is unlikely that the levels of non-infectious BV production would be significantly different. Additionally, Fang and others were able to detect viral DNA as well as the proteins GP64 and VP39 in the supernatant of transfected Sf9 cells at 72 hours p.t., presumably due to the presence of non-infectious BV at this time point (Fang et. al., 2009). Based on these results, there appears to be sufficient levels of non-infectious BV for detection at this earlier time point, however, we could not duplicate any of these results with our recombinant virus. On a side note, the presence of GP64-containing BV in the supernatant is particularly troubling considering GP64 by itself can mediate attachment and entry into insect cells (Hefferon et. al., 1999; Monsma et. al., 1996). It is therefore unclear at what stage the deletion Ac-*orf109*-produced BV become non-infectious.

A third possible explanation, which is more likely considering all the evidence, is the capsids, DNA and proteins detected in the supernatant were the product of inadvertently lysed cells. In the Materials and Methods section, Fang and others described a collection method that involved the initial use of rubber policeman to scrape the transfected Sf9cells, releasing them

from the plate into the supernatant. The cell/supernatant mixture was then separated via low speed centrifugation and the supernatant removed for later analysis. In our experiments, however, the supernatant was removed from the cells while the cells were still attached to the plates. It was then clarified by low speed centrifugation to remove any cells or debris prior to storage for later analysis. This subtle difference in collection methods may account for the identification of non-infectious BV by Fang and others, whereas we could not detect any evidence of this.

The phenotype of the deletion Ac-*orf109* virus noted by Lin and others is starkly different than the one observed by Fang and others, as well as the phenotype associated with Ac-BAC-*orf109*KO. We can only hypothesize that the method of deletion strongly affected the phenotype. In the Materials and Methods section of Lin and others, a 278 base pair fragment was deleted from the center portion of Ac-*orf109* and replaced with an antibiotic-expressing cassette. This deletion method results in a large N-terminal Ac-*orf109* fragment as well as C-terminal fragment roughly twice the size of Fang and others. It is possible that a truncated Ac-orf109 protein is produced from the remaining N-terminal fragment, and this protein somehow interferes with some aspect of late gene expression and capsid formation but surprisingly not viral DNA replication. Alternatively, the phenotype observed with Lin and other's deletion Ac-*orf109* virus could be due to an errant mutation occurring during the production process independent of Ac-*orf109*. Without more evidence, such as a complementation assay, it is impossible to determine which of these explanations has more validity.

Aside from determining the phenotype arising from the deletion of Ac-*orf109*, this work also demonstrated briefly that Ac-orf109 and Ac-142, two baculovirus core genes, associate together, perhaps forming a functional complex essential for directing both capsid egress out of the nucleus for BV production and the *de novo* synthesis of the membrane encapsulating ODV. Currently, little is known about the either of these processes, which makes the interaction of Ac-orf109 and Ac-142 an ideal starting point for further study. Aside from determining the structural basis for their interaction, studies could be done to determine which, if any, viral or host proteins associate with this complex over the course of infection. In addition, even though these core genes are highly conserved, it would be interesting to determine if homologs from Group II or Granuloviruses could functionally substitute for Ac-orf109 or Ac-142, either singly or as a pair. In the same vein, a small number of Group I and Group II baculoviruses are known to form only

singly enveloped capsids prior to their being embedded into the protein matrix to form OBs. It would be interesting to determine if this phenotype could be changed to an MNPV phenotype in the presence of Ac-orf109 or Ac-142.

# Baculovirus Core Gene: Figures and Legend

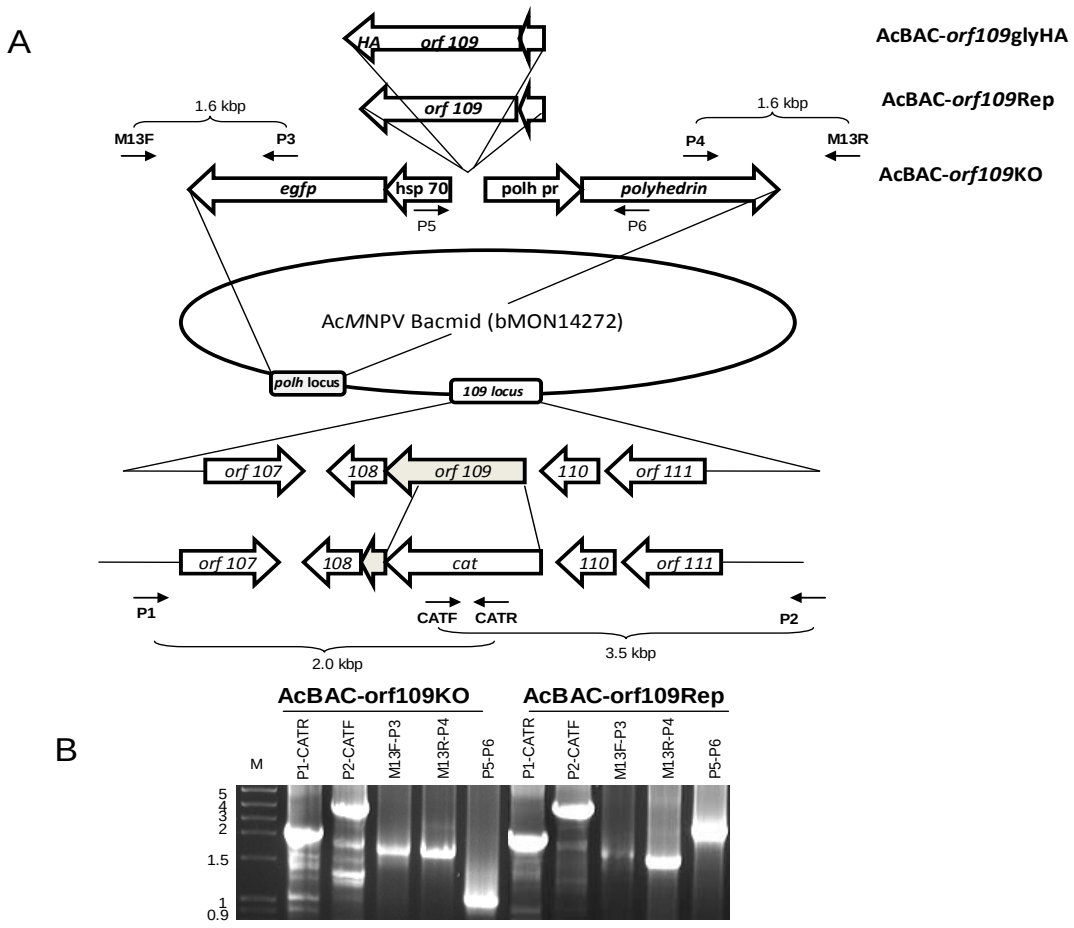


**Figure 8:** Construction of AcBAC-*orf109*KO, AcBAC-*orf109*Rep and AcBAC-*orf109*glyHA viruses A) Within the coding sequence of Ac-orf109, 94% was replaced through homologous recombination with the chloramphenicol acetyl transferase resistance gene leaving a 69 nucleotide C-terminal fragment as the promoter element for Ac-*orf108*. After recombination, transposition was used to reintroduce the *polyhedrin* (*polh*) gene under native promoter control and the enhanced green fluorescent protein (*eGFP*) gene under the *Drosophila heat shock protein 70* (hsp70) promoter control. For AcBAC-*orf109*Rep and AcBAC-*orf109*glyHA, in addition to transposition of *polh* and *eGFP*, Ac-*orf109* or the HA epitope tagged version of Ac-*orf109* was re-introduced into the AcBAC-orf109KO backbone driven by a 49 nucleotide native promoter element. B) To determine correct recombination and transposition events, PCR with specific primer sets was used for both the AcBAC-orf109KO and AcBAC-orf109Rep constructs.

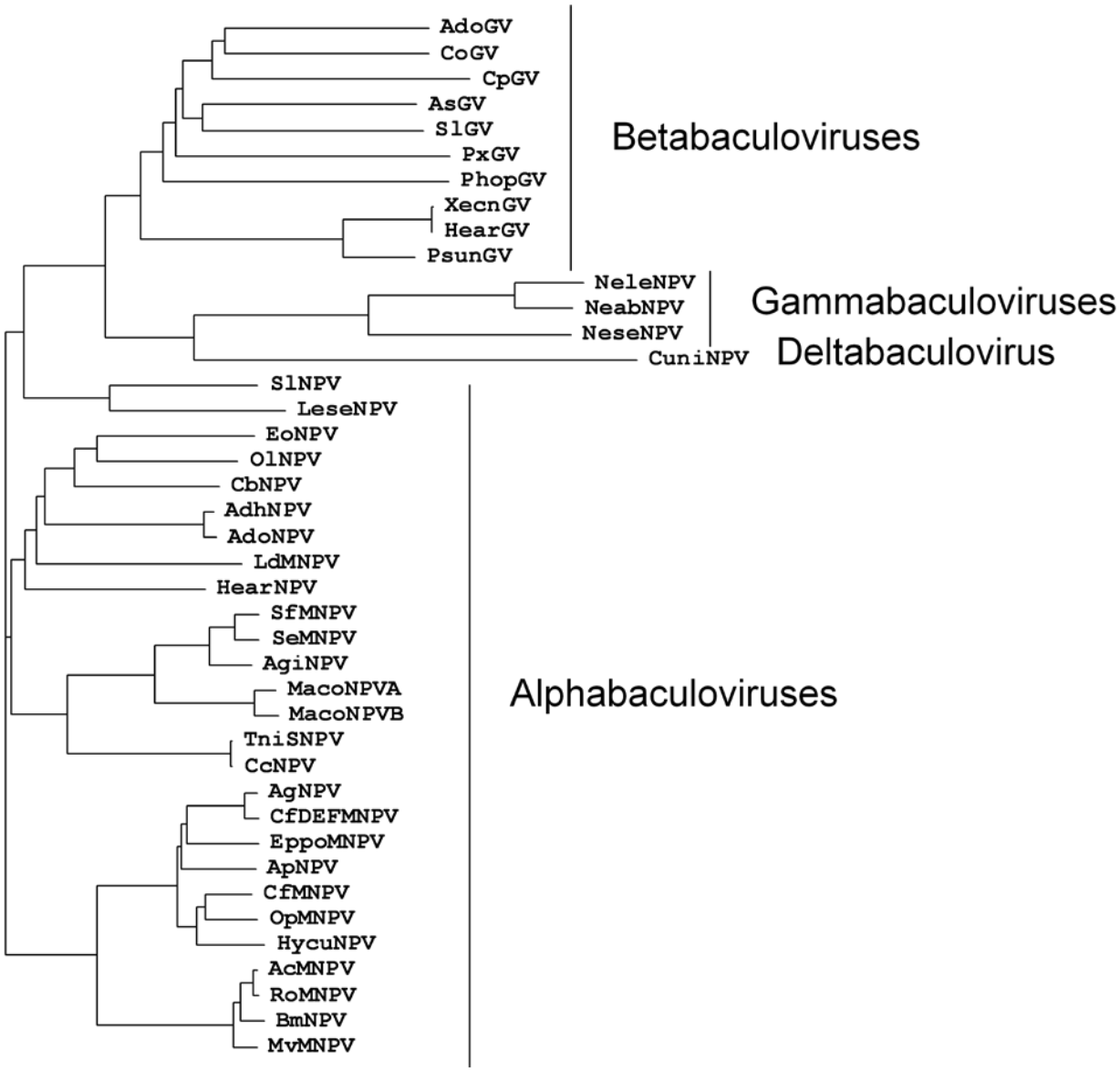


**Figure 9:** Phylogenetic analysis of Ac-*orf109* homologs. Putative protein sequences with homology to Ac-*orf109* were identified from the 53 baculoviruses genomes currently sequenced and then aligned using ClustalW software. After the alignments were completed, a phylogenetic tree was assembled using Phylip parsimony method for protein sequences. Sequence identity to Ac-orf109 ranged from 98% (RoMNPV) to 47% (CuniMNPV).

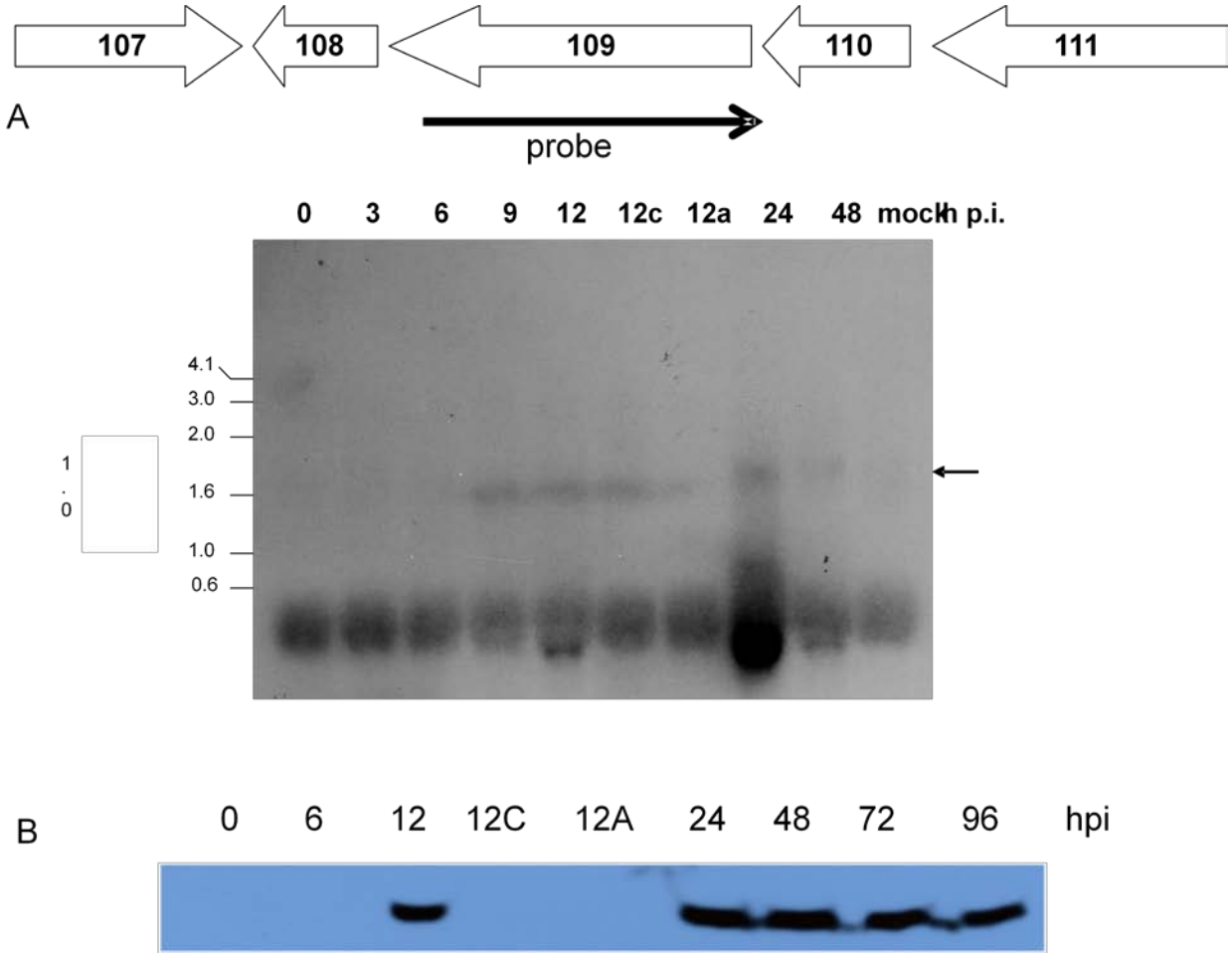


**Figure 10:** Transcription and protein expression profiles of Ac-*orf109*. A) cRNA probe complimentary to Ac-*orf109* was hybridized to a Northern blot of total RNA isolated from Ac*M*NPV-infected SF-21 cells (MOI of 20 PFU/cell) at various times p.i. indicated by the numbers along the top. One major RNA was identified at roughly 1.6 kb which corresponds to the size of the predicted Ac-*orf109* transcript. Total RNA was also collected at 12 h p.i from cells treated with cycloheximide (12c) 30 minutes prior to infection or aphidicolin (12a) immediately after infection. Numbers on the right correspond to standards in kb. B) SF-21 cells were infected (MOI 5 PFU/cell) with AcBAC-*orf109*glyHA. Two wells of cells were treated with either cycloheximide (12c) 30 minutes prior to infection or aphidicolin (12a) immediately after infection. At the times indicated (top), the cells were collected, lysed and then placed in a SDS-polyacrylamide gel. After transfer to a PVDF membrane, the samples were immunoblotted using anti-HA antibody

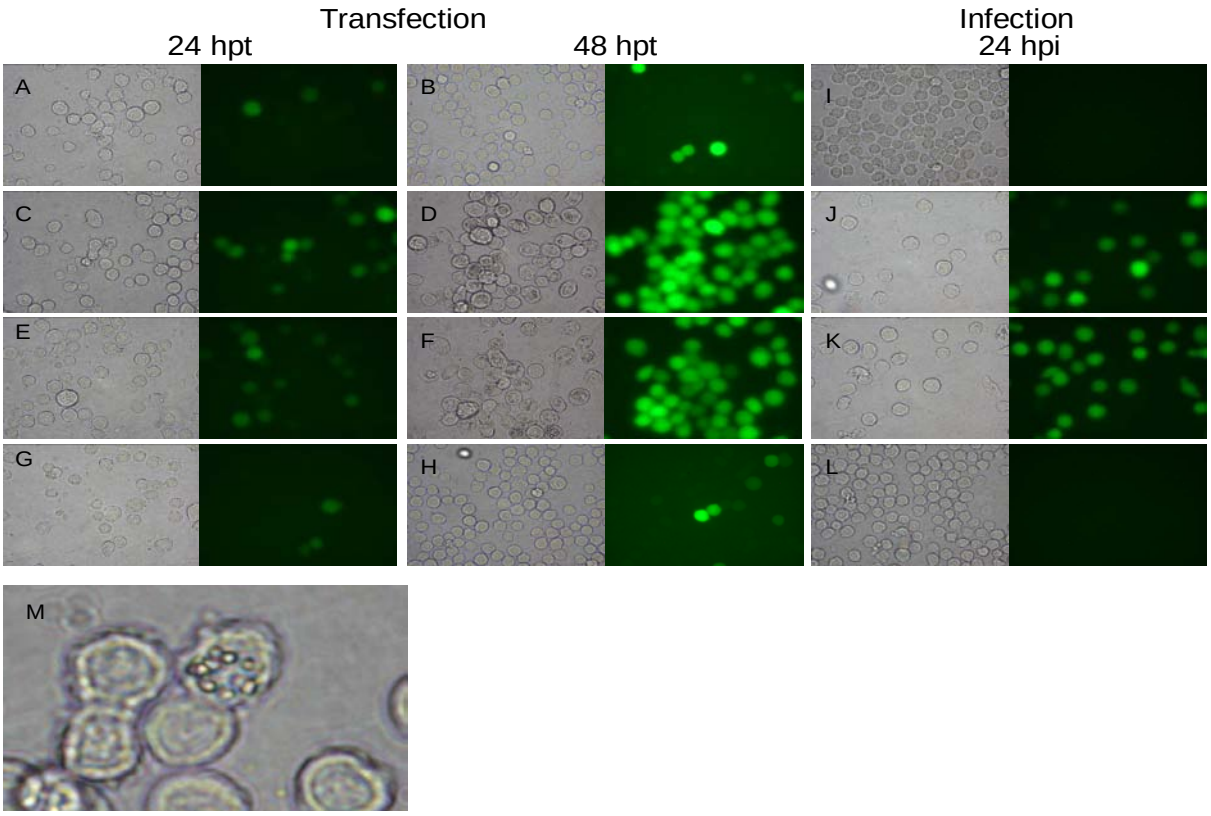


**Figure 11:** Complementation assay with AcBAC-orf109KO. AcBAC-orf109KO (A,B) or AcBAC-orf109Rep (C,D) DNA was transfected into SF-21 cells and then examined for the presence of eGFP at the times indicated. At 48 hours post transfection (p.t.), supernatant was removed from the transfected cells and used to treat naïve SF-21 cells. At 24 h post infection (p.i.), cells treated with AcBAC-orf109KO supernatant (M) or AcBAC-orf109Rep supernatant (J) were visualized for eGFP expression. In three replicate experiments, the AcBAC-orf109KO transfection failed to produce infectious budded virus. In an attempt to trans-complement the deletion phenotype, a plasmid containing Ac-orf 109 under native promoter control (p109) or a frame shift mutant (p109FS) were co-transfected with AcBAC-orf109KO into SF-21 cells. By 24 h p.t., both the p109 (E) and p109FS (G) had green fluorescent cells. By 48 h post transfection, infection had spread in the wells co-transfected with p109 (F), but not with the frame shift mutant (H). The supernatant from each transfection was collected at 48 h and used to treat naïve SF-21 cells. The supernatant from the p109-AcBAC-*orf109*KO co-transfection contained budded virus capable of infecting the SF-21 cells (K) while the co-transfection with p109FS plasmid appeared to be devoid of infectious budded virus, similar to the AcBAC-*orf109*KO (L). By 96 h p.t., occlusion bodies are clearly present in SF-21 cells transfected with AcBAC-*orf109*KO (M).

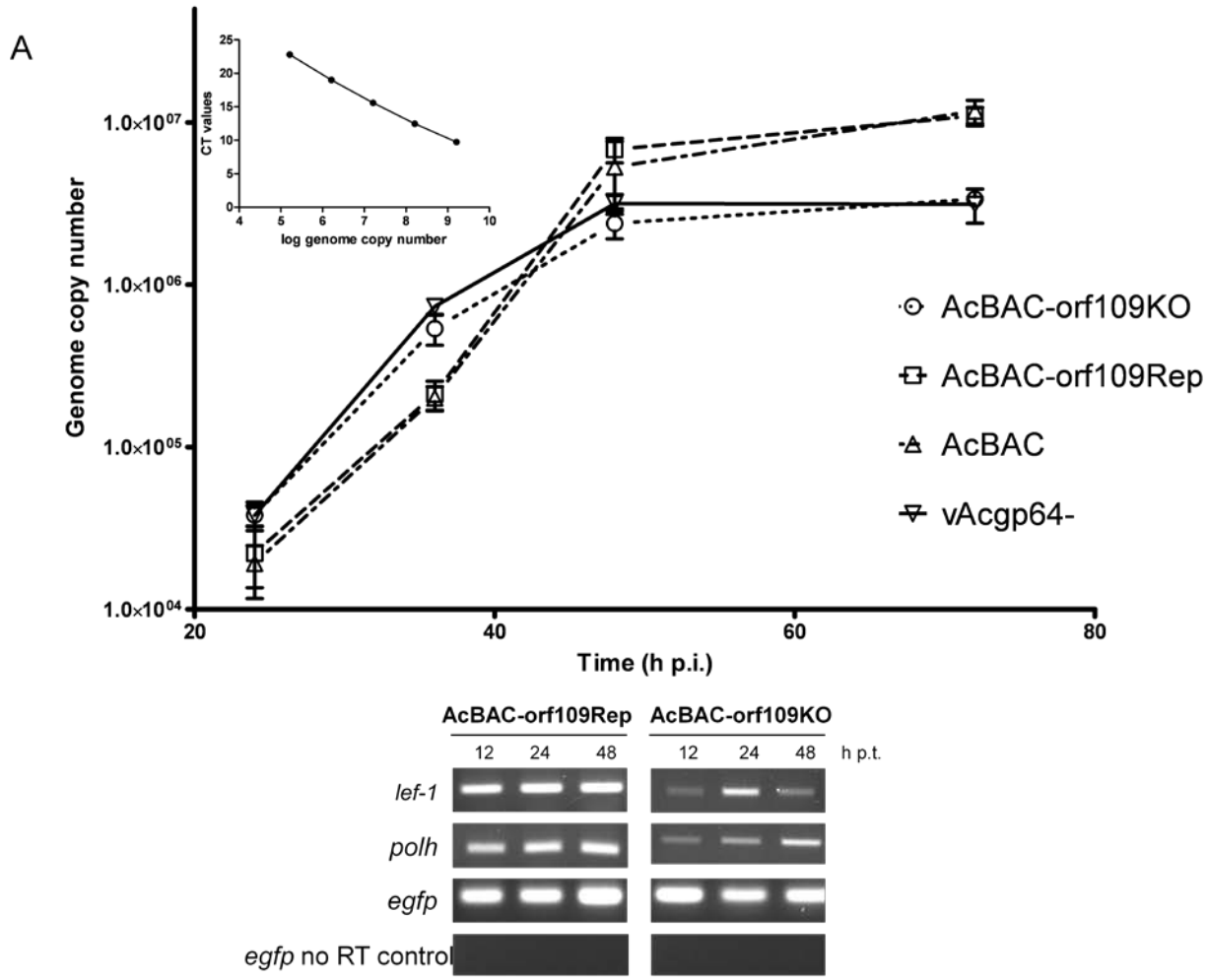


**Figure 12**: DNA replication of AcBAC, AcBAC-orf109KO, AcBAC-orf109Rep, and vAc$^{gp64}$. SF-21 cells were transfected with 1 µg of either AcBAC, AcBAC-orf109KO, AcBAC-orf109Rep, or vAc$^{gp64-}$, a mutant lacking the ability to spread systemically but still able to replicate its DNA. At specific time points post transfection, genomic DNA and total RNA were harvested from cells. (A) The genomic DNA sample (2 µg total) was treated with *Dpn* I to remove any of the transfected input viral DNA. After treatment, Q-PCR was used to amplify a segment of *gp41*. The number of viral genome copies present in the transfected cells was obtained using the standard curve (inset) (B) Total RNA (2 µg total) from the AcBAC-*orf109*Rep- and AcBAC-*orf109*KO-transfected cells was treated with DNase I to remove any viral genomic contamination and then used with specific primer sets to identify viral gene expression using reverse transcriptase (RT)-PCR.

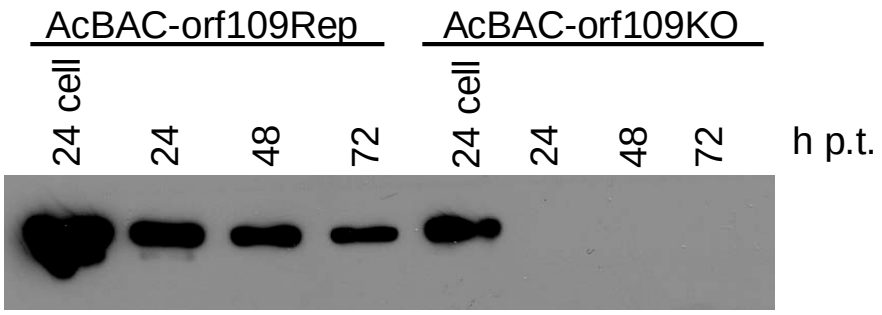


**Figure 13:** GP64 expression in AcBAC-*orf109*Rep- or AcBACorf109KO-transfected SF-21cells. SF-21 cells were transfected with AcBAC-*orf109*KO or AcBAC-*orf109*Rep DNA and then incubated for the time indicated hours post transfection (h p.t.). Supernatant was then removed from the cells and centrifuged at 24,000 x g through a 25% sucrose cushion to pellet any virus particles. The pelleted material was resuspended in 50ul of protein lysis buffer and placed on a SDS-12% acrylamide gel along with a sample of whole cell lysate from each transfection. After transfer to nitrocellulose membrane, the blot was probed with α-GP64 V5 primary antibody (1:1000) and Goat-αMouse-HRP secondary (1:3000) antibody.

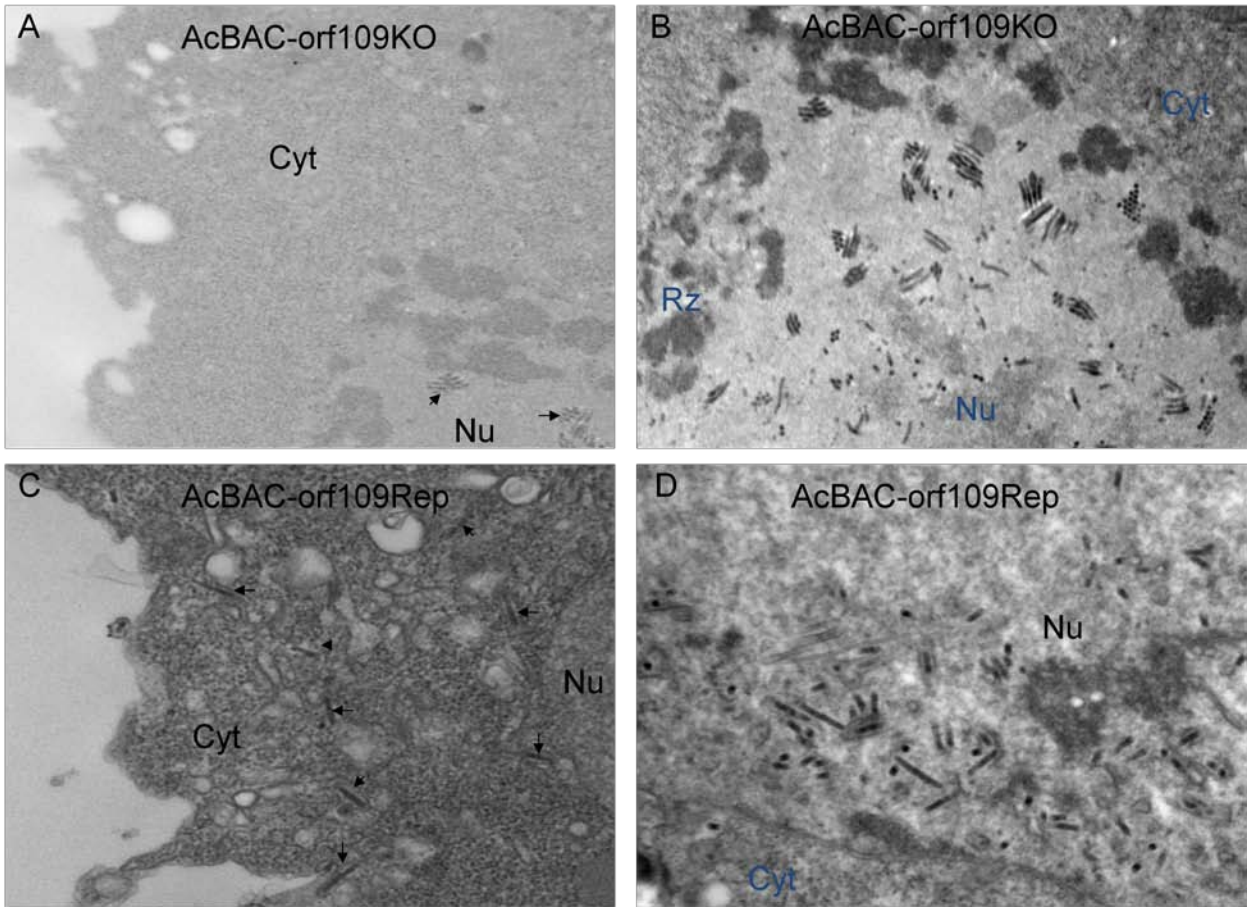


**Figure 14:** Transmission electron microscopy of AcBAC-*orf109*KO- and AcBAC-*orf109*Rep-transfected cells at early times. SF-21 cells were transfected with AcBAC-*orf109*KO(A and B) or AcBAC-*orf109*Rep (C and D) DNA, and incubated for 24 prior to fixation. Thin slices of resin-embedded cells from this time point were visualized for the presence of virus structures.. Nu = Nucleus; Cyt = cytoplasm; arrows denote capsids.

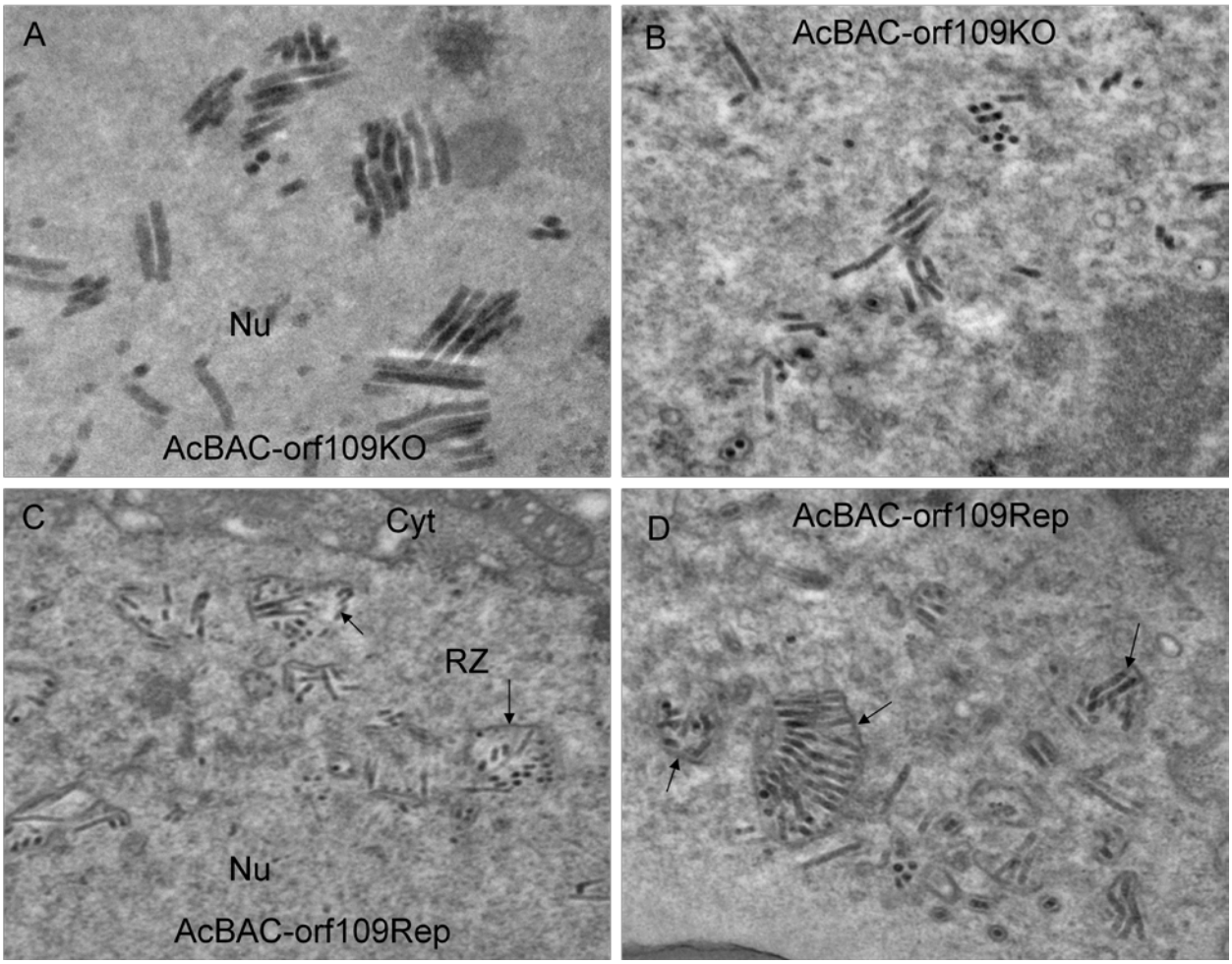


**Figure 15:** Transmission electron microscopy of AcBAC-*orf109*KO- and AcBAC-*orf109*Rep-transfected cells at late times. SF-21 cells were transfected with AcBAC-*orf109*KO (A and B) or AcBAC-*orf109*Rep (C and D) DNA, and incubated for 72 hours prior to fixation. Aligned capsids, as well as the individual capsids, in the AcBAC-*orf109*KO-transfected cells appeared to lack microvesicle envelopment compared to those found in AcBAC-*orf109*Rep-transfected cells (arrows). Nu = Nucleus; RZ = Ring Zone; VS = Virogenic Stroma.

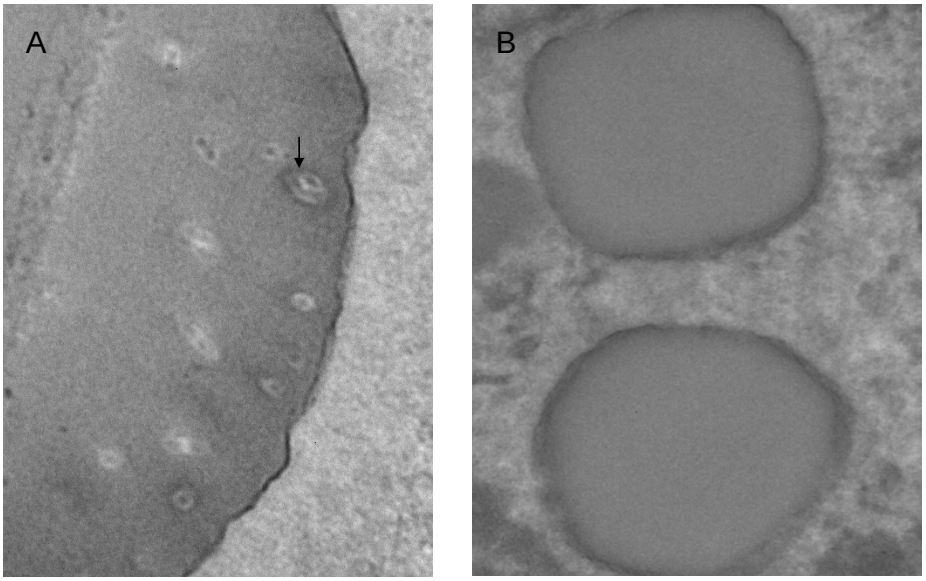


**Figure 16:** Transmission electron microscopy of AcBAC-*orf109*KO- and AcBAC-*orf109*Rep-transfected cells at very late times. SF-21 cells were transfected with AcBAC-*orf109*Rep (A) or AcBAC-*orf109*KO (B) DNA, and incubated for 96 hours prior to fixation. Occlusion bodies in the AcBAC-*orf109*Rep-transfected cells showed multiple ODV (arrow) embedded in the polyhedrin matrix. The occlusion bodies in the AcBAC-*orf109*KO-transfected cells formed normally but lacked any embedded capsids.

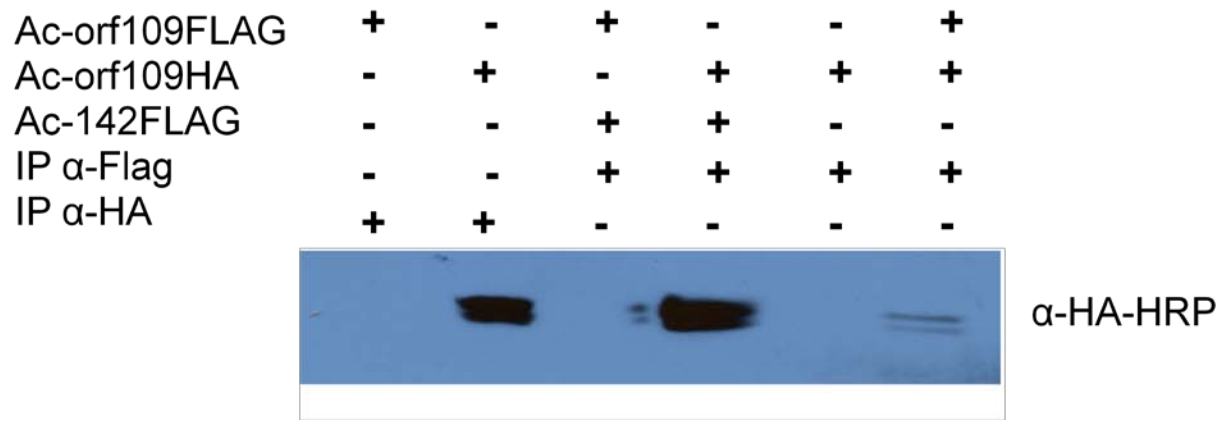


**Figure 17:** Immuno-precipitation of Ac-orf109 with Ac-142**.** Plasmids expressing either Ac-orf109HA, Ac-orf109FLAG, or Ac-142FLAG were transfected singly or together into SF-21 cells. After 24 hours incubations cells were lysed with CHAPS lysis buffer. The lysates were then immuno-precipitated with either α-HA antibody or α-Flag antibody and then placed on a 12% SDS-polyacrylamide gel. After transfer to PVDF membrane, the blot was probed with α-HA-HRP conjugated antibody. An interaction between Ac-orf109HA and Ac-142FLAG was readily detected, as well as a weaker interaction between Ac-109HA and Ac-109Flag.

# References


Adams, J. R., Goodwin, R. H., & Wilcox, T. A. (1979). Electron microscopic investigations on invasion and replication of insect baculoviruses in vitro and in vivo. *Biologie Cellulaire, 28*(1), 261-268.

Afonso, C. L., Tulman, E. R., Lu, Z., Balinsky, C. A., Moser, B. A., Becnel, J. J., et al. (2001). Genome sequence of a baculovirus pathogenic for culex nigripalpus. *Journal of Virology, 75*(22), 11157-11165.

Ahmad, S. M., & Baker, B. S. (2002). Sex-specific deployment of FGF signaling in *drosophila* recruits mesodermal cells into the male genital imaginal disc. *Cell, 109*(5), 651-661.

Allen, B. L., Filla, M. S., & Rapraeger, A. C. (2001). Role of heparan sulfate as a tissue-specific regulator of FGF-4 and FGF receptor recognition. *Journal of Cell Biology, 155*(5), 845-857.

Altschul, S.F.m Gish, W., Miller, W., Meyers, E. W., & Lipman, D. J. (1990). Basic Local Alignment Search Tool. *Journal of Molecular Biology, 215*(1), 403-410.

Ardi, V. C., Van den Steen, Philippe E., Opdenakker, G., Schweighofer, B., Deryugina, E. I., & Quigley, J. P. (2009). Neutrophil MMP-9 proenzyme, unencumbered by TIMP-1, undergoes efficient activation in vivo and catalytically induces angiogenesis via a basic fibroblast growth factor (FGF-2)/FGFR-2 pathway. *Journal of Biological Chemistry, 284*(38), 25854-25866.

Armelin, H. (1973). Pituitary extracts and steroid hormones in the control of 3T3 cell growth. *Proceedings from the National Academy of Sciences, 70*(9), 2702-2706.

Asada, M., Yoneda, A., Oda, Y., Ota, K., Ozawa, K. F., K., Omae, F., et al. (1999). Characterization of fibroblast growth factor-6 expressed by chinese hamster ovary cells as a glycosylated mitogen for human vascular endothelial cells. *Growth Factors, 16*(4), 293-303.

Ayres, M. D., Howard, S. C., Kuzio, J., Lopez-Ferber, M., & Possee, R. D. (1994). The complete DNA sequence of autographa californica nuclear polyhedrosis virus. *Virology, 202*(2), 586-605.

Baird, A., Schubert, D., Ling, N., & Guillemin, R. (1988). Receptor- and heparin-binding domains of basic fibroblast growth factor. *Proceedings from the National Academy of Sciences, 85*, 2324-2328.

Baker, B. S. (1989). Sex in flies: The splice of life. *Nature, 340*(6243), 521-524.

Baker, B. S., & Ridge, K. (1980). Sex and the single cell. I. on the action of major loci affecting sex determination in drosophila melanogaster. *Genetics, 94*(2), 383-423.

Baker, B. S., & Wolfner, M. F. (1988). A molecular analysis of doublesex, a bifunctional gene that controls both male and female sexual differentiation in drosophila melanogaster. *Genes and Development, 2*(4), 477-489.

Barrett, A. L., Kreuger, S., & Datta, S. (2008). Branchless and hedgehog operate in a positive feedback loop to regulate the initiation of neuroblast division in the drosophila larval brain. *Developmental Biology, 317*(1), 234-245.

Barrett, J. W., Brownwright, A. J., Primavera, M. J., & Palli, S. R. (1998). Studies of the Nucleopolyhedrovirus infection process in insects by using the green fluorescence protein as a reporter. *Journal of Virology, 72*(4), 3377-3382.

Bate, M. (1990). The embryonic development of larval muscles in drosophila. *Development, 110*(3), 791-804.

Beenken, A., & Mohammadi, M. (2009). The FGF family: Biology, pathophysiology and therapy. *Nature Reviews. Drug Discovery., 8*(3), 235-253.

Beer, H., Vindevoghel, L., Gait, M. J., Revest, J., Duani, D. R., Mason, I., et al. (2000). Fibroblast growth factor (FGF) receptor 1-IIIb is a naturally occurring functional receptor for FGFs that is preferentially expressed in the skin and the brain. *Journal of Biological Chemistry, 275*(21), 16091-16097.

Beiman, M., Shilo, B., & Volk, T. (1996). Heartless, a drosophila FGF receptor homolog, is essential for cell migration and establishment of several mesodermal lineages. *Genes and Development, 10*(23), 2993-3002.

Bellosta, P., Iwahori, A., Plotnikov, A. N., Eliseenkova, A. V., Basilico, C., & Mohammadi, M. (2001). Identification of receptor and heparin binding sites in fibroblast growth factor 4 by structure-based mutagenesis. *Molecular and Cellular Biology, 21*(17), 5946-5957.

Bideshi, D. K., & Federici, B. A. (2000). The Trichoplusia ni granulovirus helicase is unable to support replication of autographa californica multicapsid Nucleopolyhedrovirus in cells and larvae of T. ni. *Journal of General Virology, 81*(6), 1593-1599.

Birnbaum, D., Popovici, C., & Roubin, R. (2005). A pair as a minimum: The two fibroblast growth factors of the nematode *caenorhabditis elegans*. *Developmental Dynamics, 232*(2), 247-255.

Blissard, G. W., Kogan, P. H., Wei, R., & Rohrman, G. F. (1992). A synthetic early promoter from a baculovirus: Roles of the TATA box and conserved start site CAGT sequence in basal levels of transcription. *Virology, 190*(2), 783-793.

Blissard, G. W., & Rohrman, G. F. (1989). Location, sequence, transcriptional mapping, and temporal expression of the gp64 envelope glycoprotein gene of the orgyia pseudotsugata multicapsid nuclear polyhedrosis virus. *Virology, 170*(2), 537-555.

Blissard, G. W., & Wenz, J. R. (1992). Baculovirus gp64 envelope glycoprotein is sufficient to mediate pH-dependent membrane fusion. *Journal of Virology, 66*(11), 6829-6835.

Braunagel, S.C., Burks, J. K., Rosas-Acosta, G., Harrison, R. L., Ma, H., & Summers, M. D. (1999). Mutations within the autographa californica Nucleopolyhedrovirus FP25K gene decrease the accumulation of ODV-E66 and alter its intranuclear transport. *Journal of Virology, 73*(10), 8559-8570.

Braunagel, S.C., Cox, V., & Summers, Max D. (2008). Baculovirus data suggest a common but multifaceted pathway for sorting proteins to the inner nuclear membrane. *Journal of Virology, 83*(3), 1280-1288.

Braunagel, S. C., Parr, R., Belyavskyi, M., & Summers, Max D. (1998). Autographa californica Nucleopolyhedrovirus infection results in Sf9 cell cycle arrest at G2/M phase. *Virology, 244*(1), 195-211.

Braunagel, S. C., Russell, W. K., Rosas-Acosta, G., & Russell D.H., Summers, Max D. (2003). Determination of the protein composition of the occlusion-derived virus of *autographa californica* Nucleopolyhedrovirus. *Proceedings from the National Academy of Sciences, 100*(17), 9797-9802.

Braunagel, S. C., & Summers, M. D. (2007). Molecular biology of the baculovirus occlusion-derived virus envelope. *Current Drug Targets, 8*(10), 1084-1095.

Carbonell, L. F., Klowden, M. J., & Miller, L. K. (1985). Baculovirus-mediated expression of bacterial genes in dipteran and mammalian cells. *Journal of Virology, 1*(153), 160.

Carstens, E. B. and Wu, Y. (2007). No single homologous repeat region is essential for DNA replication of the baculovirus *Autographa californica multiple Nucleopolyhedrovirus. Journal of General Virology 88*(1), 114-122.

Carlsson, P., Presto, J., Spillmann, D., Lindahl, U., & Kjellen, L. (2008). Heparin/heparan sulfate biosynthesis: Processive formation of N-sulfated domains. *Journal of Biological Chemistry, 283*(29), 20008-20014.

Chaabihi, H., Ogliastro, M. H., Martin, M., Giraud, C., Devauchelle, G., & Cerutti, M. (1993). Competition between baculovirus polyhedrin and p10 gene expression during infection of insect cells. *Journal of Virology, 67*(5), 2664-2671.

Chapman, R. F. (1998). *The insects: Structure and function* (4th Edition ed.). Cambridge, United Kingdom: Cambridge University Press.

Charlton, C. A., & Volkman, L. E. (1991). Sequential rearrangement and nuclear polymerization of actin in baculovirus-infected spodoptera frugiperda cells. *Journal of Virology, 65*(3), 1219-1227.

Charlton, C. A., & Volkman, L. E. (1993). Penetration of autographa californica nuclear polyhedrosis virus nucleocapsids into IPLB sf 21 cells induces actin cable formation. *Virology, 197*(1), 245-254.

Chellaiah, A., Yuan, W., Chellaiah, M., & Ornitz, D. M. (1999). Mapping ligand binding domains in chimeric fibroblast growth factor receptor molecules. multiple regions determine ligand binding specificity. *Journal of Biological Chemistry, 274*(49), 34785-34794.

Chen, Y., Wu, C., Lee, S., Wu, Y., Lo, C., Tsai, M., et al. (2008). Genomic and host range studies of maruca vitrata Nucleopolyhedrovirus. *Journal of General Virology, 89*(9), 2315-2330.

Cheng, X., & Lynn, D. E. (2009). Baculovirus interactions in vitro and in vivo. *Advances in Applied Microbiology, 68*(217), 239.

Cherbas, L., & Cherbas, P. (1993). The arthropod initiator: The capsite consensus plays an important role in transcription. *Insect Biochemistry and Molecular Biology, 23*(1), 81-90.

Chikhalya, A., Luu, D. D., Carrera, M., De La Cruz, A., Torres, M., Martinez, E. N., et al. (2009). Pathogenesis of autographa californica multiple Nucleopolyhedrovirus in fifth-instar anticarsia gemmatalis larvae. *Journal General Virology, 90*(8), 2023-2032.

Clarke, T. E., & Clem, R. J. (2002). Lack of involvement of haemocytes in the establishment and spread of infection in spodoptera frugiperda larvae infected with the baculovirus autographa californica M Nucleopolyhedrovirus by intrahaemocoelic injection. *Journal of General Virology, 83*(7), 1565-1572.

Clem, R. J., Robson, M., & Miller, L. K. (1994). Influence of infection route on the infectivity of baculovirus mutants lacking the apoptosis-inhibiting gene p35 and the adjacent gene p94. *Journal of Virology, 68*(10), 6759-6762.

Costell, M., Mann, K., Yamada, Y., & Timpl, R. (1997). Characterization of recombinant perlecan domain I and its substitution by glycosaminoglycans and oligosaccharides. *European Journal of Biochemistry, 243*(1-2), 115-121.

Cote, G. J., Huang, E. S. C., Jin, W., & Morrison, R. S. (1997). Sequence requirements for regulated RNA splicing of the human fibroblast growth factor receptor-1 alpha exon. *Journal of Biological Chemistry, 272*(2), 1054-1060.

Coulier, F., Pontarotti, P., Roubin, R., Hartung, H., Goldfarb, M., & Birnbaum, D. (1997). Of worms and men: An evolutionary perspective on the fibroblast growth factor (FGF) and FGF receptor families. *Journal of Molecular Evolution, 44*(1), 43-56.

Crouch, E. A., & Passarelli, A. L. (2005). Effects of baculovirus transactivators IE-1 and IE-2 on the drosophila heat shock 70 promoter in two insect cell lines. *Archives of Virology, 150*(8), 1563-1578.

Datta, S. (1995). Control of proliferation activation in quiescent neuroblasts of the drosophila central nervous system. *Development, 121*(4), 1173-1182.

Dell, K. R., & Williams, L. T. (1992). A novel form of fibroblast growth factor receptor 2. alternative splicing of the third immunoglobulin-like domain confers ligand binding specificity. *Journal of Biological Chemistry, 267*(29), 21225-21229.

Derksen, A. C., & Granados, R. R. (1988). Alteration of a lepidopteran peritrophic membrane by baculoviruses and enhancement of viral infectivity. *Virology, 167*(1), 242-250.

Detvisitsakun, C., Berretta, M. F., Lehiy, C., & Passarelli, A. L. (2005). Stimulation of cell motility by a viral fibroblast growth factor homolog: Proposal for a role in viral pathogenesis. *Virology, 336*(2), 308-317.

Detvisitsakun, C., Hutfless, E. L., Berretta, M. F., & Passarelli, A. L. (2006). Analysis of a baculovirus lacking a functional viral fibroblast growth factor homolog. *Virology, 346*(2), 258-265.

Döller, G., Gröner, A., & Straub, O. C. (1983). Safety evaluation of nuclear polyhedrosis virus replication in pigs. *Applied Environmental Microbiology, 45*(4), 1229-1233.

Du, X., & Thiem, S. M. (1997). Responses of insect cells to baculovirus infection: Protein synthesis shutdown and apoptosis. *Journal of Virology, 71*(10), 7866-7872.

Duan, D. R., Werner, S., & Williams, L. T. (1992). A naturally occurring secreted form of fibroblast growth factor (FGF) receptor 1 binds basic FGF in preference over acidic FGF. *Journal of Biological Chemistry, 267*(23), 16076-16080.

Duffy, S. P., Becker, E. M., Whittome, B. H., Lucarotti, C. J., & Levin, D. B. (2007). In vivo replication kinetics and transcription patterns of the Nucleopolyhedrovirus (NeabNPV) of the balsam fir sawfly, neodiprion abietis. *Journal of General Virology, 88*(7), 1945-1951.

Duffy, S. P., Young, A. M., Morin, B., Lucarotti, C. J., Koop, B. F., & Levin, D. B. (2006). Sequence analysis and organization of the neodiprion abietis Nucleopolyhedrovirus genome. *Journal of Virology, 80*(14), 6952-6963.

Duisit, G., Saleun, S., Douthe, S., Barsoum, J., Chadeuf, G., & Moullier, P. (1999). Baculovirus vector requires electrostatic interactions including heparan sulfate for efficient gene transfer in mammalian cells. *Journal of Gene Medicine, 1*(2), 93-102.

Dutta, D., Shaw, S., Maqbool, T., Pandya, H., & Raghavan, K. V. (2005). Drosophila heartless acts with Heartbroken/Dof in muscle founder differentiation. *PLoS Biology, 3*(10), 1789-1800.

Eason, J. E., Hice, R. H., Johnson, J. J., & Federici, B. A. (1998). Effects of substituting granulin or a granulin-polyhedrin chimera for polyhedrin on virion occlusion and polyhedral

morphology in autographa californica multinucleocapsid nuclear polyhedrosis virus. *Journal of Virology, 72*(7), 6237-6243.

Engelhard, E. K., Kam-Morgan, L. N., Washburn, J. O., & Volkman, L. E. (1994). The insect tracheal system: A conduit for the systemic spread of autographa californica M nuclear polyhedrosis virus. *Proceedings from the National Academy of Sciences, 91*(8), 3224-3227.

Engelhard, E. K., & Volkman, L. E. (1995). Developmental resistance in fourth instar trichoplusia ni orally inoculated with autographa californica M nuclear polyhedrosis virus. *Virology, 202*(2), 384-389.

Eriksson, A. E., Cousens, L. S., Weaver, L. H., & Matthews, B. W. (1991). Three-dimensional structure of human basic fibroblast growth factor. *Proceedings from the National Academy of Sciences, 88*(8), 3441-3445.

Fan, H., Duan, Y., Zhou, H., Li, W., Li, F., Guo, L., et al. (2002). Selection of peptide ligands binding to fibroblast growth factor receptor 1. *International Union of Biochemistry and Molecular Biology Life, 54*(2), 67-72.

Fang, M., Dai, X., & Theilmann, D. A. (2007). Autographa californica multiple Nucleopolyhedrovirus EXON0 (ORF141) is required for efficient egress of nucleocapsids from the nucleus. *Journal of Virology, 81*(18), 9859-9869.

Fang, M., Nie, Y., Dai, X., & Theilmann, D. A. (2008). Identification of AcMNPV EXON0 (ac141) domains required for efficient production of budded virus, dimerization and association with BV/ODV-C42 and FP25. *Virology, 375*(1), 265-276.

Fang, M., Nie, Y., Harris, S., Erlandson, M. A., & Theilmann, D. A. (2009). Autographa californica multiple Nucleopolyhedrovirus core gene ac96 encodes a per os infectivity factor (PIF-4). *Journal of Virology, 83*(23), 12569-12578.

Fang, M., Nie, Y., & Theilmann, D. A. (2009). AcMNPV EXON0 (AC141) which is required for the efficient egress of budded virus nucleocapsids interacts with beta-tubulin. *Virology, 385*(2), 496-504.

Fang, M., Nie, Y., & Theilmann, D. A. (2009). Deletion of the AcMNPV core gene ac109 results in budded virions that are non-infectious. *Journal of Virology, 389*(1-2), 66-74.

Fang, M., Wang, H., Wang, H., Yuan, L., Chen, X., Vlak, J. M., et al. (2003). Open reading frame 94 of helicoverpa armigera single nucleocapsid Nucleopolyhedrovirus encodes a novel conserved occlusion-derived virion protein, ODV-EC43. *Journal of General Virology, 84*(11), 3021-3027.

Federici, B. A., & Lowe, R. E. (1972). Studies on the pathology of a baculovirus in aedes triseriatus. *Journal of Invertebrate Pathology, 20*(1), 14-21.

Federici, B. A., & Miller, L. K. (Eds.). (1997). *The baculoviruses*. New York, New York: Plenum.

Flipsen, J. T., Marten, J. W., van Oers, M. M., Vlak, J. M., & van Lent, J. W. (1995). Passage of autographa californica nuclear polyhedrosis virus through the midgut epithelium of spodoptera exigua larvae. *Virology, 208*(1), 328-335.

Ford-Perriss, M., Guimond, S. E., Greferath, U., Kita, M., Grobe, K., Habuchi, H., et al. (2002). Variant heparan sulfates synthesized in developing mouse brain differentially regulate FGF signaling. *Glycobiology, 12*(11), 721-727.

Frasier, M. J. (1986). Ultrastructural observations of virion maturation in *autographa californica* nuclear polyhedrosis virus infected *spodoptera frugip*erda cell cultures. *Journal of Ultrastructure and Molecular Structure Research, 95*(3), 189-195.

Friedrich, M. V. K., Schneider, M., Timpl, R., & Baumgartner, S. (2000). Perlecan domain V of drosophila melanogaster. sequence, recombinant analysis and tissue expression. *European Journal of Biochemistry, 267*(11), 3149-3159.

Friesen, P. D., & Miller, L. K. (1988). Temporal regulation of baculovirus RNA: Overlapping early and late transcripts. *Journal of Virology, 54*(2), 392-400.

Friesen, P. D., & Miller, L. K. (Eds.). (1997). *The baculoviruses*. New York, New York: Plenum.

Fuller, A. O., & Lee, W. (1992). Herpes simplex virus type 1 entry through a cascade of virus-cell interactions requires different roles of gD and gH in penetration. *Journal of Virology, 66*(8), 5002-5012.

Furdui, C. M., Lew, E. D., Schlessinger, J., & Anderson, K. S. (2006). Autophosphorylation of FGFR1 kinase is mediated by a sequential and precisely ordered reaction. *Molecular Cell, 21*(5), 711-717.

Gambarini, A. G., & Armelin, H. A. (1981). Pituitary fibroblast growth factors: Partial purification and characterization. *Brazilian Journal of Medical and Biological Research, 14*(1), 19-27.

Garcia-Maruniak, A., Maruniak, J. E., Zanotto, P. M. A., Doumbouya, A. E., Liu, J., Merritt, T. M., et al. (2004). Sequence analysis of the genome of the neodiprion sertifer Nucleopolyhedrovirus. *Journal of Virology, 78*(13), 7036-7051.

Gattineni, J., & Baum, M. (2009). Regulation of phosphate transport by fibroblast growth factor 23 (FGF23): Implications for disorders of phosphate metabolism. *Pediatric Nephrology,*

Gimenez-Gallego, G., Conn, G., Hatcher, V. B., & Thomas, K. A. (1986). Human brain-derived acidic and basic fibroblast growth factors: Amino terminal sequences and specific mitogenic activities. *Biochemical and Biophysical Research Communications, 135*(2), 541-548.

Gisselbrecht, S., Skeath, J. B., Doe, C. Q., & Michelson, A. M. Heartless encodes a fibroblast growth factor receptor (DFR1/DFGF-R2) involved in the directional migration of early mesodermal cells in the drosophila embryo. *Genes and Development, 10*(23), 3003-3017.

Glazer, L., & Shilo, B. (1991). The *drosophila* FGF-R homolog is expressed in the embryonic tracheal system and appears to be required for directed tracheal cell extension. *Genes and Development, 5*(4), 697-705.

Goetz, R., Beenken, A., Ibrahimi, O. A., Kalinina, J., Olsen, S. K., Eliseenkova, A. V., et al. (2007). Molecular insights into the klotho-dependent, endocrine mode of action of fibroblast growth factor 19 subfamily members. *Molecular and Cellular Biology, 27*(9), 3417-3428.

Goldfarb, M. (2005). Fibroblast growth factor homologous factors: Evolution, structure, and function. *Cytokine & Growth Factor Reviews, 16*(2), 215-220.

Gonzalez, M. A., Smith, G. E., & Summers, M. D. (1989). Insertion of the SfMNPV polyhedrin gene into an AcMNPV polyhedrin deletion mutant during viral infection. *Virology, 170*(1), 160-175.

Gospodarowicz, D., Lui, G., & Cheng, J. (1982). Purification in high yield of brain fibroblast growth factor by preparative isoelectric focusing at pH 9.6. *J. Biol. Chem., 257*(20), 12266-12276.

Gospodarwicz, D. (1974). Localisation of a fibroblast growth factor and its effect alone and with hydrocortisone on 3T3 cell growth. *Nature, 249*(453), 123-127.

Grainge, I., & Jayaram, M. (1999). The integrase family of recombinase: Organization and function of the active site. *Molecular Microbiology, 33*(3), 449-456.

Granados, R. R. (1978). Early events in the infection of Heliothis zea midgut cells by a baculovirus. *Virology, 90*(1), 170-174.

Granados, R. R., & Federici, B. A. (Eds.). (1986). *The biology of baculoviruses.* Boca Raton, Florida: CRC Press.

Granados, R. R., & Lawler, K. A. (1981). In vivo pathway of autographa californica baculovirus invasion and infection. *Virology, 108*(2), 297-308.

Groffen, A. J. A., Buskens, C. A. F., van Kuppevelt, T. H., Veerkamp, J. H., Monnens, L. A. H., & van den Heuvel, L. (1998). Primary structure and high expression of human agrin in basement membranes of adult lung and kidney. *European Journal of Biochemistry, 254*(1), 123-128.

Groth, C., & Lardelli, M. (2002). The structure and function of vertebrate fibroblast growth factor receptor 1. *International Journal of Developmental Biology, 46*(4), 393-400.

Gryzik, T., & Müller, H. -. J. (2004). FGF8-like1 and FGF8-like2 encode putative ligands of the FGF receptor htl and are required for mesoderm migration in the drosophila gastrula. *Current Biology, 14*(8), 659-667.

Guillonneau, X., Régnier-Ricard, F., Jeanny, J. C., Thomasseau, S., Courtois, Y., & Mascarelli, F. (2000). Regulation of FGF soluble receptor type 1 (SR1) expression and distribution in developing, degenerating, and FGF2-treated retina. *Developmental Dynamics, 217*(1), 24-36.

Guillonneau, X., Régnier-Ricard, F., Laplace, O., Jonet, L., Bryckaert, M., Courtois, Y., et al. (1998). Fibroblast growth factor (FGF) soluble receptor 1 acts as a natural inhibitor of FGF2 neurotrophic activity during retinal degeneration. *Molecular Biology of the Cell, 9*(10), 2785-2802.

Guimond, S., & Turnbull, J. (1999). Fibroblast growth factor receptor signalling is dictated by specific heparan sulphate saccharides. *Current Biology, 9*(22), 1343-1346.

Haas-Stapleton, E. J., Washburn, J. O., & Volkman, L. E. (2003). Pathogenesis of autographa californica M Nucleopolyhedrovirus in fifth instar spodoptera frugiperda. *Journal General Virology, 84*(8), 2033-2040.

Haas-Stapleton, E. J., Washburn, J. O., & Volkman, L. E. (2004). P74 mediates specific binding of autographa californica M Nucleopolyhedrovirus occlusion-derived virus to primary cellular targets in the midgut epithelia of heliothis virescens larvae. *Journal of Virology, 78*(13), 6786-6791.

Häcker, U., Lin, X., & Perrimon, N. (1997). The drosophila sugarless gene modulates wingless signaling and encodes an enzyme involved in polysaccharide biosynthesis. *Development, 124*(18), 3565-3573.

Hakim, R. S., Baldwin, K., & Smagghe, G. (2010). Regulation of midgut growth, development, and metamorphosis. *Annual Review of Entomology, 55*, 593-608.

Hanneken, A., Ying, W., Ling, N., & Baird, A. (1994). Identification of soluble forms of the fibroblast growth factor receptor in blood. *Proceedings from the National Academy of Sciences, 91*(19), 9170-9174.

Harmer, N. J., Pellegrini, L., Chirgadze, D., Fernandez-Recio, J., & Blundell, T. L. (2004). The crystal structure of fibroblast growth factor (FGF) 19 reveals novel features of the FGF family and offers a structural basis for its unusual receptor affinity. *Biochemistry, 43*(3), 629-640.

Harrison, R. (2009). Structural divergence among genomes of closely related baculoviruses and its implications for baculovirus evolution. *Journal of Invertebrate Pathology, 101*(3), 181-186.

Hawtin, R. E., Arnold, K., Ayres, M. D., Zanotto, P. M., Howard, S. C., Gooday, G. W., et al. (1995). Identification and preliminary characterization of a chitinase gene in the autographa californica nuclear polyhedrosis virus genome. *Virology, 212*(2), 673-685.

Hawtin, R. E., Zarkowska, T., Arnold, K., Thomas, C. J., Gooday, G. W., King, L. A., et al. (1997). Liquefaction of autographa californica Nucleopolyhedrovirus-infected insects is dependent on the integrity of virus-encoded chitinase and cathepsin genes. *Virology, 238*(2), 243-253.

Hefferon, K., Oomens, A. G., Monsma, S., Finnerty, C. M., & Blissard, G. W. (1999). Host cell receptor binding by baculovirus GP64 and kinetics of virion entry. *Virology, 258*(2), 455-468.

Herniou, E. A., & Jehle, J. A. (2007). Baculovirus phylogeny and evolution. *Current Drug Targets, 8*(10), 1043-1050.

Herniou, E. A., Olszewski, J. A., Cory, J. S., & O'Reilly, D. R. (2003). The genome sequence and evolution of baculoviruses. *Annual Review of Entomology, 48,* 211-234.

Herniou, E. A., Olszewski, J. A., O'Reilly, D. R., & Cory, J. S. (2004). Ancient coevolution of baculoviruses and their insect hosts. *Journal of Virology, 78*(7), 3244-3251.

Hildreth, P. E. (1965). DOUBLESEX, RECESSIVE GENE THAT TRANSFORMS BOTH MALES AND FEMALES OF DROSOPHILA INTO INTERSEXES. *Genetics, 51,* 659-678.

Hilton, S. (2008). Baculoviruses: Molecular biology of granuloviruses. In B. W. J. Mahy, & M. H. van Regenmortel (Eds.), (Third ed., pp. 211-219) Science Direct.

Holley, R. W., & Kiernan, J. A. (1974). Control of the initiation of DNA synthesis in 3T3 cells: Serum factors. *Proceedings from the National Academy of Sciences, 71*(7), 2908-2911.

Hong, T., Braunagel, S. C., & Summers, M. D. (19944). Transcription, translation, and cellular localization of PDV-E66: A structural protein of the PDV envelope of autographa californica nuclear polyhedrosis virus. *Virology, 204*(1), 210-222.

Hong, T., Summers, M. D., & Braunagel, S. C. (1997). N-terminal sequences from autographa californica nuclear polyhedrosis virus envelope proteins ODV-E66 and ODV-E25 are sufficient to direct reporter proteins to the nuclear envelope, intranuclear microvesicles and the envelope of occlusion-derived virus. *Proceedings from the National Academy of Sciences, 94*(8), 4050-4055.

Horton, H. M., & Burand, J. P. (1993). Saturable attachment sites for polyhedron-derived baculovirus on insect cells and evidence for entry via direct membrane fusion. *Journal of Virology, 67*(4), 1860-1868.

Hu, Y. (2008). Baculoviral vectors for gene delivery: A review. *Current Gene Therapy, 8*(1), 54-65.

Hu, Z., Yuan, M., Wu, W., Liu, C., Yang, K., & Pang, Y. (2010 Epub ahead of print). Autographa californica multiple Nucleopolyhedrovirus ac76 is involved in intranuclear microvesicle formation. *Journal of Virology,*

Huh, N. E., & Weaver, R. F. (1990). Identifying the RNA polymerases that synthesize specific transcripts of the autographa californica nuclear polyhedrosis virus. *Journal of General Virology, 71*(1), 195-201.

Hung, K., Kumar, K. T. S., Kathir, K. M., Xu, P., Ni, F., Ji, H., et al. (2005). Solution structure of the ligand binding domain of the fibroblast growth factor receptor: Role of heparin in the activation of the receptor. *Biochemistry, 44*(48), 15787-15798.

Hunt, L. T., & Dayhoff, M. O. (1970). The occurrence in proteins of the tripeptides asn-X-ser and asn-X-thr and of bound carbohydrate. *Biochemical and Biophysical Research Communications, 39*(4), 757-765.

Hynes, R. O., & Zhao, Q. (2000). The evolution of cell adhesion. *Journal of Cell Biology, 150*(2), 89-96.

Ibrahimi, O. A., Yeh, B. K., Eliseenkova, A. V., Zhang, F., Olsen, S. K., Igarashi, M., et al. (2005). Analysis of mutations in fibroblast growth factor (FGF) and a pathogenic mutation in FGF receptor (FGFR) provides direct evidence for the symmetric two-end model for FGFR dimerization. *Molecular and Cellular Biology, 25*(2), 671-684.

IJkel, W. F., Westenberg, M., Goldbach, R. W., Blissard, G. W., Vlak, J. M., & Zuidema, D. (2000). A novel baculovirus envelope fusion protein with a proprotein convertase cleavage site. *Virology, 275*(1), 30-41.

Imam, F., Sutherland, D., Huang, W., & Krasnow, M. A. (1999). Stumps, a drosophila gene required for fibroblast growth factor (FGF)-directed migrations of tracheal and mesodermal cells. *Genetics, 152*(1), 307-318.

Itoh, N. (2007). The fgf families in humans, mice, and zebrafish: Their evolutional processes and roles in development, metabolism, and disease. *Biological & Pharmaceutical Bulletin, 30*(10), 1819-1825.

Jarecki, J., Johnson, E., & Krasnow, M. A. (1999). Oxygen regulation of airway branching in drosophila is mediated by branchless FGF. *Cell, 99*(2), 211-220.

Jaye, M., Schlessinger, J., & Dionne, C. A. (1992). Fibroblast growth factor receptor tyrosine kinases: Molecular analysis and signal transduction. *Biochimica Et Biophysica Acta (BBA) - Molecular Cell Research, 1135*(2), 185-199.

Jeffers, M., Shimkets, R., Prayaga, S., Boldog, F., Yang, M., Burgess, C., et al. (2001). Identification of a novel human fibroblast growth factor and characterization of its role in oncogenesis. *Cancer Research, 61*(7), 3131-3138.

Jehle, J. A., Blissard, G. W., Bonning, B. C., Cory, J. S., Herniou, E. A., Rohrmann, G. F., et al. (2006). On the classification and nomenclature of baculoviruses: A proposal for revision. *Archives of Virology, 151*(7), 1257-1266.

Ji, X., Sutton, G., Evans, G., Axford, D., Owen, R., & Stuart, D. I. (2010). How baculovirus polyhedra fit square pegs into round holes to robustly package viruses. *EMBO Journal, 29*(2), 505-514.

Jiang, S. S., Chang, I., Huang, L., Chen, P., Wen, C., Liu, S., et al. (2006). Temporal transcription program of recombinant autographa californica multiple nucleopolyhedrosis virus. *Journal of Virology, 80*(18), 8989-8999.

Johnson, D. E., Lee, P. L., Lu, J., & Williams, L. T. (1990). Diverse forms of a receptor for acidic and basic fibroblast growth factors. *Molecular and Cellular Biology, 10*(9), 4728-4736.

Johnson, D. E., Lu, J., Chen, H., Werner, S., & Williams, L. T. (1991). The human fibroblast growth factor receptor genes: A common structural arrangement underlies the mechanisms for generating receptor forms that differ in their third immunoglobulin domain. *Molecular and Cellular Biology, 11*(9), 4627-4634.

Johnson, D. E., & Williams, L. T. (1993). Structural and functional diversity in the FGF receptor multigene family. *Advances in Cancer Research, 60*, 1-41.

Kamimura, K., Koyama, T., Habuchi, H., Ueda, R., Masu, M., Kimata, K., et al. (2006). Specific and flexible roles of heparan sulfate modifications in drosophila FGF signaling. *Journal of Cell Biology, 174*(6), 773-778.

Katsuma, S., Daimon, T., Horie, S., Kobayashi, M., & Shimada, T. (2006). N-linked glycans of bombyx mori Nucleopolyhedrovirus fibroblast growth factor are crucial for its secretion. *Biochemical and Biophysical Research Communications, 350*(4), 1069-1075.

Katsuma, S., Daimon, T., Mita, K., & Shimada, T. (2006). Lepidopteran ortholog of drosophila breathless is a receptor for the baculovirus fibroblast growth factor. *Journal of Virology, 80*(11), 5474-5481.

Katsuma, S., Horie, S., Daimon, T., Iwanaga, M., & Shimada, T. (2006). In vivo and in vitro analyses of a bombyx mori Nucleopolyhedrovirus mutant lacking functional vfgf. *Virology, 355*(1), 62-70.

Katsuma, S., Horie, S., & Shimada, T. (2008). The fibroblast growth factor homolog of bombyx mori Nucleopolyhedrovirus enhances systemic virus propagation in B. mori larvae. *Virus Research, 137*(1), 80-85.

Katsuma, S., Shimada, T., & Kobayashi, M. (2004). Characterization of the baculovirus bombyx mori Nucleopolyhedrovirus gene homologous to the mammalian FGF gene family. *Virus Genes, 29*(2), 211-217.

Kawasaki, Y., Matsumoto, S., & Nagamine, T. (2004). Analysis of baculovirus IE1 in living cells: Dynamics and spatial relationships to viral structural proteins. *Journal General Virology, 85*(12), 3575-3583.

Ke, J., Wang, J., Deng, R., & Wang, X. (2008). Autographa californica multiple Nucleopolyhedrovirus ac66 is required for the efficient egress of nucleocapsids from the nucleus, general synthesis of preoccluded virions and occlusion body formation. *Virology, 374*(2), 421-431.

Keddie, B. A., Aponte, G. W., & Volkman, L. E. (1989). The pathway of infection of autographa californica nuclear polyhedrosis virus in an insect host. *Science, 243*(4899), 1728-1730.

Kelly, D. C. (1982). Baculovirus replication. *Journal of General Virology, 63*, 1-13.

Kenoutis, C., Efrose, R. C., Swevers, L., Lavdas, A. A., Gaitanou, M., Matsas, R., et al. (2006). Baculovirus-mediated gene delivery into mammalian cells does not alter their transcriptional and differentiating potential but is accompanied by early viral gene expression. *Journal of Virology, 80*(8), 4135-4146.

Khare, N., & Baumgartner, S. (2000). Dally-like protein, a new drosophila glypican with expression overlapping with wingless. *Mechanisms of Development, 99*(1-2), 199-202.

Kharitonenkov, A. (2009). FGFs and metabolism. *Current Opinion in Pharmacology,*

Khosaka, T., Himeno, M., & Onodera, K. (1971). Separation and structure of components of nuclear polyhedrosis virus of the silkworm. *Journal of Virology, 7*(2), 267-273.

Kiselyov, V. V., Bock, E., Berezin, V., & Poulsen, F. M. (2006). NMR structure of the first ig module of mouse FGFR1. *Protein Sci., 15*(6), 1512-1515.

Klagsbrun, M., & Baird, A. (1981). A dual receptor system is required for basic fibroblast growth factor activity. *Cell, 67*(2), 229-231.

Klambt, C., Glazer, L., & Shilo, B. (1992). Breathless, a drosophila FGF receptor homolog, is essential for migration of tracheal and specific midline glial cells. *Genes and Development, 6*(9), 1668-1678.

Klowden, M. J. (2007). *Physiological systems in insects* (Second Edition ed.) Elsevier.

Knebel-Mörsdorf, D., Flipsen, J. T., Roncarati, R., Jahnel, F., Kleefsman, A. W., & Vlak, J. M. (1996). Baculovirus infection of spodoptera exigua larvae: LacZ expression driven by promoters of early genes pe38 and me53 in larval tissue. *Journal of General Virology, 77*(5), 815-824.

Knudson, D. L., & Harrap, K. A. (1975). Replication of nuclear polyhedrosis virus in a continuous cell culture of spodoptera frugiperda: Microscopy study of the sequence of events of the virus infection. *Journal of Virology, 17*(1), 254-268.

Kogan, P. H., Chen, X., & Blissard, G. W. (1995). Overlapping TATA-dependent and TATA-independent early promoter activities in the baculovirus gp64 envelope fusion protein gene. *Journal of Virology, 69*(3), 1452-1461.

Kozuma, K., & Hukuhara, T. (1994). Fusion characteristics of a nuclear polyhedrosis virus in cultured cells: Time course and effect of a synergistic factor and pH. *Journal of Invertebrate Pathology, 63*(1), 63-67.

Krejci, P., Prochazkova, J., Bryja, V., Kozubik, A., & Wilcox, W. R. (2009). Molecular pathology of the fibroblast growth factor family. *Human Mutation, 30*(9), 1245-1255.

Kurosu, H., & Kuro-o, M. (2009). Endocrine fibroblast growth factors as regulators of metabolic homestasis. *Biofactors, 35*(1), 52-60.

Kurosu, H., Ogawa, Y., Miyoshi, M., Yamamoto, M., Nandi, A., Rosenblatt, K. P., et al. (2006). Regulation of fibroblast growth factor-23 signaling by klotho. *Journal of Biological Chemistry, 281*(61), 6120-6123.

Lanier, L. M., & Volkman, L. E. (1998). Actin binding and nucleation by autographa california M Nucleopolyhedrovirus. *Virology, 243*(1), 167-177.

Laurie, G. W., Inoue, S., Bing, J. T., & Hassell, J. R. (1988). Visualization of the large heparan sulfate proteoglycan from basement membrane. *American Journal of Anatomy, 181*(3), 320-326.

Lauzon, H. A. M., Lucarotti, C. J., Krell, P. J., Feng, Q., Retnakaran, A., & Arif, B. M. (2004). Sequence and organization of the neodiprion lecontei Nucleopolyhedrovirus genome. *Journal of Virology, 78*(13), 7023-7035.

Lavine, M. D., & Strand, M. R. (2002). Insect hemocytes and their role in immunity. *Insect Biochemistry and Molecular Biology, 32*(10), 1295-1309.

Lee, S. Y., Poloumienko, A., Belfry, S., Qu, X., Chen, W., MacAfee, N., et al. (1996). A common pathway for p10 and calyx proteins in progressive stages of polyhedron envelope assembly in AcMNPV-infected spodoptera frugiperda larvae. *Archives of Virology, 141*(7), 1247-1258.

Lee, T., Hacohen, N., Krasnow, M., & Montell, D. J. (1996). Regulated breathless receptor tyrosine kinase activity required to pattern cell migration and branching in the drosophila tracheal system. *Genes and Development, 10*(22), 2912-2921.

Lehane, M. J. (1997). Peritrophic matrix structure and function. *Annual Review of Entomology, 42,* 525-550.

Lepore, L. S., Roelvink, P. R., & Granados, R. R. (1996). Enhancin, the granulosis virus protein that facilitates Nucleopolyhedrovirus (NPV) infections, is a metalloprotease. *Journal of Invertebrate Pathology, 68*(2), 131-140.

Lew, E. D., Furdui, C. M., Anderson, K. S., & Schlessinger, J. (2009). The precise sequence of FGF receptor autophosphorylation is kinetically driven and is disrupted by oncogenic mutations. *Science Signaling, 2*(58)

Li, H., Tang, H., Harrison, R. L., & Bonning, B. C. (2007). Impact of a basement membrane-degrading protease on dissemination and secondary infection of autographa californica multiple Nucleopolyhedrovirus in heliothis virescens (fabricus). *Journal of General Virology, 88*(4), 1109-1119.

Li, S., & Skinner, A. C. (2005). Influence of larval stage and virus inoculum on virus yield in insect host neodiprion abietis (hymenoptera: Diprionidae). *Journal of Economic Entomology, 98*(6), 1876-1879.

Li, Z., & Blissard, G. W. (2009). The pre-transmembrane domain of the autographa californica multicapsid Nucleopolyhedrovirus GP64 protein is critical for membrane fusion and virus infectivity. *Journal of Virology, 83*(21), 10993-11004.

Lieleg, O., Baumgärtel, R. M., & Bausch, A. R. (2009). Selective filtering of particles by the extracellular matrix: An electrostatic bandpass. *Biophysical Journal, 97*(6), 1568-1577.

Lin, L., Wang, J., Deng, R., Ke, H., Wu, J., & Wang, X. (2009). ac109 is required for the nucleocapsid assembly of autographa californica multiple Nucleopolyhedrovirus. *Virus Research, 142*(1-2), 130-135.

Lin, X., Buff, E. M., Perrimon, N., & Michelson, A. M. (1999). Heparan sulfate proteoglycans are essential for FGF receptor signaling during drosophila embryonic development. *Development, 126*(17), 3715-3723.

Lin, X., & Perrimon, N. (1999). Dally cooperates with drosophila frizzled 2 to transduce wingless signalling. *Nature, 400*(6741), 281-284.

Lin, X., & Perrimon, N. (2000). Role of heparan sulfate proteoglycans in cell-cell signaling in *drosophila*. *Matrix Biology, 19*(4), 303-307.

Lindner, J. R., Hillman, P. R., Barrett, A. L., Jackson, M. C., Perry, T. L., Park, Y., et al. (2007). The drosophila perlecan gene trol regulates multiple signaling pathways in different developmental contexts. *BMC Developmental Biology, 7*(121), 1-14.

Liu, Z., Ishiwata, T., Zhou, S., Maier, S., Henne-Bruns, D., Korc, M., et al. (2007). Human fibroblast growth factor receptor 1-IIIb is a functional fibroblast growth factor receptor expressed in the pancreas and involved in proliferation and movement of pancreatic ductal cells. *Pancreas, 35*(2), 147-157.

Locke, M. (1985). The structure of epidermal feet during their development. *Tissue and Cell, 17*(6), 901-921.

Locke, M. (1997). Caterpillars have evolved lungs for hemocyte gas exchange. *Journal of Insect Physiology, 44*(1), 1-20.

Long, G., Pan, X., Kormelink, R., & Vlak, J. M. (2006). Functional entry of baculovirus into insect and mammalian cells is dependent on clathrin-mediated endocytosis. *Journal of Virology, 80*(17), 8830-8833.

Long, G., Pan, X., & Vlak, J. M. (2008). Conserved leucines in N-terminal heptad repeat HR1 of envelope fusion protein F of group II Nucleopolyhedroviruses are important for correct processing and essential for fusogenicity. *Journal of Virology, 82*(5), 2437-2447.

Lu, S., Yi-Peng, Q., & Ge, G. (2002). Interaction of heliothis armigera nuclear polyhedrosis viral capsid protein with its host actin. *Journal of Biochemistry and Molecular Biology, 35*(6), 562-567.

Lübbert, H., & Doerfler, W. (1984). Transcription of overlapping sets of RNAs from the genome of autographa californica nuclear polyhedrosis virus: A novel method for mapping RNAs. *Journal of Virology, 52*(1), 255-265.

Lung, O. Y., Cruz-Alvarez, M., & Blissard, G. W. (2003). Ac23, an envelope fusion protein homolog in the baculovirus autographa californica multicapsid Nucleopolyhedrovirus, is a viral pathogenicity factor. *Journal of Virology, 77*(1), 328-339.

Lung, O. Y., Westenberg, M., Vlak, J. M., Zuidema, D., & Blissard, G. W. (2002). Pseudotyping autographa californica multicapsid Nucleopolyhedrovirus (AcMNPV): F proteins from group II NPVs are functionally analogous to AcMNPV GP64. *Journal of Virology, 76*(11), 5729-5736.

Maina, J. N. (1989). Scanning and transmission electron microscopic study of the tracheal air sac system in a grasshopper chrotogonus senegalensis (kraus)--orthoptera: Acrididae: Pyrgomorphinae. *The Anatomical Record, 223*(4), 393-405.

Markovic, I., Pulyaeva, H., Sokoloff, A., & Chernomordik, L. V. (1998). Membrane fusion mediated by baculovirus gp64 involves assembly of stable gp64 trimers into multiprotein aggregates. *Journal of Cell Biology, 143*(5), 1155-1166.

Marsh, M., & Helenius, A. (2006). Virus entry: Open sesame. *Cell, 124*(4), 729-740.

Mathieu, M., Chatelain, E., Ornitz, D., Bresnick, J., Mason, I., Kiefer, P., et al. (1995). Receptor binding and mitogenic properties of mouse fibroblast growth factor 3. modulation of response by heparin. *Journal of Biological Chemistry, 270*(41), 24197-24203.

Matzner, Y., Bar-Nor, M., Yahalom, J., Ishai-Michaeli, R., Fuks, Z., & Vlodavsky, I. (1985). Degradation of heparan sulfate in the subendothelial extracellular matrix by a readily released heparanase from human neutrophils. possible role in invasion through basement membranes. *Journal of Clinical Investigation, 76*(4), 1306-1313.

Maves, L., & Schubiger, G. (1999). Cell determination and transdetermination in drosophila imaginal discs. *Current Topics in Developmental Biology, 43*, 115-151.

McCarthy, C. B., Dai, X., Donly, C., & Theilmann, D. A. (2008). Autographa californica multiple Nucleopolyhedrovirus ac142, a core gene that is essential for BV production and ODV envelopment. *Virology, 372*(2), 325-339.

McCarthy, C. B., & Theilmann, D. A. (2008). AcMNPV ac143 (odv-e18) is essential for mediating budded virus production and is the 30th baculovirus core gene. *Virology, 375*(1), 277-291.

McIntosh, A. H., & Shamy, R. (1980). Biological studies of a baculovirus in a mammalian cell line. *Intervirology, 13*(6), 331-341.

McLachlin, J. R., & Miller, L. K. (1994). Identification and characterization of VLF-1, a baculovirus gene involved in very late gene expression. *Journal of Virology, 68*(12), 7746-7756.

McNeil, J., Cox-Foster, D., Gardner, M., Slavicek, J., Thiem, S. M., & Hoover, K. (2010). Pathogenesis of lymantria dispar multiple Nucleopolyhedrovirus in L. dispar and mechanisms of developmental resistance. *Journal of General Virology, 91*(6), 1590-1600.

Means, J., & Passarelli, A. L. (Epublished ahead of print 2010). Viral fibroblast growth factor, matrix metalloproteases, and caspases are associated with enhancing systemic infection by baculoviruses. *Proceedings from the National Academy of Sciences,*

Merry, C. L. R., Bullock, S. L., Swan, D. C., Backen, A. C., Lyon, M., Beddington, R. S. P., et al. (2001). The molecular phenotype of heparan sulfate in the Hs2st-/- mutant mouse. *Journal of Biological Chemistry, 276*(38), 35429-35434.

Michelson, A. M., Gisselbrecht, S., Zhou, Y., Baek, K., & Buff, E. M. (1998). Dual functions of the heartless fibroblast growth factor receptor in development of the drosophila embryonic mesoderm. *Developmental Genetics, 22*(3), 212-229.

Mikhailov, V. S., & Rohrmann, G. F. (2002). Binding of the baculovirus very late expression factor 1 (VLF-1) to different DNA structures. *BMC Molecular Biology, 3*(14), 1-11.

Miki, T., Bottaro, D. P., Fleming, T. P., Smith, C. L., Burgess, W. H., Chan, A., et al. (1992). Determination of ligand-binding specificity by alternative splicing: Two distinct growth factor receptors encoded by a single gene. *Proceedings from the National Academy of Sciences, 89*(1), 246-250.

Miller, L. K., & Lu, A. (Eds.). (1997). *The baculoviruses*. New York, New York: Plenum Press.

Min, H., Danilenko, D. M., Scully, S. A., Bolon, B., Ring, B. D., Tarpley, J. E., et al. (1998). *Fgf-10* is required for both limb and lung development and exhibits striking functional similarity to *drosophila branchless*. *Genes and Development, 12*(20), 3156-3161.

Mistretta, T. A., & Guarino, L. A. (2005). Transcriptional activity of baculovirus very late factor 1. *Journal of Virology, 79*(3), 1958-1960.

Miyakawa, K., Hatsuzawa, K., Kurokawa, T., Asada, M., Kuroiwa, T., & Imamura, T. (1999). A hydrophobic region locating at the center of fibroblast growth factor-9 is crucial for its secretion. *Journal of Biological Chemistry, 274*(41), 29352-29357.

Miyakawa, K., & Imamura, T. (2003). Secretion of FGF-16 requires an uncleaved bipartite signal sequence*. *The Journal of Biological Chemistry, 278*(37), 35718-35724.

Miyakawa, K., & Imamura, T. (2003). Secretion of FGF-16 requires an uncleaved bipartite signal sequence. *Journal of Biological Chemistry, 278*(37), 35718-35724.

Mohammadi, M., Dikic, I., Burgess, W. H., Jaye, M., & Schlessinger, J. (1996). Identification of six novel autophosphorylation sites on fibroblast growth factor receptor 1 and elucidation of their importance in receptor activation and signal transduction. *Molecular and Cellular Biology, 16*(3), 977-989.

Mohammadi, M., Olsen, S. K., & Goetz, R. (2005b). A protein canyon in the FGF-FGF receptor dimer selects from an à la carte menu of heparan sulfate motifs. *Current Opinions in Structural Biology, 15*(5), 505-516.

Mohammadi, M., Olsen, S. K., & Ibrahimi, O. A. (2005a). Structural basis for fibroblast growth factor receptor activation. *Cytokine & Growth Factor Reviews, 16*(2), 107-137.

Monsma, S., Oomens, A. G., & Blissard, G. W. (1996). The GP64 envelope fusion protein is an essential baculovirus protein required for cell-to-cell transmission of infection. *Journal of Virology, 70*(7), 4607-4617.

Moy, F. J., Safran, M., Seddon, A. P., Kitchen, D., Böhlen, P., Aviezer, D., et al. (1997). Properly oriented heparin-decasaccharide-induced dimers are the biologically active form of basic fibroblast growth factor. *Biochemistry, 36*(16), 4782-4791.

Murges, D., Kremer, A., & Knebel-Mörsdorf, D. (1997). Baculovirus transactivator IE1 is functional in mammalian cells. *Journal of General Virology, 78*(6), 1507-1510.

Murzina, A. G., Leskc, A. M., & Chothia, C. (1992). β-Trefoil fold : Patterns of structure and sequence in the kunitz inhibitors interleukins-1β and 1α and fibroblast growth factors. *Journal of Molecular Biology, 223*(2), 531-543.

Nagamine, T., Kawasaki, Y., & Matsumoto, S. (2006). Induction of a subnuclear structure by the simultaneous expression of baculovirus proteins, IE1, LEF3, and P143 in the presence of hr. *Virology, 352*(2), 400-407.

Nagendra, H. G., Harrington, A. E., Harmer, N. J., Pellegrini, L., Blundell, T. L., & Burke, D. F. (2001). Sequence analyses and comparative modeling of fly and worm fibroblast growth factor receptors indicate that the determinants for FGF and heparin binding are retained in evolution. *FEBS Letters, 501*(1), 51-58.

Nakato, H., Futch, T. A., & Selleck, S. B. (1995). The division abnormally delayed (dally) gene: A putative integral membrane proteoglycan required for cell division patterning during postembryonic development of the nervous system in drosophila. *Development, 121*(11), 3687-3702.

Neufeld, G., & Gospodarowicz, D. (1985). The identification and partial characterization of the fibroblast growth factor receptor of baby hamster kidney cells. *Journal of Biological Chemistry, 260*(25), 13860-13868.

Nickel, W. (2003). The mystery of nonclassical protein secretion. A current view on cargo proteins and potential export routes. *European Journal of Biochemistry, 270*(10), 2109-2119.

Noonan, D. M., Fulle, A., Valente, P., Cai, S., Horigan, E., Sasaki, M., et al. (1991). The complete sequence of perlecan, a basement membrane heparan sulfate proteoglycan, reveals extensive similarity with laminin A chain, low density lipoprotein-receptor, and the neural cell adhesion molecule. *Journal of Biological Chemistry, 266*(34), 22939-22947.

Ogawa, Y., Kurosu, H., Yamamoto, M., Nandi, A., Rosenblatt, K. P., Goetz, R., et al. (2007). βKlotho is required for metabolic activity of fibroblast growth factor 21. *Proceedings from the National Academy of Sciences, 104*(18), 7432-7437.

Ohkawa, T., Washburn, J. O., Sitapara, R., Sid, E., & Volkman, L. E. (2005). Specific binding of autographa californica M Nucleopolyhedrovirus occlusion-derived virus to midgut cells of heliothis virescens larvae is mediated by products of pif genes Ac119 and Ac022 but not by Ac115. *Journal of Virology, 79*(24), 15258-15264.

Olsen, S. K., Garbi, M., Zampieri, N., Eliseenkova, A. V., Ornitz, D. M., Goldfarb, M., et al. (2003). Fibroblast growth factor (FGF) homologous factors share structural but not functional homology with FGFs. *The Journal of Biological Chemistry, 278*, 34226-34236.

Olsen, S. K., Ibrahimi, O. A., Raucci, A., Zhang, F., Eliseenkova, A. V., Yayon, A., et al. (2004). Insights into the molecular basis for fibroblast growth factor receptor autoinhibition and ligand-binding promiscuity. *Proceedings from the National Academy of Sciences, 104*(4), 935-940.

Olsen, S. K., Li, J. Y. H., Bromleigh, C., Eliseenkova, A. V., Ibrahimi, O. A., Lao, Z., et al. (2006). Structural basis by which alternative splicing modulates the organizer activity of FGF8 in the brain. *Genes and Development, 20*(2), 185-198.

Olszewski, J., & Miller, L. K. (1997). A role for baculovirus GP41 in budded virus production. *Virology, 233*(2), 292-301.

Oomens, A. G., & Blissard, G. W. (1999). Requirement for GP64 to drive efficient budding of autographa californica multicapsid Nucleopolyhedrovirus. *Virology, 254*(2), 297-314.

Ornitz, D. M. (2000). FGFs, heparan sulfate and FGFRs: Complex interactions essential for development. *Bioessays, 22*(2), 108-112.

Ornitz, D. M., & Itoh, N. (2001). Fibroblast growth factors. *Genome Biology, 2*(3), Reviews 3005.1-Reviews 3005.12.

Ornitz, D. M., & Itoh, N. (2004). Evolution of the fgf and fgfr gene families. *Trends in Genetics, 20*(11), 563-569.

Ornitz, D. M., Xu, J., Colvin, J. S., McEwen, D. G., MacArthur, C. A., Coulieri, F., et al. (1996). Receptor specificity of the fibroblast growth factor family. *Journal of Biological Chemistry, 271*(25), 15292-15297.

Osslund, T. D., Syed, R., Singer, E., Hsu, E. W., Nybo, R., Harvey, T., et al. (1998). Correlation between the 1.6 Å crystal structure and mutational analysis of keratinocyte growth factor. *Protein Science, 7*(8), 1681-1690.

Park, Y., Rangel, C., Reynolds, M., Caldwell, M. C., Johns, M., Nayak, M., et al. (2003). Drosophila perlecan modulates FGF and hedgehog signals to activate neural stem cell division. *Developmental Biology, 253*(2), 247-257.

Pasquale, E. B., & Singer, S. J. (1989). Identification of a developmentally regulated protein-tyrosine kinase by using anti-phosphotyrosine antibodies to screen a cDNA expression library. *Proceedings from the National Academy of Sciences, 86*(14), 5449-5453.

Passarelli, A. L., & Guarino, L. A. (2007). Baculovirus late and very late gene regulation. *Current Drug Targets, 8*(10), 1103-1115.

Pearson, M. N., Groten, C., & Rohrmann, G. F. (2000). Identification of the *lymantria dispar* Nucleopolyhedrovirus envelope fusion protein provides evidence for a phylogenetic division of the *Baculovirus*. *Journal of Virology, 74*(13), 6126-6134.

Pearson, M. N., & Rohrman, G. F. (2002). Transfer, incorporation, and substitution of envelope fusion proteins among members of the Baculovirus, orthomyxoviridae, and metaviridae (insect retrovirus) families. *Journal of Virology, 76*(11), 5301-5304.

Pearson, M. N., Russell, R. L. Q., & Rohrmann, G. F. (2001). Characterization of a baculovirus-encoded protein that is associated with infected-cell membranes and budded virions. *Virology, 291*(1), 22-31.

Pellegrini, L., Burke, D. F., von Delft, F., Mulloy, B., & Blundell, T. L. (2000). Crystal structure of fibroblast growth factor receptor ectodomain bound to ligand and heparin. *Nature, 407*(6807), 1029-1034.

Peng, K., Wu, M., Deng, F., Song, J., Dong, C., Wang, H., et al. (2010). Identification of protein-protein interactions of the occlusion-derived virus-associated proteins of helicoverpa armigera Nucleopolyhedrovirus. *Journal of General Virology, 91*(3), 659-670.

Perrimon, N., & Bernfield, M. (2000). Specificities of heparan sulphate proteoglycans in developmental processes. *Nature, 404*(6779), 725-728.

Plotnikov, A. N., Eliseenkova, A. V., Ibrahimi, O. A., Shriver, Z., Sasisekharan, R., Lemmon, M. A., et al. (2001). Crystal structure of fibroblast growth factor 9 reveals regions implicated in dimerization and autoinhibition. *Journal of Biological Chemistry, 2776*(6), 4322-4329.

Plotnikov, A. N., Hubbard, S. R., Schlessinger, J., & Mohammadi, M. (2000). Crystal structures of two FGF-FGFR complexes reveal the determinants of ligand-receptor specificity. *Cell, 101*(4), 413-424.

Plotnikov, A. N., Schlessinger, J., Hubbard, S. R., & Mohammadi, M. (1999). Structural basis for FGF receptor dimerization and activation. *Cell, 98*(5), 641-650.

Plymale, R., Grove, M. J., Cox-Foster, D., Ostiguy, N., & Hoover, K. (2008). Plant-mediated alteration of the peritrophic matrix and baculovirus infection in lepidopteran larvae. *Journal of Insect Physiology, 54*(4), 737-749.

Popovici, C., Roubin, R., Coulier, F., & Birnbaum, D. (2005). An evolutionary history of the FGF superfamily. *Bioessays, 27*(8), 849-857.

Prudovsky, I., Mandinova, A., Soldi, R., Bagala, C., Graziani, I., Landriscina, M., et al. (2003). The non-classical export routes: FGF1 and IL-1alpha point the way. *Journal of Cell Science, 116*(24), 4871-4881.

Prydz, K., & Dalen, K. T. (2000). Synthesis and sorting of proteoglycans. *Journal of Cell Science, 113*(2), 193-205.

Pullen, S. S., & Friesen, P. D. (1995). The CAGT motif functions as an initiator element during early transcription of the baculovirus transregulator ie-1. *Journal of Virology, 69*(6), 3575-3583.

Puntervoll, P., Linding, R., Gemünd, C., Chabanis-Davidson, S., Mattingsdal, M., Cameron, S., et al. (2003). ELM server: A new resource for investigating short functional sites in modular eukaryotic proteins. *Nucleic Acids Research, 31*(13), 3625-3630.

Pye, D. A., Vivès, R. R., Hyde, P., & Gallagher, J. T. (2000). Regulation of FGF-1 mitogenic activity by heparan sulfate oligosaccharides is dependent on specific structural features: Differential requirements for the modulation of FGF-1 and FGF-2. *Glycobiology, 10*(11), 1183-1192.

Rahman, M. M., & Gopinathan, K. P. (2004). Systemic and in vitro infection process of bombyx mori Nucleopolyhedrovirus. *Virus Research, 101*(2), 109-118.

Rankin, C., Ooi, B. G., & Miller, L. K. (1988). Eight base pairs encompassing the transcriptional start point are the major determinant for baculovirus polyhedrin gene expression. *Gene, 70*(1), 39-49.

Rapp, J. C., Wilson, J. A., & Miller, L. K. (1998). Nineteen baculovirus open reading frames, including LEF-12, support late gene expression. *Journal of Virology, 72*(12), 10197-10206.

Rapraeger, A. C., Krufka, A., & Olwin, B. B. (1991). Requirement of heparan sulfate for bFGF-mediated fibroblast growth and myoblast differentiation. *Science, 252*(5013), 1705-1708.

Reddy, J. T., & Locke, M. (1990). The size limited penetration of gold particles through insect basal laminae. *Journal of Insect Physiology, 396*(6), 397-403.

Reichman-Fried, M., Dickson, B., Hafen, E., & Shilo, B. (1994). Elucidation of the role of breathless, a drosophila FGF receptor homolog, in tracheal cell migration. *Genes and Development, 8*(4), 428-439.

Revest, J., DeMoerlooze, L., & Dickson, C. (2000). Fibroblast growth factor 9 secretion is mediated by a non-cleaved amino-terminal signal sequence. *The Journal of Biological Chemistry, 275*(11), 8083-8090.

Ribeiro, C., & Brehélin, M. (2006). Insect haemocytes: What type of cell is that? *Journal of Insect Physiology, 52*(5), 417-429.

Rivkin, H., Kroemer, J. A., Bronshtein, A., Belausov, E., Webb, B. A., & Chejanovsky, N. (2006). Response of immunocompetent and immunosuppressed spodoptera littoralis larvae to baculovirus infection. *Journal of General Virology, 87*(8), 2217-2225.

Rohel, D. Z., Cochran, M. A., & Faulkner, P. (1983). Characterization of two abundant mRNAs of autographa californica nuclear polyhedrosis virus present late in infection. *Virology, 124*(2), 357-365.

Roncarati, R., & Knebel-Mörsdorf, D. (1997). Identification of the early actin-rearrangement-inducing factor gene, arif-1, from autographa californica multicapsid nuclear polyhedrosis virus. *Journal of Virology, 71*(10), 7933-7941.

Root, L. L., & Shipley, G. D. (2000). Normal human fibroblasts produce membrane-bound and soluble isoforms of FGFR-1. *Molecular Cellular Biology Research Communications, 3*(2), 87-97.

Saksela, O., Moscatelli, D., Sommer, A., & Rifkin, D. B. (1988). Endothelial cell-derived heparan sulfate binds basic fibroblast growth factor and protects it from proteolytic degradation. *Journal of Cell Biology, 107*(2), 743-751.

Saksena, S., Summers, M. D., Burks, J. K., Johnson, A. E., & Braunagel, S. C. (2006). Importin-alpha-16 is a translocon-associated protein involved in sorting membrane proteins to the nuclear envelope. *Nature Structural & Molecular Biology, 13*(6), 500-508.

Sánchez, L., & Guerrero, I. (2001). The development of the drosophila genital disc. *Bioessays, 23*(8), 698-707.

Sanchez-Heras, E., Howell, F. V., Williams, G., & Doherty, P. (2006). The fibroblast growth factor receptor acid box is essential for interactions with N-cadherin and all of the major isoforms of neural cell adhesion molecule. *Journal of Biological Chemistry, 281*(46), 35208-35216.

Sanderson, R. D., Yang, Y., Kelly, T., MacLeod, V., Dai, Y., & Theus, A. (2005). Enzymatic remodeling of heparan sulfate proteoglycans within the tumor microenvironment: Growth regulation and the prospect of new cancer therapies. *Journal of Biological Chemistry, 96*(5), 897-905.

Sato, M., & Kornberg, T. B. (2002). FGF is an essential mitogen and chemoattractant for the air sacs of the drosophila tracheal system. *Developmental Cell, 3*(2), 195-207.

Schäfer, T., Zentgraf, H., Zehe, C., Brügger, B., Bernhagen, J., & Nickel, W. (2004). Unconventional secretion of fibroblast growth factor 2 is mediated by direct translocation across the plasma membrane of mammalian cells. *The Journal of Biological Chemistry, 279*(8), 6244-6251.

Schlessinger, J., Plotnikov, A. N., Ibrahimi, O. A., Eliseenkova, A. V., Yeh, B. K., Yayon, A., et al. (2000). Crystal structure of a ternary FGF-FGFR-heparin complex reveals a dual role for heparin in FGFR binding and dimerization. *Molecular Cell, 6*(3), 743-750.

Schultz, G. S., & Wysocki, A. (2009). Interactions between extracellular matrix and growth factors in wound healing. *Wound Repair and Regeneration, 17*(2), 153-162.

Schultz, K. L., & Friesen, P. D. (2009). Baculovirus DNA replication-specific expression factors trigger apoptosis and shutoff of host protein synthesis during infection. *Journal of Virology, 83*(21), 11123-11132.

Seno, M., Sasada, R., Kurokawa, T., & Igarashi, K. (1990). Carboxyl-terminal structure of basic fibroblast growth factor significantly contributes to its affinity for heparin. *European Journal of Biochemistry, 180*(2), 239-245.

Sher, I., Lang, T., Lubinsky-Mink, S., Kuhn, J., Adir, N., Chatterjee, S., et al. (2000). Identification of residues important both for primary receptor binding and specificity in fibroblast growth factor-7. *Journal of Biological Chemistry, 275*(45), 34881-34886.

Sher, I., Weizman, A., Lubinsky-Mink, S., Lang, T., & Noam Adir§, Dietmar Schomburg¶, and Dina Ron‡i. (1999). Mutations uncouple human fibroblast growth factor (FGF)-7 biological activity and receptor binding and support broad specificity in the secondary receptor binding site of FGFs. *Journal of Biological Chemistry, 274*(49), 35016-35022.

Shing, Y., Folkman, J., Sullivan, R., Butterfield, C., Murray, J., & Klagsbrun, M. (1984). Heparin affinity: Purification of a tumor-derived capillary endothelial cell growth factor. *Science, 223*(4642), 1296-1299.

Shishido, E., Higashijima, S., Emori, Y., & Saigo, K. (1993). Two FGF-receptor homologues of drosophila: One is expressed in mesodermal primordium in early embryos. *Development, 117*(2), 751-761.

Simón, O., Williams, T., López-Ferber, M., & Caballero, P. (2004). Virus entry or the primary infection cycle are not the principal determinants of host specificity of spodoptera spp. Nucleopolyhedroviruses. *Journal of General Virology, 85*(10), 2845-2855.

Slack, J. M., Kuzio, J., & Faulkner, P. (1995). Characterization of v-cath, a cathepsin L-like proteinase expressed by the baculovirus autographa californica multiple nuclear polyhedrosis virus. *Journal of General Virology, 76*(5), 1091-1098.

Slavicek, J. M., & Popham, H. J. R. (2005). The lymantria dispar Nucleopolyhedrovirus enhancins are components of occlusion-derived virus. *Journal of Virology, 79*(16), 10578-10588.

Smith-Johannsen, H., Witkiewicz, H., & Iatrou, K. (1986). Infection of silkmoth follicular cells with *bombyx mori* nuclear polyhedrosis virus. *Journal of Invertebrate Pathology, 48*(1), 74-84.

Spring, J., Paine-Saunders, S. E., Hynes, R. O., & Bernfield, M. (1994). Drosophila syndecan: Conservation of a cell-surface heparan sulfate proteoglycan. *Proceedings from the National Academy of Sciences, 91*(8), 3334-3338.

Springer, B. A., Pantoliano, M. W., Barberall, F. A., Gunyuzlu, P. L., Thompson, L. D., Herblin, W. F., et al. (1994). Identification and concerted function of two receptor binding surfaces on basic fibroblast growth factor required for mitogenesis. *The Journal of Biological Chemistry, 269*(43), 26879-26884.

Srahna, M., Leyssen, M., Choi, C. M., Fradkin, L. G., Noordermeer, J. N., & Hassan, B. A. (2006). A signaling network for patterning of neuronal connectivity in the drosophila brain. *PLoS Biology, 4*(11), 2076-2090.

Stathopoulos, A., Tam, B., Ronshaugen, M., Frasch, M., & Levine, M. (2004). Pyramus and thisbe: FGF genes that pattern the mesoderm of drosophila embryos. *Genes and Development, 18*(6), 687-699.

Stolz, D. B. (1981). A putative baculovirus in the ichneumonid parasitoid, mesoleius tenthredinis. *Canadian Journal of Microbiology, 27*(1), 116-122.

Summerford, C., & Samulski, R. J. (1998). Membrane-associated heparan sulfate proteoglycan is a receptor for adeno-associated virus type 2 virions. *Journal of Virology, 72*(2), 1438-1445.

Summers, M. D. (1971). Electron microscopic observations on granulosis virus entry, uncoating and replication processes during infection of the midgut cells of trichoplusia ni. *Journal of Ultrastructural Research, 35*(5), 606-625.

Summers, M. D., & Smith, G. E. (1975). Comparative studies of baculovirus granulins and polyhedrins. *Intervirology, 6*(3), 168-180.

Summers, M. D., & Smith, G. E. (1978). Baculovirus structural polypeptides. *Virology, 84*(2), 390-402.

Sutherland, D., Samakovlis, C., & Krasnow, M. A. (1996). *Branchless* encodes a *drosophila* FGF homolog that controls tracheal cell migration and the pattern of branching. *Cell, 87*(6), 1091-1101.

Szewczyk, B., Hoyos-Carvajal, L., Paluszek, M., Skrzecz, I., & Lobo de Souza, M. (2006). Baculoviruses-- re-emerging biopesticides. *Biotechnology Advances, 24*(2), 143-160.

Takaishi, S., Sawada, M., Morita, Y., Seno, H., Fukuzawa, H., & Chiba, T. (2000). Identification of a novel alternative splicing of human FGF receptor 4: Soluble-form splice variant expressed in human gastrointestinal epithelial cells. *Biochemical and Biophysical Research Communications, 267*(2), 658-662.

Tani, H., Nishijima, M., Ushijima, H., Miyamura, T., & Matsuura, Y. (2001). Characterization of cell-surface determinants important for baculovirus infection. *Virology, 279*(1), 343-353.

Theilmann, D. A., & Blissard, G. W. (2008). Baculoviruses:Molecular biology of Nucleopolyhedroviruses. In B. W. J. Mahy, & M. H. van Regenmortel (Eds.), (Third ed., pp. 254-265) Science Direct.

Theilmann, D. A., & Stewart, S. (1991). Identification and characterization of the IE-1 gene of orgyia pseudotsugata multicapsid nuclear polyhedrosis virus. *Virology, 180*(2), 492-508.

Thiem, S. M., & Miller, L. K. (1989). Identification, sequence, and transcriptional mapping of the major capsid protein gene of the baculovirus autographa californica nuclear polyhedrosis virus. *Journal of Virology, 63*(5), 2008-2018.

Tholozan, F. M. D., Gribbon, C., Li, Z., Goldberg, M. W., Prescott, A. R., McKie, N., et al. (2007). FGF-2 release from the lens capsule by MMP-2 maintains lens epithelial cell viability. *Molecular Biology of the Cell, 18*(11), 4222-4231.

Thomas, K. A., Rios-Candelore, M., Gimenez-Gallego, G., Disalvo, J., Bennett, C., Rodkey, J., et al. (1985). Pure brain-derived acidic fibroblast growth factor is a potent angiogenic vascular endothelial cell mitogen with sequence homology to interleukin 1. *Proceedings from the National Academy of Sciences, 82*(19), 6409-6413.

Thompson, L. D., Pantoliano, M. W., & Springer Barry A. (1994). Energetic characterization of the basic fibroblast growth factor-heparin interaction: Identification of the heparin binding domain. *Biochemistry, 33*(13), 3831-3840.

Thornton, S. C., Mueller, S. N., & Levine, E. M. (1983). Human endothelial cells: Use of heparin in cloning and long-term serial cultivation. *Science, 222*(4624), 623-625.

Todd, J. W., Passarelli, A. L., & Miller, L. K. (1995). Eighteen baculovirus genes, including lef-11, p35, 39K, and p47, support late gene expression. *Journal of Virology, 69*(2), 968-974.

Trudeau, D., Washburn, J. O., & Volkman, L. E. (2001). Central role of hemocytes in autographa californica M Nucleopolyhedrovirus pathogenesis in heliothis virescens and helicoverpa zea. *Journal of Virology, 75*(2), 996-1003.

Trudeau, D., Washburn, J. O., & Volkman, L. E. (2001). Central role of hemocytes in autographa californica M Nucleopolyhedrovirus pathogenesis in heliothis virescens and helicoverpa zea. *Journal of Virology, 75*(2), 996-1003.

Tsen, G., Halfter, W., Kröger, S., & Cole, G. J. (1995). Agrin is a heparan sulfate proteoglycan. *Journal of Biological Chemistry, 270*(7), 3392-3399.

Turnbull, J., Drummond, K., Huang, Z., Kinnunen, T., Ford-Perriss, M., Murphy, M., et al. (2003). Heparan sulphate sulphotransferase expression in mice and *caenorhabditis elegans*. *Biochemical Society Transactions, 31*(2), 343-348.

Tweeten, K. A., Bulla, L. A. J., & Consigli, R. A. (1977). Isolation and purification of a granulosis virus from infected larvae of the indian meal moth, plodia interpunctella. *Applied Environmental Microbiology, 34*(3), 320-327.

Vanarsdall, A. L., Okano, K., & Rohrman, G. F. (2006). Characterization of the role of very late expression factor 1 in baculovirus capsid structure and DNA processing. *Journal of Virology, 80*(4), 1724-1733.

Vanarsdall, A. L., Okano, K., & Rohrmann, G. F. (2004). Characterization of a baculovirus with a deletion of VLF-1. *Virology, 326*(1), 191-201.

Vanarsdall, A. L., Pearson, M. N., & Rohrman, G. F. (207). Characterization of baculovirus constructs lacking either the ac 101, ac 142, or the ac 144 open reading frame. *Virology, 367*(1), 187-195.

Venkataraman, G., Raman, R., Sasisekharan, V., & Sasisekharan, R. (1999). Molecular characteristics of fibroblast growth factor-fibroblast growth factor receptor-heparin-like glycosaminoglycan complex. *Proceedings from the National Academy of Sciences, 96*(7), 3658-3663.

Vialard, J. E., Arif, B., & Richardson, C. D. (1995). Introduction to the molecular biology of baculoviruses. *Methods of Molecular Biology, 39*, 1-24.

Vincent, T., Hermansson, M., Bolton, M., Wait, R., & Saklatvala, J. (2002). Basic FGF mediates an immediate response of articular cartilage to mechanical injury. *Proceedings from the National Academy of Sciences, 99*(12), 8259-8264.

Vlodavsky, I., Korner, G., Ishai-Michaeli, R., Bashkin, P., Bar-Shavit, R., & Fuks, Z. (1990). Extracellular matrix-resident growth factors and enzymes: Possible involvement in tumor metastasis and angiogenesis. *Cancer Metastasis Review, 9*(3), 203-226.

Vlodavsky, I., Folkmann, J., Sullivan, R., Fridman, R., Ishai-Michaeli, R., Sasse, J., et al. (1987). Endothelial cell-derived basic fibroblast growth factor: Synthesis and deposition into subendothelial extracellular matrix. *Proceedings from the National Academy of Sciences, 84*(8), 2292-2296.

Voigt, A., Pflanz, R., Schäfer, U., & Jäckle, H. (2002). Perlecan participates in proliferation activation of quiescent drosophila neuroblasts. *Developmental Dynamics, 224*(4), 403-412.

Volkman, L. E., & Goldsmith, P. A. (1983). In vitro survey of autographa californica nuclear polyhedrosis virus interaction with nontarget vertebrate host cells. *Applied Environmental Microbiology, 45*(3), 1085-1093.

Volkman, L. E., & Goldsmith, P. A. (1984). Budded autographa californica NPV 64K protein: Further biochemical analysis and effects of postimmunoprecipitation sample preparation conditions. *Virology, 139*(2), 295-302.

Volkman, L. E., & Goldsmith, P. A. (1985). Mechanism of neutralization of budded *autographs californica* nuclear polyhedrosis virus by a monoclonal antibody: Inhibition of entry by adsorptive endocytosis. *Virology, 143*(1), 185-195.

Volkman, L. E., Goldsmith, P. A., & Hess, R. T. (1986). Alternate pathway of entry of budded autographa californica nuclear polyhedrosis virus: Fusion at the plasma membrane. *Virology, 148*(2), 288-297.

Wang, F., Kan, M., Xu, J., Yan, G., & McKeehan, W. L. (1995). Ligand-specific structural domains in the fibroblast growth factor receptor. *The Journal of Biological Chemistry, 270*(17), 10222-10230.

Wang, F., Lu, W., McKeehan, K., Mohamedali, K., Gabriel, J. L., Kan, M. (1999) Common and specific determinants for fibroblast growth factors in the ectodomain of the receptor kinase complex. *Biochemistry, 38*(1), 160-171.

Wang, J., Shen, M., Fong, G., & Hill, D. J. (2000). A soluble fibroblast growth factor receptor is released from HL-60 promyelocytic leukemia cells: Implications for paracrine growth control. *Growth Factors, 17*(3), 203-214.

Wang, Q., Liu, Y., He, H., Zhao, X., & Wang, J. (2010). Immune responses of helicoverpa armigera to different kinds of pathogens. *BMC Immunology, 11*(9)

Wang, S., Ai, X., Freeman, S. D., Pownall, M. E., Lu, Q., Kessler, D. S., et al. (2004). QSulf1, a heparan sulfate 6-O-endosulfatase, inhibits fibroblast growth factor signaling in mesoderm induction and angiogenesis. *Proceedings from the National Academy of Sciences, 101*(14), 4833-4838.

Washburn, J. O., Kirkpatrick, B. A., & Volkman, L. E. (1995). Comparative pathogenesis of autographa californica M nuclear polyhedrosis virus in larvae of trichoplusia ni and heliothis virescens. *Virology, 209*(2), 561-568.

Washburn, J. O., Lyons, E. H., Haas-Stapleton, E. J., & Volkman, L. E. (1999). Multiple nucleocapsid packaging of autographa californica Nucleopolyhedrovirus accelerates the onset of systemic infection in trichoplusia ni. *Journal of Virology, 73*(1), 411-416.

Washburn, J. O., Trudeau, D., Wong, J. F., & Volkman, L. E. (2003). Early pathogenesis of autographa californica multiple Nucleopolyhedrovirus and helicoverpa zea single Nucleopolyhedrovirus in heliothis virescens: A comparison of the 'M' and 'S' strategies for establishing fatal infection. *Journal of General Virology, 84*(pt2), 343-351.

Westenberg, M., Uijtdewilligen, P., & Vlak, J. M. (2007). Baculovirus envelope fusion proteins F and GP64 exploit distinct receptors to gain entry into cultured insect cells. *Journal of General Virology, 88*(12), 3302-3306.

Westenberg, M., Veenman, F., Roode, E., Goldbach, R. W., Vlak, J. M., & Zuidema, D. (2004). Functional analysis of the putative fusion domain of the baculovirus envelope fusion protein F. *Journal of Virology, 78*(13), 9646-9654.

Westenberg, M., & Vlak, J. M. (2008). GP64 of group I Nucleopolyhedroviruses cannot readily rescue infectivity of group II f-null Nucleopolyhedroviruses. *Journal of General Virology, 89*(2), 424-431.

Weyer, U., Knight, S., & Possee, R. D. (1990). Analysis of very late gene expression by autographa californica nuclear polyhedrosis virus and the further development of multiple expression vectors. *Journal of General Virology, 71*(7), 1525-1534.

Weyer, U., & Possee, R. D. (1989). Analysis of the promoter of the autographa californica nuclear polyhedrosis virus p10 gene. *Journal of General Virology, 70*(1), 203-208.

Whitt, M. A., & Manning, J. S. (1988). A phosphorylated 34-kDa protein and a subpopulation of polyhedrin are thiol linked to the carbohydrate layer surrounding a baculovirus occlusion body. *Virology, 163*(1), 33-42.

Wickham, T. J., Shuler, M. L., Hammer, M., Granados, R. R., & Wood, H. A. (1992). Equilibrium and kinetic analysis of autographa californica nuclear polyhedrosis virus attachment to different insect cell lines. *Journal of General Virology, 73*(12), 3185-3194.

Wiedłocha, A., & Sorensen, V. (2004). Signaling, internalization, and intracellular activity of fibroblast growth factor. *Current Topics in Microbiology and Immunology, 286*, 45-79.

Williams, G. V., & Faulkner, P. (Eds.). (1997). *The baculoviruses*. New York, New York: Plenum Press.

Wood, H. A. (1980). Autographa californica nuclear polyhedrosis virus-induced proteins in tissue culture. *Virology, 102*(1), 21-27.

Wu, D., Kan, M., Sato, G. H., Okamoto, T., & Satoi, J. D. (1991). Characterization and molecular cloning ao fP utative binding protein for heparin-binding growth factors. *The Journal of Biological Chemistry, 266*(25), 16778-16785.

Wu, W., Liang, H., Kan, J., Liu, C., Yuan, M., Liang, C., et al. (2008). Autographa californica multiple Nucleopolyhedrovirus 38K is a novel nucleocapsid protein that interacts with VP1054, VP39, VP80, and itself. *Journal of Virology, 82*(24), 12356-12364.

Wu, X., Ge, H., Gupte, J., Weiszmann, J., Shimamoto, G., Stevens, J., et al. (2007). Co-receptor requirements for fibroblast growth factor-19 signaling. *Journal of Biological Chemistry, 282*(40), 29069-29072.

Xu, H., Yao, L., Lu, S., & Qi, Y. (2007). Host filamentous actin is associated with heliothis armigera single nucleopolyhedrosis virus (HaSNPV) nucleocapsid transport to the host nucleus. *Current Microbiology, 54*(3), 199-206.

Yan, D., & Lin, X. (2007). Drosophila glypican dally-like acts in FGF-receiving cells to modulate FGF signaling during tracheal morphogenesis. *Developmental Biology, 312*(1), 203-216.

Yang, S., & Miller, L. K. (1999). Activation of baculovirus very late promoters by interaction with very late factor 1. *Journal of Virology, 73*(4), 3404-3409.

Yayon, A., Klagsbrunb, M., Eskoc, J. D., Lederd, P., & Ornitz, D. M. (1991). Cell surface, heparin-like molecules are required for binding of basic fibroblast growth factor to its high affinity receptor. *Cell, 64*(4), 841-848.

Ye, S., Luo, Y., Lu, W., Jones, R. B., Linhardt, R. J., Capila, I., et al. (2001). Structural basis for interaction of FGF-1, FGF-2, and FGF-7 with different heparan sulfate motifs. *Biochemistry, 40*(48), 14429-14439.

Yeh, B. K., Igarashi, M., Eliseenkova, A. V., Plotnikov, A. N., Sher, I., Ron, D., et al. (2003). Structural basis by which alternative splicing confers specificity in fibroblast growth factor receptors. *Proceedings from the National Academy of Sciences, 100*(5), 2266-2271.

Young, J. C., McKinnon, E. A., & Faulkner, P. (1993). The architecture of the virogenic stroma in isolated nuclei of *spodoptera frugiperda* cells in vitro infected by *autographa californica* nuclear polyhedrosis virus. *Journal of Structural Biology, 110*(2), 141-153.

Zhang, F., Zhang, Z., Lin, X., Beenken, A., Eliseenkova, A. V., Mohammadi, M., et al. (2009). Compositional analysis of heparin/heparan sulfate interacting with fibroblast growth factor.fibroblast growth factor receptor complexes. *Biochemistry, 48*(35), 8379-8386.

Zhang, J. D., Cousens, L. S., Barr, P. J., & Sprang, J. R. (1991). Three-dimensional structure of human basic fibroblast growth factor, a structural homolog of interleukin 1 beta. *Proceedings from the National Academy of Sciences, 88*(8), 3446-3450.

Zhang, X., Ibrahimi, O. A., Olsen, S. K., Umemori, H. M., Moosa, & Ornitz, D. M. (2006). Receptor specificity of the fibroblast growth factor family. the complete mammalian FGF family. *Journal of Biological Chemistry, 281*(23), 15694-15700.

Zhou, J., & Blissard, G. W. (2008). Identification of a GP64 subdomain involved in receptor binding by budded virions of the baculovirus autographica californica multicapsid Nucleopolyhedrovirus. *Journal of Virology, 82*(9), 4449-4460.

Zhou, Y., Yi, Y., Zhang, Z., He, J., Zhang, Y., & Wu, X. (2003). Promoter activities in the baculovirus envelope glycoprotein gp64 gene. *Acta Biochimica Et Biophysica Sinica, 35*(1), 18-26.

Zhu, H., Ramnarayan, K., Anchin, J., Miao, W. Y., Sereno, A., & Millman, L. (1995). Glu-96 of basic fibroblast growth factor is essential for high affinity receptor binding. identification by structure-based site-directed mutagenesis. *Journal of Biological Chemistry, 270*(37), 21869-21874.

Zhu, X., Komiya, H., Chirino, A., Faham, S., Fox, G. M., Arakawa, T., et. al. (1991). Three-dimensional structures of acidic and basic fibroblast growth factors. *Science, 251*, 90-93.

Zimmer, Y., Givol, D., & Yayon, A. (1993). Multiple structural elements determine ligand binding of fibroblast growth factor receptors. evidence that both ig domain 2 and 3 define receptor specificity. *Journal of Biological Chemistry, 268*(11), 7899-7903.

# Appendix A - Materials and Methods vFGF

## Cells, viruses, and insects

The cell line IPLB-SF-21 (SF-21) (Vaughn et al., 1977) derived from the fall armyworm, *Spodoptera frugiperda*, and TN-368 cells (Hink, 1970) derived from the cabbage looper, *Trichoplusia ni*, were maintained in TC-100 medium (Invitrogen) supplemented with 10% fetal bovine serum (Atlanta Biological) and 0.26% tryptose broth as described previously (O'Reilly et al., 1994).

## Transplacement vector construction-vFGF

We constructed a transfer vector to generate a recombinant of Ac*M*NPV expressing v*fgf* under native promoter control. First, the oligonucleotides (Sac I-F 5'-CTTAAGTCT GCAGTTTTAC-3' and Sac 1-R 5'-ATAAAAATGTTTTTATTGTAAAAT ACAC-3') were used to amplify an 863-base pair fragment from a construct containing HA-tagged *vfgf* and flanking regions. DNA containing HA-tagged *vfgf* and 207-base pairs upstream of *vfgf* that serve as promoter region was ligated into the transplacement vector pFastBac–polh+gfp+ (Detvisitsakun et al., 2006) at *Sac* I sites to generate pFastBac–polh+-vFGFHA-gfp+. The correct amplified sequence was verified by nucleotide sequencing analysis. To create the transplacement vector with v*fgf* under *Drosophila* heat shock protein (*HSP*) 70 promoter control, the 207 base pair native promoter element was removed and the 739 base pair HSP 70 promoter element inserted. The correct insertion was also verified by nucleotide sequencing analysis.

## Construction of AcBAC–vfgfHARep and AcBAC-HSP70vfgfHA

AcBAC-vfgfHA Rep and AcBAC-HSP70 vfgfHA were generated by Tn7-mediated transposition by transforming MAX DH10Bac Efficiency competent *Escherichia coli* (Invitrogen) with pFastBac–polh+-vFGFHA-gfp+ or pFastBac–polh+-HSP70 vFGFHA-gfp+. Bacterial cells were incubated for 4 hours in SOC media (Invitrogen) at 37 °C and then plated on the appropriate selection media and incubated for an additional 18 hours according to the Bac-to-Bac Baculovirus Expression System Manual (Invitrogen). White colonies resistant to kanamycin and gentamicin were selected and the transposition event and flanking regions were verified by PCR analysis. Budded virus was produced by transfection of AcBAC-vfgfHARep or AcBAC-HSP70vfgfHA DNA into SF-21 cells by liposome-mediated transfection as previously described (Crouch and Passarelli, 2002).

## Virus growth curves and RT

SF-21 cells were infected at an MOI of 5 PFU/cell with AcBAC-vfgfHARep, AcBAC-HSP70vfgfHA or AcBAC. Budded virus was collected at different times p.i. and titers were determined by $TCID_{50}$ (O'Reilly et al., 1994). The graph represents 3 independent experiments for each virus. Cells from the AcBAC-vfgfHARep-infections were harvested from plates, lysed with Trizol reagent (Invitrogen), and stored at -80 °C until the entire time course was complete. Using the standard protocol, total RNA from infected cells was extracted and quantified. Aliquots (4 µg) from each time point were treated with 2 units of DNAse I for 2 hours and then heat inactivated at 72 °C for 15 minutes. After DNAse I treatment, the Access RT PCR system (Promega) was used to amplify v*fgf* specific transcripts with 1µg of treated RNA as a template and oligonucleotides (F5'- GGAGCTGTTTACG GAACCATTG-3' and R5'-CAGTGC CACATACGTCAACTTG-3') as primers. To control for DNA contamination, parallel samples lacking AMV Reverse Transcriptase were tested. PCR conditions were carried out at 45 °C for 1 hour, followed by 40 cycles of 95 °C for 2 minutes, 45 °C for 30 seconds, and 72 °C for 1 minute.

## Immunoblotting

TN-368 cells ($2 \times 10^6$) were infected at an MOI of 10 PFU/cell with AcBAC–vfgfHARep or AcBAC-vfgfKO virus. At several times p.i., cells were collected in 100 µl of Laemeli loading buffer. Proteins were resolved in a sodium dodecyl sulfate–12 % polyacrylamide gel, transferred to a PVDF membrane, and detected using 1:3000 dilution of anti-HA.11 antibody (Covance), 1:5000 dilution of goat anti-mouse IgG–horseradish peroxidase (Bio-Rad). The SuperSignal West Femto Maximum Sensitivity Substrate (Pierce) was used to detect cross-reactive proteins. Densitometry Integrated Density Values (IDV) were calculated using AlphaImager 2200 software.

## Transmission electron microscopy

SF-21 cells ($2 \times 10^8$) were infected with AcBAC–vfgfHARep, AcBAC-vfgfKO, or AcBAC-HSP70vfgfHA at an MOI of 0.1 PFU/cell. At 72 h p.i., cell supernatant was collected and budded virus isolated using density gradient centrifugation (O'Reilly et al., 1994). Purified virions were removed from sucrose or Nycoprep™ Universal (Axis Shield) gradients and resuspended in PBS, pH 6.2 (Potter and Miller, 1980). Virions (1:100 dilution) were bound to Nickel Formvar/Carbon 200 mesh grids (Ted Pella, Inc.) and immunolabeled with a 1:1500

dilution of anti-HA.11 antibody (Covance) or 1:1500 dilution of anti-GP64 (AcV1) antibody (Santa Cruz Biotechnology) and 1:100 dilution of anti-mouse IgG (whole molecule)–gold antibody (Sigma). Virions were visualized with a Philips MC-100 transmission electron microscope.

## Flow cytometry

TN-368 cells ($0.5 \times 10^6$) were infected with AcBAC–v*fgf*HARep, AcBAC-v*fgf*KO, or AcBAC-HSP70v*fgf*HA at an MOI of 5 PFU/cell. At 24 and 48 h p.i., cells were harvested, washed twice with cold PBS (pH 6.2) and then resuspended in 100 µl of 1:1000 dilution of anti-HA.11 antibody (Covance). After 1 h, the antibody solution was removed and cells were washed once with PBS. Cells were then resuspended in 100 µl of 1:2000 dilution of APC-conjugated anti-mouse IgG antibody (BD Biosciences) for 1 h in the dark. Unbound antibody was removed and the cells were washed 3 times in PBS before fixing in 100 µl of 4% paraformaldehyde-1% glutaraldehyde in 0.1 M PBS. Cells were analyzed using a FACSCalibur flow cytometer.

## Heparin binding assay

SF-21 cells ($2 \times 10^8$) were infected with AcBAC-v*fgf*HARep, AcBAC-v*fgf*KO, or AcBAC-HSP70v*fgf*HA and virions were isolated and titered as described above (O'Reilly et al., 1994). Heparin Sepharose™ 6 Fast Flow beads (Amersham Biosciences) were washed with and resuspended in PBS pH 6.2. Aliquots (100 µl) from a 50% bead slurry were mixed with $5 \times 10^7$ infectious virions and then diluted to a final volume of 1 ml. The virus-heparin-Sepharose mixture was incubated overnight at 4 °C with steady rotation. After binding, the flow-through was collected and the beads were washed with 1 ml of TC-100 incomplete media. Bound vFGF was eluted with 1.25 M NaCl solution (1 ml). The input, flow-through, wash, and elution fractions were dialyzed in TC-100 incomplete media for a minimum of four hours at 4 °C to remove excess salt and maintain comparable salt concentrations in the different samples. After dialysis, the amount of infectious virions in each sample was determined by $TCID_{50}$. Results are reported as a percentage of the total viral infectious units present in each sample treatment.

## Transmigration assay

SF-21 cell migration was assessed using 8 µM pore size Costar transwells with polycarbonate membrane inserts. Approximately $2 \times 10^4$ cells were loaded onto transwell inserts and allowed to settle for 30 minutes. The transwell inserts were then transferred to 24-well plates containing virus and incubated for 4 h at 27 °C. Purified infectious virions ($1 \times 10^5$ to 1 x

$10^7$) from AcBAC-v*fgf*HARep-, AcBAC-HSP70v*fgf*HA- or AcBAC-v*fgf*KO-infected cells were placed in the lower transwell chamber along with 500 ul of PBS, pH 6.2. After incubation, the transwell inserts were removed and cells that had migrated downward were quantified using CellTiter-Glo luminescent substrate to measure ATP, according to the protocol provided by the manufacturer (Promega). The level of luminescence was determined with the Wallac Victor$^3$ 1420 Multilabel counter (Perkin-Elmer). To remove virion-bound vFGF, 3 x $10^7$ AcBAC-HSP70vFGFHA virions in 3 mL final volume of 20 mM Tris-HCl, pH 7, containing 0.1mg/ml BSA and 4 mM CaCl2 were treated with 1IU of Heparinase III from *Flavobacterium heparinum (*Sigma Aldritch) at 27 ºC for 4 hours. After treatment, the virions were separated from supernatant through centrifugation at 24,000 x G through a 25% Nycoprep cushion. The supernatant and cushion were carefully removed and the pelleted virus reconstituted in 1mL of PBS pH 6.2. In the assay, 500 uL of clarified supernatant was used to induce motility.

## Virus attachment assay

SF-21 cells (8 x $10^7$) were infected at an MOI of 0.1 PFU/cell with AcBAC-v*fgf*HARep, AcBAC-v*fgf*KO or AcBAC-HSP70v*fgf*HA. The supernatant was removed 29 h p.i. and replaced with Grace's Insect Medium lacking L-methionine and unsupplemented (Invitrogen). After 1 h, EasyTag™ EXPRESS $^{35}$S Protein Labeling Mix (Perkin Elmer) was added to a final concentration of 10 µCi/ml and cells were incubated at 27 °C for 10 h. Cells were then supplemented with 10 mM unlabeled methionine and 10% FBS and incubated for an additional 48 h. After incubation, the supernatant was removed and centrifuged at 1000 x g for 5 minutes to remove any debris present. The cleared supernatant was centrifuged at 80,000 x g for 75 minutes at 4 °C through a 25% sucrose cushion to pellet the virus and then resuspended in 10 ml of TC-100 complete media supplemented with 10% FBS. The radiolabeled virus was titered using $TCID_{50}$ end point dilution methods for a total of 3 times and radioactivity in the virus suspension measured by mixing 10 µl of virus with 1.5 ml of NET lysis buffer (20 mM Tris, 150 mM NaCl, 0.5% deoxycholate, 1% Nonidet P-40 1 mM EDTA, pH 7.5) and 3.5 ml of EcoLUME ™ Scintillation fluid (MP Biomedicals). Cells (1 x $10^6$) were plated on a 35-mM tissue culture dish and allowed to attach for 1 h at 27 °C before placing at a 4 °C for 3 h. After chilling, the cells were placed on ice blocks and the supernatant removed. Chilled virus was then added to each well (MOI of 1 PFU/cell, 500 µl total volume) and removed at specific time intervals (0, 5, 10, 20 30 and 60 minutes). Immediately after, the cells were washed with 3 ml of ice-cold PBS,

pH 6.2 and then lysed with 1.5 ml of NET buffer. The lysate was transferred to scintillation vials along with 3.5 ml of EcoLume $^{TM}$ Liquid Scintillation fluid. Radioactivity was determined for 1 minute using a Beckman-Coulter LS6500 Scintillation counter. To normalize all samples, the CPM counts on all samples were adjusted relative to initial CPM counts.

## Endosomal acidification assay

SF-21 cells ($1x\ 10^{6}$) were allowed to attach for 1 h at 27 °C prior to incubation at 4 °C for 2 h and infected at an MOI of 1 PFU/cell for 1 h at 4 °C with pre-chilled AcBAC-vfgfHARep or AcBAC-HSP70vfgfHA. After 1 h, the virus supernatant was removed and cells washed 3 times with pre-chilled PBS, pH 6.2. After washing, the cells were treated with warm TC-100 complete media and returned to a 27 °C incubator. At 0, 5, 10, 20, 30 and 60 minutes post attachment, ammonium chloride was added to the wells (final concentration of 25 mM) to inhibit endosome acidification. As a control, a well of infected cells was left untreated allowing endosomal acidification to continue normally. 24 h post attachment, the cells were removed from the plates, fixed with 100 µL of 4% paraformaldehyde-1% glutaraldehyde in 0.1 M PBS. Cells were analyzed using a FACSCalibur flow cytometer and the results of two independent experiments were shown here.

## Analysis of data

Analysis of standard deviations and statistical significance was done using Graphpad Prism® software. For comparisons of interaction between three or more experimental conditions, two-way Anova analysis was employeed with p values listed.

# Appendix B - Materials and Methods Ac-orf109

## Cells, viruses, and insects

The cell line IPLB-SF-21 (SF-21) (Vaughn *et al*., 1977) were derived from the fall armyworm, *Spodoptera frugiperda*, and were maintained in TC-100 medium (Invitrogen) supplemented with 10% fetal bovine serum (Atlanta Biological) and 0.26% tryptose broth.

## Northern Blot

SF-21 cells (2 x$10^6$) were infected with Ac*M*NPV at an MOI of 20 pfu/cell for one hour. The virus was aspirated off the cells, and then the cells were washed one time before being overlayed with TC 100 media supplemented with FBS (10%). At specified time points post infection, the cells were harvested with Trizol (Invitrogen) reagent and RNA extracted following the manufacturer's protocol. For the cycloheximide treatment, 30 minutes prior to infection, cells were treated with the protein synthesis inhibitor at a final concentration of 100µg/ml and this was maintained throughout the course of infection. For aphidicolin treatment, cells were treated with the DNA replication inhibitor immediately after virus infection at a final concentration of 5µg/ml. Samples of total RNA (20 µg per lane) were electrophoresed on a formaldehyde–1% agarose gel, transferred to a nylon membrane, and hybridized to α-$^{32}$P-radiolabeled riboprobes. The probe was generated by first PCR-amplifying Ac-orf109 from the translational start codon to the translational stop codon (Ayers *et al.* 1994). PCR products were cloned into an expression vector using the TA Cloning kit (Invitrogen) and the cRNA probes were synthesized by in vitro transcription using T7 RNA polymerase in the presence of a-32P[UTP].

## Transfection of SF-21 cells

In experiments in which DNA was introduced into 1 x $10^6$ SF-21 cells, 1 µg of Bacmid DNA or 2 µg of plasmid DNA was mixed with 4 µl of liposome preparation as previously described (Crouch and Passarelli, 2002). Cells were maintained at 27° C for four hours in the liposome-DNA mixture, then the media was removed from the cells and the cells washed once with TC-100 media. After washing, TC-100 media containing 10% fetal bovine serum was placed on the cells and incubated at 27° C until harvesting. The harvesting was done

by first aspirating the supernatant from the cells or removing it via pipet. The cells were then washed one time with PBS pH 6.2 prior to removal with careful agitation.

## Imaging eGFP expression

Cells were imaged on a Nikon Eclipse TE200 microscope with a 40X lens. Pictures were captured with a Nikon Coolpix 955 camera set at maximum resolution. The images shown are representative of four independent experiments.

## Generation of AcBAC-Δorf109

Ac*M*NPV DNA was digested with *Eco* RI and the 4035 fragment (93589-97624) was ligated into pBlueScript vector (Stratagene), creating pBIE4-3 plasmid. pBIE4-3 was digested with *Nde* I (96379-96385) and *Mlu* I (94788- 94793) to remove 1592 bp, including Ac-orfs 111, 110 and 94% of 109. Using 109MLUI (F 5'- GAACGCGTCGTGATGTATATGTCTTACT TCA-3') and 111NDEI (R 5'- GGAATTCCATATGCATCAGTGACATTGCCT-3') and pBIE4-3 as a template, a 492-bp fragment (95893-96384) containing full length Ac-orf 111 and Ac-orf 110 was obtained using PCR amplification. This fragment was ligated into the digested pBIE4-3 vector creating pBIE4-3-Δ109. The chloramphenicol resistance gene and promoter was amplified from pUC18CMR (ATTC) using the primer set CAT1 (F 5'- GAACGCGTTCCGTCGATCAT ATCGTCAA-3') and CAT2 (R 5'- GAACGCGTCGCCACATAGCAGAACTTTA-3'). This 1866 bp fragment was ligated into *Nde* I-*Mlu* I digested pBIE4-3-Δ109, creating the recombination vector pBIE4-3-Δ109CAT. Following the method of Bideshi and Federici (2000), 100 ng of pBIE4-3-Δ109CAT was transformed into BJ5183 cells containing bMON14272, the commercially available AcMNPV bacmid (Invitrogen). After incubation (4 h) in Super Optimal broth with Catabolite repression (SOC) media at 37° C, the transformed cells were plated on Luria Broth (LB) agar plates supplemented with kanamycin (50 µg/ml) and chloramphenicol (100 µg/ml). Colonies growing after 24 h were screened using PCR for the presence of the chloramphenicol resistance gene in the Ac-orf 109 locus. The primer sets used were P1 and CAT-R primers (F 5'-TGTGCTGCTTACTGTGCCTGTAT-3'and R 5'-AACGTTTTCATCGCTCTGGAGT-3', respectively), and CAT-F and P2 primers (F 5'-CCAGGTTTTCACCG TAACACG and R-5'- CGACATTAACAAAGAGCCA TTGA, respectively). Both P1 (93336-93358) and P2 (97918-97940) were well outside of the possible

area of recombination in order to confirm the correct insertion site. Next, bacmid DNA was co-transformed into MAX Efficiency DH10B competent *E. coli* cells (Invitrogen) along with the T7 translocation helper plasmid pMON7124 and plated on LB plates supplemented with kanamycin (50 µg/ml), chloramphenicol (100 µg/ml) and tetracycline (15 µg/ml). A single colony from this plate was used to generate the final constructs AcBAC-orf109KO and subsequently AcBAC-orf109Rep.

## Generation of AcBAC-orf109KO

To construct AcBAC-orf109KO, DH10B bacteria containing AcBAC-Δorf109 and the T7 helper plasmid were transformed with the T7 transplacement vector pFastBac–polh+gfp+ (Detvisitsakun et al., 2006). After transformation, the bacteria were plated on LB plates supplemented with kanamycin (50 µg/ml), chloramphenicol (100 µg/ml), gentamicin (7 µg/ml), tetracycline (15 µg/ml), 100 µg/ml 5-bromo-4- chloro-3-indoxyl-beta-D-galactopyranoside, and 40 µg/ml isopropyl-1-thio-β-D- galactoside as directed in the Bac-to-Bac Baculovirus Expression System Manual (Invitrogen). White colonies were selected and screened for the presence of the enhanced green fluorescent protein gene (*egfp*) and the polyhedrin *(polh)* gene transposition using PCR. The primer sets used were M13F (F 5'- GTTTTCCCA GTCACGAC-3') with P3 (R 5'- CATGGAC GAGCTGTACAAGTAAAGC-3'), P5 (F 5'-CTGCAACTACTGAAAT CAAC-3') with P6 (R 5'- CAAG GAAAACATCCA TCACTTCTTG-3') and P4 (F 5'-CGAACAT GAGATCGAAGAGGCTAC-3') with M13R (R 5'-CAGGAAACAGCTATGAC-3').

## Construction of AcBAC–orf109Rep

We constructed a transfer vector to generate a recombinant of AcMNPV expressing Ac-orf109 under native promoter control. First, the oligonucleotides (Sac I-F 5'- CGGTACG AGCTCACAAATTAAAATAATCTAAAG-3' and Sac 1-R 5'-GACGTGAGCTC CTACAAATAATAGTTGTACTTGA-3') were used to amplify a 1222-bp fragment from pBIE4-3 consisting of a 49 bp leader sequence and the complete Ac-orf109 coding sequence. The PCR product was cloned into the transplacement vector pFastBac–polh+gfp+ (Detvisitsakun *et al*., 2006) at *Sac* I sites to generate pFastBac−polh+-orf109-gfp+. The correct amplified sequence was verified by nucleotide sequencing analysis. DH10B cells containing the AcBAC-Δorf 109 backbone and T7 helper plasmid were transformed with pFastBac−polh+-orf109-gfp+.

Transformed cells were incubated on kanamycin (50 μg/ml), chloramphenicol (100 μg/ml), gentamicin (7 μg/ml), tetracycline (15gμ/ml), 100 μg/ml 5-bromo-4- chloro-3-indoxyl-beta-D-galactopyranoside, and 40 μg/ml isopropyl-1-thio-β-D- galactoside media according to the Bac-to-Bac Baculovirus Expression System Manual (Invitrogen). White colonies were selected and the transposition event and flanking regions were verified by PCR analysis. Budded virus was produced by transfection of AcBAC-orf109Rep DNA into SF-21 cells by liposome-mediated transfection as previously described (Crouch and Passarelli, 2002).

## Construction of AcBAC–orf109HA

Using the same strategy to create AcBAC-orf109Rep, a recombinant Ac*M*NPV expressing an epitope tagged version of Ac-orf109 under native promoter control was constructed. To prevent interference with Ac-orf109 function, a glycine linker (gly-gly-gly) was employed to provide space between the epitope tag and the C-terminal sequence of Ac-orf109. First, the oligonucleotides (Sac I-F 5'- CGGTACG AGCTCACAAATTAAAATAATCT AAAG-3' and Sac 1-R 5'- CTAGGCGTAATCTGGGACGTCGTATGGGTATCCTCCTCCCA AATAATAGTTGTACTTGACG-3') were used to amplify a 1258-bp fragment from pBIE4-3 consisting of a 49 bp leader sequence and the complete Ac-orf109 coding sequence, the glycine linker and the HA epitope tag. The PCR product was cloned into the transplacement vector pFastBac–polh+gfp+ (Detvisitsakun *et al*., 2006) at *Sac* I sites to generate pFastBac–polh+-orf109HA-gfp+. After sequencing, using the same method outlined above, AcBAC-orf109HA was constructued.

## Immunoblotting

SF-21 cells ($2 \times 10^6$) were infected at an MOI of 10 PFU/cell with AcBAC–orf109HA virus. At several times p.i., cells were collected in 100 μl of Laemeli loading buffer. Proteins were resolved in a sodium dodecyl sulfate–12 % polyacrylamide gel, transferred to a PVDF membrane, and detected using 1:3000 dilution of anti-HA.11 antibody (Covance), 1:5000 dilution of goat anti-mouse IgG–horseradish peroxidase (Bio-Rad). The SuperSignal West Pico Substrate (Pierce) was used to detect cross-reactive proteins.

For co-immunoprecipitations, SF-21cells were initially transfected either singly with pHS-orf109HA, pHS-orf109FLAG, or pHS-142FLAG or in pairs (Ac-109HA/Ac-109FLAG; Ac-109HA/Ac-142FLAG). After 24 hours incubation, the supernatant was removed and cells

washed one time with PBS pH 6.2. The cells were then lysed with 200 µL of CHAPS lysis buffer (Sambrook, Molecular Cloning 3rd edition) and placed at -80°C overnight. The lysates were then immunprecipitated with either 0.5 µl of anti-FLAG M2 antibody (Sigma) or 2.0 µl of anti-HA.11 monoclonal antibody (Covance) bound to 100 µl of a 10% solution of Protein G-Sepharose Fast Flow beads (Sigma) at 4 °C overnight. After IP, the beads were mixed with 100 µl of Laemeli loading buffer and proteins resolved using a sodium dodecyl sulfate–12 % polyacrylamide gel. After transfer to PVDF, the blot was probed with α-HA-HRP (Invitrogen) at a 1:1000 concentration. The SuperSignal West Pico Substrate (Pierce) was used to detect cross-reactive proteins.

## Complementation assay

SF-21 cells were transfected with 1 µg AcBAC-orf109KO with either 1 µg p109 plasmid which contains Ac-orf109 and Ac-orf110 or 1 µg p109FS plasmid which is the p109 plasmid digested with Nco1, blunt ended with T4 DNA ligase and then re-ligated to introduce a premature stop codon in Ac-orf109. As a control, SF-21 cells were also transfected with AcBAC-orf109Rep DNA with 1 µg pBluescript vector. At 24 and 48 h p.t., cells were examined for *egfp* expression. The supernatant from the 48 h p.t sample was removed and placed on 1 x $10^6$ naïve SF-21 cells. After 1h incubation at 27° C, the supernatant was removed and the cells were replenished with TC-100 media supplemented with 10% fetal bovine serum. At 24 hours post treatment, cells were observed for *egfp* expression.

## Virus growth curves

SF-21 cells were infected at an MOI of 5 PFU/cell with AcBAC-*orf109*Rep or AcBAC. Budded virus was collected at different times p.i. and titers were determined by $TCID_{50}$. To calculate the virus growth curve of AcBAC-*orf109*KO, SF-21 cells were first transfected with 1µg of AcBAC-*orf109*KO DNA. At 48 h p.t., the supernatant was removed from cells, and used to infect naïve SF-21 cells. After 1h incubation at 27° C, the supernatant was removed and the cells were replenished with TC-100 media supplemented with 10% fetal bovine serum. At specified time intervals, the supernatant was collected and assayed for the presence of infectious budded virus using the $TCID_{50}$ method.

## RT-PCR

SF-21 cells were transfected with 1 µg AcBAC-orf109KO DNA and at specific times p.t. lysed with Trizol reagent (Invitrogen), and stored at -80 °C until the entire time course was complete. Total RNA from infected cells was extracted and quantified. Aliquots (4 µg) from each time point were treated with 2 units of DNAse I for 2 h and then heat inactivated at 72° C for 15 minutes. After DNAse I treatment, the Access RT-PCR system (Promega) was used to amplify viral specific transcripts with 1 µg of DNase I-treated RNA as a template and the following oligonucleotides: gp64 primer set: F 5'- GCGTGTGTTGGGATCCAGCGA -3' and R 5'- GCGCATTCTGCCTTTGCGGC -3'; polyhedrin primer set: F 5'- ATGCCGGATTATTCA TACCGTCCCACCAT-3' and R 5'- CCTTTCCTGGGACCCGGCAAGAACC-3'; lef-1 primer set: F 5'- AGTCGTCTGCATTGAACCG-3 and R 5'- GAGAACGTGTCAAGAGTCATG TATAC-3'; To control for DNA contamination, parallel samples lacking AMV Reverse Transcriptase were subjected to amplification. PCR conditions were carried out at 45° C for 1 h, followed by 40 cycles of 95° C for 2 minutes, 45° C for 30 seconds, and 72 °C for 1 minute.

## Transmission electron microscopy

SF-21 cells ($2 \times 10^8$) were transfected with 1µg of AcBAC–*orf109*Rep, AcBAC-*orf109*KO, or AcBAC DNA. At 24 and 48 h p.t., cells were collected, fixed with 2% paraformaldehyde/0.2% glutaraldehyde overnight and then embedded in resin for sectioning as previously described (Lehiy et. al., 2010). Cell sections were placed on Formvar carbon 500 mesh grids and then visualized with a Philips MC-100 transmission electron microscope.

## Genomic Copy Number

To generate a standard curve, purified Ac*M*NPV DNA from budded virus was serially diluted 5 times from 230 ng/µl to 23 ng/µl. Using the protocol outlined by Vanarsdall *et al.* (2006), the template DNA along with the gp41 primer set was used with the iQ Sybr Green Supermix® (BioRad) and the BioRad ICycler system with Optical system software version 3.1. To convert from DNA concentration to copy number, 1 copy of Ac*M*NPV genome used as equivalent to $1.34 \times 10^{-4}$ pg of DNA (Carstens and Wu, 2007). CT values were plotted against $\log_{10}$ genome copy number to generate graph and line slope equations. Sample DNA was obtained from the SF-21 cells transfected with 1 µg of AcBAC, AcBAC-*orf109*KO, AcBAC-

*orf109*Rep, or vAc$^{gp64-}$. At specified time points, cells were harvested and washed 3 times with PBS prior to addition of Trizol reagent (Invitrogen). Following the manufacturers protocol, genomic DNA was isolated and quantified using spectrophotometry. DNA (2 µg) was then digested with *Dpn* I for 4 h to remove any input bacmid DNA carried from transfection. Using the same protocol outlined earlier, CT values and melt curves were generated for the individual samples. Using the standard curve generated from purified viral DNA, CT values were converted to genome copy number.

## Plasmid Construction

To construct the epitope tagged versions of Ac-*orf109* and Ac-*142*, PCR was used to amplify the genes using either genomic DNA (Ac-142) or pBIE4-3 (Ac-orf109) as the template. To prevent the C-terminal tag from interfering with Ac-orf109 function, a glycine linker sequence (gly-gly) was included between the Ac-orf109 coding sequence and the HA or FLAG (Invitrogen) epitope tags. The oligionucleotides sets used for amplification included: F 5'-CCTAAGGATGGAGTGCCCGTTTCAGATTCAAGTTTGTATT-3' and R 3'- CCTAA GGCTAGGCGTAATCTGGGACGTCGTATGGGTATCCTCCCAAATAATAGTTGTACTTG ACG-5' (Ac-orf109HA); F 5'- CCTAAGGATGGAGTGCCCGTTTCAGATTCAA TTTGTATT-3' and R 3'-CCTAAGGCTACTTATCGTCGTCATCCTTGTAATCTCCTC CAAATAAAGTTGTACTTGACG-5' (Ac-orf109FLAG); and F 5'- CCTAAGGAT GAGTGGTGGCGGCAACTTGTTGACTCTGGAAAG-3' and R 3'- CCTAAGGCTA CTTATCGTCGTCATCCTTGTAATCTTGTACCGAGTCGGGGAT TAATAAT-5' (Ac-142 FLAG). After amplification, the PCR products were cloned into the pHSGFP plasmid previously described by Crouch and Passarelli (2002) after restriction digest removal of the GFP coding sequence. This resulted in three clones with either Ac-orf109HA, Ac-orf109FLAG or Ac-142FLAG under *hsp70* promoter control.